

# Vulnerability Assessment of Electric Power Supply under Extreme Weather Conditions

THÈSE N° 4873 (2010)

PRÉSENTÉE LE 9 DÉCEMBRE 2010

À LA FACULTÉ ENVIRONNEMENT NATUREL, ARCHITECTURAL ET CONSTRUIT  
LABORATOIRE DES SYSTÈMES ÉNERGÉTIQUES  
PROGRAMME DOCTORAL EN ENERGIE

ÉCOLE POLYTECHNIQUE FÉDÉRALE DE LAUSANNE

POUR L'OBTENTION DU GRADE DE DOCTEUR ÈS SCIENCES

PAR

Raphaël BARBEN

acceptée sur proposition du jury:

Prof. H. B. Püttgen, président du jury  
Dr E. Gnansounou, directeur de thèse  
Prof. F. Golay, rapporteur  
Dr E. Marthe, rapporteur  
Dr A. Schenk, rapporteur



ÉCOLE POLYTECHNIQUE  
FÉDÉRALE DE LAUSANNE

Suisse  
2010



---

## Summary of the thesis

This thesis analyses and models the vulnerability of the electricity power supply under extreme weather conditions. The system under study is the electric supply system that includes major power plants to main load centers. Extreme weather conditions can cause common mode contingencies (CMCs) of overhead power lines, which endanger the security of electricity supply. Planning and operation of transmission systems are subject to N-1 criterion, which requires that all single failures of network elements do not cause a breach of safety limits. This criterion does not guarantee the security of electricity supply at the time of extreme weather conditions. The objective of this research is to identify critical and plausible CMCs, taking into account space-time correlations of extreme weather conditions and possible states of the network. The most vulnerable zones are focused on to determine appropriate countermeasures for reducing vulnerability.

In the past, extreme weather events have caused major disruptions. For example, the blackout in New York in 1977 was initiated by three impacts of lightning on high voltage lines. In 1999, hurricane Lothar caused damage to power grids in several countries, leaving hundreds of thousands of people in darkness. These examples demonstrate the vulnerability of power systems to CMCs. Current transmission networks are expected to undergo significant changes in response to developments such as increases in consumption and newly installed capacity. These changes provide an opportunity to strengthen the security of electricity supply in the perspective of extreme weather conditions and even improve the resilience of electric supply systems.

The use of the proposed methodology allows reducing the level of vulnerability by reinforcing only few points or change of the topology of the network. Faced with uncertainties about the evolution of networks and plausible extreme weather conditions, a methodology based on scenarios has been selected. The methodology allows the modeler to reproduce the complexity of the problem while still encouraging the learning process.

The core of the methodology is founded on a scenario of electric supply systems and a scenario of extreme weather events. The first scenario includes three models: electric, geographic, and reliability. The electric model comprises components of the network compatible with load flow calculations. The geographic model contains a representation of each power line in a geographic information system, and each of these lines is divided into segments that are associated with a reliability model. The reliability model evaluates failure rates related to exposure to extreme weather conditions. Scenarios of extreme weather events are built on data from weather stations or by numerical simulations implemented in a geographic information system.

A vulnerability level index is calculated on the basis of probability and severity indices of a priori possible CMCs. These probabilities are evaluated by a simulation of the interaction between the scenario of transmission network and scenario of extreme weather event. They are

---

a subjective and temporal measure of plausibility of CMCs stemming from interactions in space and time of the two systems previously mentioned. The severity index of CMCs is calculated by a contingency analysis that involves the evaluation of security limit violations. A matrix of vulnerability is constructed as a projection of the vulnerability level in two dimensions, including the lines involved in overload and those being overloaded. This matrix allows the identification of the infrastructures involved in the vulnerability and the determination of major zones of vulnerability. Countermeasures are then proposed to reduce the vulnerability of these zones, and these measures may include additions or retirement of lines or other network topology changes.

This methodology is applied to the Swiss transmission network in 2018 subject to summer thunderstorms. A reference case from 2006 is compared in terms of vulnerability to a plausible scenario of transmission network 2018. The latter includes an increased consumption of 20%, around 3 GW of pumped-storage power plants, and network changes proposed by the electricity sector plan supported by the Swiss Federal Office of Energy.

On another level, two scenarios of extreme weather events were constructed. The first is an intense thunderstorm occurring in the past, where lightning strikes were recorded by a tracking system. The second case stems from a simulation of a thunderstorm event composed of six cells passing over the Swiss territory. The vulnerability of both scenarios of electric supply system impacted by both scenarios of extreme weather events was evaluated.

Two major zones of vulnerability were detected both in the reference case 2006 and the plausible scenario 2018. They are in mountainous regions near major centers of production. The network changes between 2006 and 2018 did not decrease the vulnerability. This is due to the installation of large generation capacity and the difficulty of building lines as a result of the topography in these regions.

To reduce vulnerability, the addition of a 380 kV overhead line is proposed for the plausible scenario 2018. This line allows draining off the new hydro generation by offering a new route to major consumption centers and drastically reduces the vulnerability of the two zones mentioned. This measure illustrates the methodology's ability to identify areas of vulnerability and propose actions to increase network resilience.

One of the major contributions and innovative points of this research is the consideration of the spatiotemporal correlations of extreme weather conditions for the geographical distribution and structural resistance of transmission lines. In the application of the Swiss 2018 scenario of transmission network, the concept of major zones of vulnerability was useful in identifying the weakest zones and in finding a measure capable of increasing network resilience.

Keywords: Vulnerability analysis, extreme weather conditions, electricity power supply, contingency analysis, geographic information system

---

## Résumé de la thèse

Cette thèse est consacrée à l'évaluation de la vulnérabilité de l'approvisionnement en électricité dans des conditions météorologiques extrêmes (CME). Le système étudié est le système d'approvisionnement en énergie électrique. Les CME peuvent engendrer des contingences en mode commun (CMC) des lignes aériennes de transport qui influencent négativement la sécurité d'approvisionnement en électricité. En effet, la planification et l'opération des réseaux de transport sont soumises au critère N-1 qui impose que toute défaillance unique d'élément du réseau ne provoque pas de violation des limites de sécurité. Ce critère n'assure donc pas la sécurité d'approvisionnement lors de CME. Cette recherche vise à identifier des CMC plausibles et critiques en tenant compte des corrélations spatiotemporelles ainsi que des états possibles du réseau. Les zones les plus vulnérables sont mises en évidence pour déterminer des contre-mesures aptes à réduire la vulnérabilité.

Par le passé, les CME ont provoqué des perturbations importantes. Par exemple, le blackout de New York en 1977 a été initié par trois impacts de foudre sur des lignes à très haute tension. Plus récemment en 1999, l'ouragan Lothar a causé des dégâts aux réseaux électriques de plusieurs pays plongeant dans le noir des centaines de milliers de personnes. Ces deux exemples montrent que la vulnérabilité des réseaux électriques aux CME est réelle. D'autre part, les réseaux de transport actuels vont subir des modifications importantes pour répondre à de profonds changements comme la hausse de la consommation ou des nouvelles capacités de productions envisagées. Ces changements sont une opportunité à saisir pour renforcer la sécurité d'approvisionnement lors de CME. Une meilleure résilience des réseaux de transport vis-à-vis des CME est non seulement possible mais souhaitable.

La méthodologie proposée permet de diminuer le niveau de vulnérabilité en prenant en compte les infrastructures existantes et leurs possibles alternatives de développement. Face aux incertitudes concernant l'évolution des réseaux et des CME plausibles, une méthodologie sur base de scénarios a été retenue. Elle permet au modélisateur de restituer la complexité du problème tout en encourageant les processus d'apprentissage. Le cœur de la méthodologie a donc pour fondement un scénario du réseau électrique de transport et un scénario d'événement météorologique extrême. Le scénario du réseau comprend un modèle électrique, un modèle géographique et un modèle de défaillance. Le modèle électrique contient les composants du réseau compatible avec un calcul de load flow. Le modèle géographique contient une représentation de chaque ligne électrique dans un système d'information géographique. Chacune de ces lignes est divisée en segments qui sont associés à un modèle de défaillance. Celui-ci permet d'évaluer son taux de défaillance à la suite d'une exposition à des CME. Quant au scénario météorologique, il est construit sur la base d'informations fournies par des stations météorologiques ou à partir de simulations numériques implémentées sous un système d'information géographique.

Un indice de niveau de vulnérabilité est calculé sur la base des probabilités et des indices de sévérité des CMC a priori possibles. Ces probabilités sont évaluées par une simulation de

---

l'interaction entre le scénario de réseau et le scénario météorologique. Elles sont une mesure subjective et temporelle de la plausibilité de CMC engendrés par les interactions dans l'espace et le temps de deux scénarios mentionnés. L'indice de sévérité des CMC est calculé à la suite d'une analyse de contingence qui consiste à évaluer des violations de limites de sécurité. D'autre part, une matrice de vulnérabilité est construite comme projection du niveau de vulnérabilité sur deux dimensions, les lignes impliquées dans des surcharges et celles qui sont surchargées. Cette matrice permet l'identification des infrastructures participant à la vulnérabilité afin définir des zones de vulnérabilité. Des contre-mesures sont ensuite proposées pour en diminuer la vulnérabilité. Ces mesures peuvent comprendre des ajouts ou suppressions de lignes ou d'autres modifications topologiques du réseau.

Cette méthodologie est appliquée au réseau de transport suisse d'électricité de 2018 soumis à des orages estivaux. Un cas de référence de 2006 est comparé à un scénario du réseau plausible pour 2018. Ce dernier comprend une augmentation de la consommation de 20%, l'installation de 3 GW de centrales de pompage-turbinage et des modifications du réseau proposées par le plan sectoriel d'électricité soutenu par l'office fédéral de l'énergie. Sur un autre plan, deux scénarios météorologiques ont été constitués. Le premier reprend un cas d'orages passés très intenses dont les impacts de foudre ont été enregistrés par un système de localisation. Le deuxième cas provient d'une simulation d'un passage de six cellules orageuses sur le territoire suisse. La vulnérabilité des deux scénarios du réseau impactés par les deux scénarios d'orage a été évaluée.

Deux mêmes zones majeures de vulnérabilité ont été détectées pour les scénarios réseaux de 2006 et 2018. Elles se situent dans des régions montagneuses proches de grands centres de production d'électricité. Les modifications apportées au réseau entre 2006 et 2018 n'ont pas diminué la vulnérabilité certainement en raison des nouvelles capacités de production installées et de la difficulté de construction de lignes dues à la topographie accidentée de ces régions.

Afin de réduire la vulnérabilité, l'ajout d'une ligne aérienne de 380 kV a été proposé pour le scénario 2018. Cette ligne permet un drainage de la nouvelle production hydraulique en offrant un nouveau passage vers les grands centres de consommation d'électricité. Cette ligne diminue drastiquement la vulnérabilité des deux zones mentionnées. Cette mesure doit être considérée comme une illustration de l'aptitude de la méthodologie à identifier des zones de vulnérabilité puis de proposer des actions visant à augmenter la résilience du réseau.

La prise en compte des corrélations spatiotemporelles des CME, de la distribution géographique des lignes de transport, ainsi que de leur résistance aux CME par les probabilités de CMC est une contribution majeure et novatrice de cette recherche. Lors de l'application à un scénario du réseau Suisse en 2018, le concept de zones majeures de vulnérabilité s'est révélé utile pour identifier les zones les plus faibles et pour trouver une mesure capable d'augmenter la résilience du réseau.

Mots clés : Analyse de vulnérabilité, conditions météorologiques extrêmes, système d'approvisionnement en électricité, analyse de contingence, système d'information géographique

---

## Acknowledgments

I would like to express my gratitude to all the people who helped me during these four years of hard but inspiring work.

I would like to first thank my thesis advisor, Dr. Edgard Gnansounou, who proposed the subject of research and undertook the search for financing support. His recommendations, faultless guidance and everlasting patience allowed me to cope with the inherent difficulties related to this thesis work.

I would like to thank my colleagues Arnaud Dauriat, Dr. Abdel Lahlou, Dr. Denis Bednyagin, Luis Panichelli, Juan David Villegas Gomez, Simone Chiesa and Jairo Alexander Lozano Moreno for the moments and valuable conversations we shared.

I am grateful to Professor Hans-Björn Püttgen and Professor François Golay from EPFL, Dr. Emmanuel Marthe from Alpiq and Dr. Alain Schenk from BKW-FMB for accepting the position of referees for my thesis and acting as members of the jury.

I would also like to thank numerous collaborators from the Swiss electric industry, including BKW-FMB, Alpiq, Swissgrid and importantly, Swisselectric Research, which funded most of the project leading to this thesis. Also, special thanks to Dr. Peter Burri, Charles Moser and Dr. Patrick Braun from BKW-FMB, Dr. Stephane Gerbex, Dr. Daniel Tabara and Dr. Philippe Méan from Alpiq, Philippe Huber from Swissgrid, Dr. Martin Kauert, and Dr. Michael Paulus from SER, Dr. Rachid Cherkaoui from EPFL, for providing a wide range of services including guidance, useful feedback, and electric and geographic data.

I also thank my family and friends for supporting me during the four years of intense work. Last but not least, I want to express all my gratitude to Janice Byrd for her understanding and unconditional support during this process.

---

# Table of contents

<b>1 INTRODUCTION.....</b>	<b>1</b>
1.1 CONTEXT .....	1
1.1.1 <i>How do extreme weather events affect the security of the electricity supply?</i> .....	1
1.1.2 <i>The Swiss transmission network</i> .....	3
1.2 PROBLEM DEFINITION: VULNERABILITY ASSESSMENT AND REDUCTION .....	6
1.3 OBJECTIVES AND SCOPE OF THE RESEARCH .....	8
1.4 CONCEPTUAL FRAMEWORK OF THE METHODOLOGY .....	9
1.4.1 <i>Vulnerability, security of supply and related analysis methods</i> .....	9
1.4.2 <i>Handling of uncertainties</i> .....	12
1.4.3 <i>Geographic information systems</i> .....	15
1.5 ESSENTIAL AND ORIGINAL POINTS OF THE RESEARCH .....	16
1.6 ORGANIZATION OF THE THESIS .....	17
<b>2 STATE OF THE ART .....</b>	<b>19</b>
2.1 INTRODUCTION .....	19
2.2 PRESENTATION AND ANALYSIS OF THE THREE MAIN APPROACHES.....	19
2.3 SUMMARY .....	21
<b>3 METHODOLOGY OF THE VULNERABILITY ASSESSMENT.....</b>	<b>23</b>
3.1 INTRODUCTION .....	23
3.2 OVERVIEW OF THE METHODOLOGY .....	25
3.3 MODELS OF THE ELECTRIC POWER TRANSMISSION SYSTEM .....	27
3.3.1 <i>The electric model</i> .....	27
3.3.2 <i>The geographic model</i> .....	32
3.3.3 <i>The reliability model</i> .....	35
3.4 SCENARIO OF EXTREME WEATHER EVENT .....	39
3.5 PROBABILITY EVALUATION OF PLAUSIBLE COMMON MODE CONTINGENCIES .....	43
3.6 SEVERITY ASSESSMENT.....	46
3.7 VULNERABILITY QUANTIFICATION.....	49
3.7.1 <i>Vulnerability indexes</i> .....	49
3.7.2 <i>Matrix of vulnerability</i> .....	51
3.7.3 <i>Zones of vulnerability</i> .....	53
3.8 PROPOSAL OF SUITABLE COUNTERMEASURES.....	55
<b>4 DEFINITION OF SCENARIOS FOR THE APPLICATION TO THUNDERSTORMS ....</b>	<b>59</b>
4.1 CONTEXT .....	59
4.2 SCENARIOS OF EXTREME THUNDERSTORM EVENT .....	60
4.2.1 <i>Simulated event of an extreme thunderstorm</i> .....	62
4.2.2 <i>Real past thunderstorms event</i> .....	64
4.3 SCENARIOS OF THE SWISS ELECTRIC POWER SYSTEM .....	65
4.3.1 <i>Electric model for RS 2006 and PS 2018</i> .....	65
4.3.2 <i>Geographic model of RS 2006 and PS 2018</i> .....	68
4.3.3 <i>Hazard function of the reliability model</i> .....	70
4.3.4 <i>Reconnection rate of the reliability model</i> .....	74
<b>5 VULNERABILITY ASSESSMENT OF THE SWISS ELECTRIC POWER SYSTEM.....</b>	<b>77</b>
5.1 PERFORMING THE SIMULATIONS .....	77



---

5.1.1	<i>Main stages of the vulnerability assessment</i>	77
5.1.2	<i>Parameters of the simulations</i>	78
5.1.3	<i>Simulations</i>	81
5.1.4	<i>Sensitivity analyses</i>	83
5.2	VULNERABILITY ASSESSMENT OF THE PS 2018 IMPACTED BY THE SEWE 1	83
5.2.1	<i>Identification of vulnerable zones</i>	84
5.2.2	<i>Temporal analysis of the vulnerability</i>	87
5.3	VULNERABILITY ASSESSMENT OF OTHER SCENARIOS	90
5.4	CONCLUSIONS	92
<b>6</b>	<b>PROPOSAL OF COUNTERMEASURES TO REDUCE VULNERABILITY</b>	<b>93</b>
6.1	INTRODUCTION	93
6.2	PROPOSAL OF A MORE RESILIENT ALTERNATIVE TO THE PS 2018	94
6.2.1	<i>Reduction in vulnerability</i>	98
6.3	CONCLUSIONS	99
<b>7</b>	<b>CONCLUSIONS</b>	<b>101</b>
7.1	OVERVIEW OF THE RESEARCH	101
7.2	MAIN FINDINGS OF THE RESEARCH	103
7.3	MAIN CONTRIBUTIONS AND LIMITATIONS	104
7.4	FUTURE WORKS	105
<b>8</b>	<b>BIBLIOGRAPHY</b>	<b>107</b>
<b>9</b>	<b>APPENDIX</b>	<b>113</b>
9.1	POWER SYSTEM ANALYSIS	113
9.1.1	<i>AC power flow model</i>	113
9.1.2	<i>DC power flow model</i>	115
9.1.3	<i>Contingency analysis</i>	115
9.2	CONCEPTS FROM RELIABILITY THEORY	117
9.3	EQUIVALENCE BETWEEN THE INDEX AND THE MATRIX OF VULNERABILITY	119
9.4	SCENARIOS OF EXTREME THUNDERSTORM EVENT	120
9.5	SCENARIOS OF POWER TRANSMISSION SYSTEM	122
9.5.1	<i>Characteristics of the electric models</i>	122
9.5.2	<i>Electric schemas</i>	123
9.5.3	<i>Geographical models</i>	127
9.6	DATA OF THE REFERENCE SCENARIO	129
<b>10</b>	<b>CURRICULUM VITAE</b>	<b>130</b>

---

## List of acronyms

CMC	Common Mode Contingency
EWE	Extreme Weather Event
GIS	Geographic Information System
MZV	Major Zone of Vulnerability
RS 2006	Reference Scenario 2006
SEWE	Scenario of Extreme Weather Event
SPTS	Scenario of Power Transmission System
PS 2018	Plausible Scenario 2018
TSO	Transmission System Operator
UCTE	Union for the Coordination of Transmission of Electricity

---

## List of figures

Figure 1: Evolution of the net electricity generation for continental Europe.....	4
Figure 2: System operating states related to outages location .....	11
Figure 3: The four main stages of the methodology .....	25
Figure 4: Scenario of the power transmission system and its three models.....	27
Figure 5: Illustration of the electric model.....	29
Figure 6: Two layers of the geographic model .....	33
Figure 7: Transition in the two states model of power line l.....	36
Figure 8: Example of interpolation from 3 weather stations to a segment .....	42
Figure 9: Overview of the probability evaluation CMCs.....	43
Figure 10: The two components of the severity index .....	47
Figure 11: Overview of the vulnerability quantification.....	49
Figure 12: Methodology for suitable countermeasures proposal .....	56
Figure 13: Illustration of segment exposure to lightning strikes.....	62
Figure 14: Illustration of SEWE 1.....	63
Figure 15: Illustration of SEWE 2.....	64
Figure 16: Building of the geographic model of the RSs 2006.....	69
Figure 17: Building of the geographic model of the PSs 2018 .....	70
Figure 18: Zoom in the geographic model 2006 .....	69
Figure 19: Evaluation of number of lightning strikes with ArcInfo .....	73
Figure 20: Stages of the simulations implemented in three software .....	78
Figure 21: Numerical simulations of the unavailability under Simulink.....	80
Figure 22: Map of the vulnerable areas of the PS 2018.....	85
Figure 23: Temporal evolution of the vulnerability .....	88
Figure 24: Categorization of CMCs potentiality to threat the security of supply .....	95
Figure 25: Additional 380 kV line to reduce the vulnerability of the area A .....	97
Figure 26: Process of the contingency analysis .....	116
Figure 27: Map of lightning strikes close to transmission lines for SEWE 1 and 2 .....	120
Figure 28: Lightning impacts at 2.5 km from transmission lines for SEWE 1 .....	121
Figure 29: Lightning impacts at 2.5 km from transmission lines for SEWE 2 .....	121
Figure 30: Electric schema of the PS 2018 .....	124
Figure 31: Zoom in area A.....	125
Figure 32: Zoom in area B .....	125
Figure 33: Map of the geographic model of the RS 2006.....	127
Figure 34: Map of the geographic model of the PS 2018 .....	127

---

## List of tables

Table 1: Potential projects of hydroelectricity in Switzerland.....	5
Table 2: Issues to address before scenario creation .....	14
Table 3: Main parameters and variables required for power flow analyses.....	31
Table 4: Mathematical form of the features of the geographic model .....	34
Table 5: Cloud to ground lightning parameters .....	60
Table 6: Definition of SEWE 1 parameters .....	63
Table 7: Production, consumption and transit flows of RS 2006 for Switzerland.....	67
Table 8: Production, consumption and transit flows of PS 2018.....	68
Table 9: Calculation of the resistance factors scaled to two reference segments .....	73
Table 10: Number of outages caused by thunderstorms during four years.....	75
Table 11: Definition of the main parameters of the simulation .....	81
Table 12: Maximum number of CMCs vs. investigated CMCs.....	81
Table 13: Selected results of the contingency analyses .....	82
Table 14: Vulnerability index for the PS 2018 and the SEWE 1.....	84
Table 15: Matrix of vulnerability and MZV 1 and 2.....	86
Table 16: Zonal vulnerability ratio.....	87
Table 17: Temporal matrix of vulnerability at 60 minutes .....	89
Table 18: Zonal vulnerability ratio at 60 minutes .....	89
Table 20: CMCs as low and high threats .....	95
Table 21: Reduction of vulnerability by the SVALLO1A-FCORN11A line .....	98
Table 22: Number of elements of the AC flow model.....	122
Table 23: Installed capacity in Switzerland (> 100 MW) .....	122
Table 24: Comments on the electric schemas of the PS 2018 .....	126
Table 25: Statistics of the geographic models.....	128
Table 26: Attributes of fifth first lines of the geographic model 2006 .....	128
Table 27: Attributes of six first segments in the geographic model 2006.....	128
Table 28: Estimation of the average unavailability.....	129
Table 29: Normalized vulnerability of the reference scenario.....	129

---

“When one admits that nothing is certain one must, I think, also admit that some things are much more nearly certain than others.”

Bertrand Russell (1872 - 1970), British philosopher, logician and essayist

“No model is absolutely correct. In particular situations, however, some models are more useful than others.”

George E.P. Box (1919), British statistician



---

# 1 Introduction

## 1.1 Context

### *1.1.1 How do extreme weather events affect the security of the electricity supply?*

Extreme weather events are considered to be major threats, even for our modern society. Despite the high level of protection procured by sophisticated engineering techniques, extreme weather conditions are still able to disturb the smooth running of vital energy infrastructures. In particular, the electricity system, including production and transmission, has failed numerous times in the past because of natural hazards. Extreme weather conditions are the strong expressions of variability of the atmospheric system. According to Beniston (2004), no single definition is found in the literature. However, the following two definitions are most often encountered:

- Their frequency of occurrence is low. The Intergovernmental Panel on Climate Change agrees in its third assessment report (IPCC, 2001) that extreme weather conditions are referred to as occurring above the 90<sup>th</sup> percentile of a statistical distribution of precipitation, wind speed, and other key characteristics.
- They are intense and able to cause large human losses and/or significant economic costs

The intensity of extreme weather conditions is one factor that accounts for their capacity to cause disruptions in electric power systems. Their rarity and variability are other factors that impede a total protection of energy infrastructures. Failures of elements of those systems are more likely during extreme weather conditions than during normal weather conditions. Therefore, extreme weather conditions are threats to the security of the electricity supply. The working group of the security of the electricity supply of Eurelectric proposes a relevant definition for this research:

"The ability of the electrical power system to provide electricity to end-users with a specified level of continuity and quality in a sustainable manner." (Eurelectric, 2004)

In a secure power system, the demand of electricity is continuously and sustainably assured by the appropriate level of production. Moreover, the transfer of energy from power plants to end-users is also and sustainably assured by transmission and distribution networks. Transmission networks are characterized by their large transport capacity of very high voltage overhead power lines connecting large power plants to main centers of electrical consumption. These networks are meshed to assure minimal resilience in case of components failures.

Distribution networks connect transmission networks and power plants of smaller capacity to end-users. These networks are composed of overhead power lines and buried cables with a

---

decreasing redundancy as their voltage diminishes.

Extreme weather conditions are able to unbalance production and consumption or impede electricity transmission in both types of networks. This research focuses exclusively on transmission networks, which have been the source of large disturbances during past extreme weather conditions.

Large electricity disruptions or blackouts are often consequences of successive minor failures. According to Makarov et al. (2005), it generally starts with initial overhead power line breakdowns due to extreme weather conditions. Most of the time, these breakdowns are contained because of the natural resilience of meshed network. In certain unpredictable conditions, initial breakdowns are amplified by hidden failures in protective systems or accident-prone operations, which lead to cascading failures and blackouts. The following two examples give more insight into these phenomena.

The New York blackout of 1977 plunged 9 million people into darkness for up to 26 hours (Corwin and Miles, 1979). Lightning struck three overhead transmission lines during a thunderstorm event. Several power lines tripped off in less than an hour leading to the slow islanding of New York. Power generation had to be reduced to alleviate the overload of power lines while consumption was still high. The system finally collapsed because of the inadequacy of production and consumption.

This example shows the phenomenon of cascading failures. When preconditions are present such as high load or power line maintenance, a few power line failures can precipitate a whole system to ground. A sequence of unpredictable and highly unlikely failures can lead to a blackout. Once a blackout sequence is initiated, a dramatic outcome is generally unavoidable. This thunderstorm event was not considered extreme in intensity, but it was intense enough to trigger three simultaneous outages of transmission lines. In this example, the space-time patterns of the thunderstorm cells played a great role in the dangerousness of this event.

In December 1999 in Western Europe, hurricanes Lothar and Martin caused billion of euro in damages. The French electric power system in particular suffered from these two intense winter storms. According to Piketty et al. (2000), the cost of damages for Electricité de France was estimated at around 1.5 billion euro. The costs stemmed primarily from repair and reconstruction at the distribution network level (86%), the transmission network (11%) and generation (3%). Around 415 million kWh were not supplied in time, mostly by the distribution network (73%). The cost of the energy not supplied for the consumers was estimated at 4.1 billion euro.

The distribution network was responsible for the majority of the damage costs and for the energy not supplied. Most of the French distribution network was composed of overhead power lines, which are less resistant than transmission lines, and their limited height fosters hazardous interactions with vegetation.

At the transmission network level, most of the damage was recorded in eight circuits. The foundations of the pylons were responsible for the majority of the outages. The under sizing of these infrastructures has been deemed as the main cause of failure. It is mentioned in



---

Piketty's reports that the transmission network would have been responsible for a large proportion of the energy not served if the load was higher at the time of the two hurricanes. Indeed, thousands of fugitive failures were recorded. They could have triggered cascading failures in a more heavily loaded system. These two hurricanes are perfect examples of extreme weather events because their return period is estimated at around 100 years and they provoked billions of euros of losses for society.

They are representative of the capability of extreme weather conditions to endanger the security of the electricity supply. They demonstrate that most of the costs stem from energy not supplied in time, not from physical damages to infrastructures. Although distribution networks are vulnerable in case of widespread extreme weather conditions such as hurricanes, transmission networks are prone to cascading failures having the capacity to propagate to a large portion of the system. Distribution networks can be extensively cabled while transmission networks cannot at reasonable costs. These networks are resilient up to a critical point where they exhibit chaotic behaviors (Dobson, 2002). Even, two simultaneous and fugitive outages can lead to huge blackouts.

Simultaneous outages triggered by the same cause are named common mode contingencies (CMCs). Initial outages can cause violation of security limits, such as overloads or inadmissible voltage deviations, turning into an uncontrolled series of disconnections. This phenomenon of cascading failures is responsible for the biggest blackouts recorded in the past 50 years (Carreras et al., 2004). Because cascading failures are highly unpredictable, everything should be made to avoid entering these hazardous sequences of disruptive events. It is worth mentioning that extreme weather conditions are not the only factor which endangers the security of the electricity supply. The cause of vulnerability is multifactorial including, but not limited to, such issues as high consumption, ageing infrastructures, and disrespect of operational rules (Novosel et al., 2004).

In conclusion, extreme weather conditions may endanger the security of the electricity supply at the level of transmission networks by means of cascading failures. Once they are unleashed, they are difficult, if not impossible, to stop. Therefore, it is important to thoroughly plan transmission networks to reduce the likelihood of violation of security limits in case of plausible CMCs. Especially at the planning stage, it may be preferable to build more resilient transmission networks.

### *1.1.2 The Swiss transmission network*

Understanding the context of the electric power systems under investigation is essential to assessing why they are vulnerable and what measures can reasonably be undertaken to reduce vulnerability. Since the methodology of vulnerability assessment is applied to the Swiss case, the focus is given specifically to the Swiss transmission network interconnected to the European Transmission Network. Factual information is presented in the next paragraphs as well as possible future developments relating to those two transmission networks.

The European transmission network spread across 34 countries and was managed by 42

transmission system operators integrated in 2008 in the association named European network of transmission system operators for electricity. This network is divided into several regions, and the most important is the continental Europe region, formerly named UCTE. For the year 2008, the statistical year book for the continental Europe region mentions that the net electricity generation reached 2643 TWh after a long increasing trend of more than 25 years (ENTSO-E, 2008).

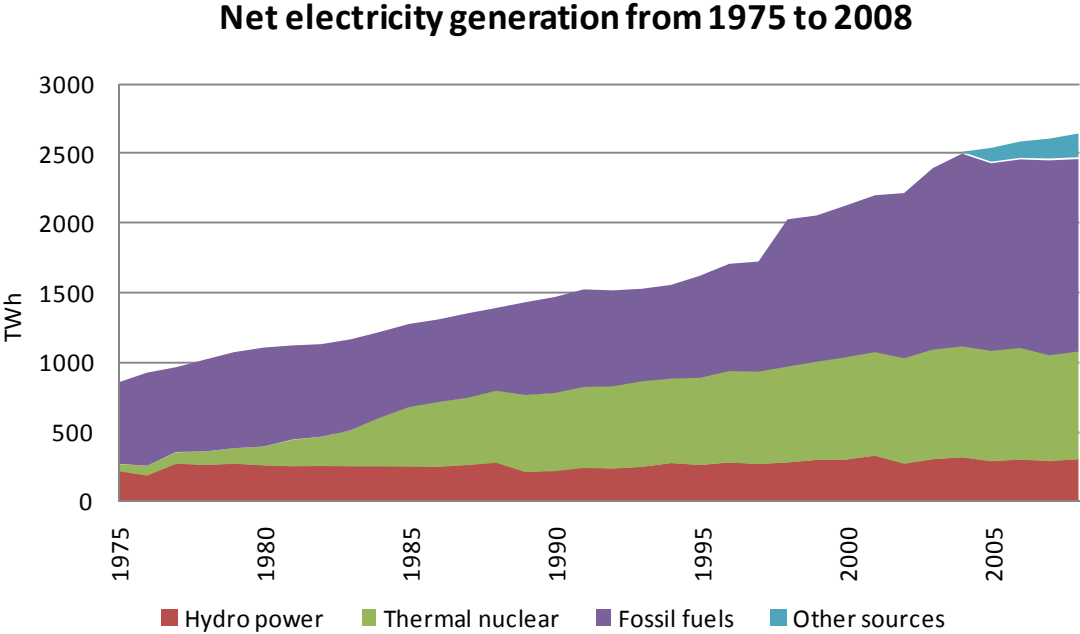


Figure 1: Evolution of the net electricity generation for continental Europe

Generation is constantly rising from 1975 to 2008 to meet ever growing demand. The sudden raise in 1998 and 2003 is due to the integration of former Eastern European countries in the continental Europe region. As seen in Figure 1, the other resources category has been rising since 2005. It is primarily constituted of renewable energies such as wind power, which was counted in the fossil fuels category. From the beginning, generation adequacy has been essentially met by thermal nuclear and fossil fuels energy sources. This fact will certainly remain true in coming years, even if the installed capacity of renewable energy is augmented. Green energy is one of the priorities of the European energy policy along with competitiveness and security of supply of the electricity sector (CEC, 2006).

Growing concerns regarding greenhouse gases and their potential effects on climate change positively influence the share of renewable energy in the generation mix. According to the report on system adequacy forecast from 2010 to 2025 (ENTSO-E, 2009b), the installed capacity of wind farms could reach in 2020 about 21% of a total of 878 GW net generating capacity. After 2020, the expected wind power capacity in Europe is likely to foster cross-border exchanges, and thus, exacerbate the current zones of congestion (Van Hulle, 2009). Indeed, much of the present transmission infrastructure was built in the 1950s and 1960s (Silvast and Kaplinsky, 2007). At this time, national monopolies were the rule of thumb where each country had a primary objective to supply its own load by conventional productions. Interconnection power lines were used to guarantee the security of supply in

case of shortages or generation breakdowns. Since the EU liberalization of electricity, exchange between countries has raised and is even encouraged by the European Council (CEC, 2007). Major investments in the European transmission network will take place in coming years to help ensure the security of the electricity supply, international energy exchanges and the integration of renewable intermittent energy sources.

Switzerland shows similar trends regarding its ageing transmission infrastructures and rise in consumption. However, its topography enables hydro energy instead of wind energy. In 2008, 55% of Swiss generation stemmed from hydro power, the rest being generated by thermal nuclear power plants (40%) and conventional thermal power plants (5%) (OFEN, 2009c). On an annual basis, Switzerland exports more electricity than it imports. In general, Switzerland imports electricity during off-peak hours and exports during peak hours because of its high hydro power capacity. According to the Swiss association of electricity, the constant rise in consumption combined with the difficulty of building new power plants of large capacity in the territory could lead to electricity shortages beginning in the winter of 2020 (AES-VSE, 2006). Nevertheless, this potential shortage is unlikely to happen because of several projects of gas-fired power plants in the short term, and the possible construction or renovation of nuclear power plants. Therefore, generation adequacy appears to be secure, at least for the next decade.

By contrast, the network adequacy is certainly more at risk. The Swiss transmission network has not been significantly upgraded over the past decades. However, consumption has doubled in less than forty years, and power transits through Switzerland have also increased (OFEN, 2009c). Importantly, around 3.6 GW of pumped-storage power plants are under construction or will be commissioned between 2010 and 2020. Information regarding these new power plants has been gathered from experts and other sources, but the actual realization of these projects is not yet certain.

Table 1: Potential projects of hydroelectricity in Switzerland

<b>Name</b>	<b>Type</b>	<b>Installed capacity [MW]</b>	<b>Total</b>
Bieudron	Hydro-turbine	1200	
Handeck	Hydro-turbine	90	
Innertkirchen	Hydro-turbine	170	1460
Nant de Drance	Pumped-storage	600	
Nestil	Pumped-storage	140	
Grimsel	Pumped-storage	400	
Linthal	Pumped-storage	1000	2140
	<b>Total</b>		<b>3600</b>

These installations will not significantly augment the generation adequacy level. Their main purpose is the trade of electricity with neighboring countries during peak hours. Equally important, they could store the surplus of intermittent European production such as wind energy. However, the Swiss transmission network has to be developed to withstand additional electricity generation and transit. The transmission lines and supply security workgroup

---

proposed the implementation of 39 modifications prior to 2015 (TLSSW, 2007). It has acknowledged the necessity of upgrading the network to its future environment. Existing overhead power lines of voltages over 220 kV are considered a strategic interest for the country. Important financial resources will be committed in development projects assuring the following objectives:

- Adaptation to the global rise in consumption and changes of load patterns
- Connection of new or upgraded power plants or better connection with lower voltages network
- Reduction of bottlenecks
- Respect of the N-1 security criteria in normal conditions (also in case of maintenance and outages)
- Interconnection to the European transmission network
- Modification of overhead power line paths aged more than 50 years

All these modification are integrated within the frame of the transmission lines sectoral plan. It sets out “*demand and corridor variations for transmission line projects, identify conflicts and find solutions for resolving them, and determine the most suitable corridor for planned transmission line construction projects*” (OFEN and ARE, 2001). Therefore, this plan sets the milestones for the development of the Swiss transmission network, and supports its improvements through the approval process.

To conclude, massive investments supporting major network changes are expected to follow the growing demand, integrate intermittent renewable energies, and allow increasing energy exchanges while guarantying an appropriate level of security of the electricity supply. This situation is ideal for the integration of measures aiming to reduce the vulnerability during extreme weather conditions. Since the development plan of the Swiss transmission network is still under construction, resilient alternatives could be suggested based on a novel vulnerability assessment methodology. Alternative scenarios of this network would meet the objectives mentioned here above with low level of vulnerability during extreme weather conditions.

## **1.2 Problem definition: Vulnerability assessment and reduction**

Extreme weather conditions can endanger the security of the electricity supply by leading electric power systems to disturbed states. One of the most fragile subsystems is transmission networks, which are directly exposed to adverse and extreme meteorological conditions. Although overhead power lines are designed according to strict standards, failures are still possible. A particular type of failure, namely CMCs, is more likely than under clement weather. Electric power systems are prone to large disturbances in case of CMCs at the transmission systems level. They are planned and operated to withstand single contingencies according to the N-1 criterion. Cascading failures triggered by initial CMCs related to extreme weather conditions cause large disturbances. Lasting CMCs can also impede

---

electricity supply at regional scales by cutting vital electricity paths. At the planning stage, appropriate counter-measures have to be identified to reduce the vulnerability of weak zones in the network.

Suitable countermeasures should assist in alleviating plausible violation of security limits caused by CMCs. Plausible and severe CMCs have to be identified to efficiently reduce vulnerability. Plausibility is a function of the space-time correlations of extreme weather events, the geographic distribution of transmission lines and their physical resistance. Severity is a function of violation of security limits stemming from the limited ability of transmission networks to transfer power in degraded states. All underlying features of CMCs are very dependent on the states of the electric power system and on particularly of extreme weather events under investigation.

The problem is addressed by the following points:

- What are the relevant models of power transmission systems impacted by extreme weather events in the context of the vulnerability analysis?
- How are plausible and severe CMCs identified?
- How to assess vulnerability and locate the weak zones of the network?
- What countermeasures can be proposed to reduce vulnerability?

A novel methodology of vulnerability assessment combining space-time models of electric power systems and extreme weather conditions is required in order to answer these questions. This methodology should first be able to model the two studied systems and their interactions. Numerous models exist for power transmission systems from full dynamic simulations to linearized static analysis (Tleis, 2008). For planning purposes, AC power flow supporting contingency analyses is an appropriate model to determine CMCs severity (Stott et al., 1987). It allows taking into account all major network components such as generation, loads, transformers and power lines. Any past or future transmission systems can be simulated taking into account their possible components failures.

Nevertheless, AC power flow model is not designed to integrate space-time extreme weather event models and their plausible CMCs. GISs are able to store and process spatiotemporal information related to extreme weather events and geography of the transmission lines path (Snaider, 2005). The space-time interactions between extreme weather events and transmission lines strongly influence the plausibility of CMCs. The mechanical resistance of overhead power lines is also an important factor in determining plausibility. Fortunately, reliability theory contains the appropriate concepts to derive probability of component failures from their exposure to forces of nature. In summary, theories and tools exist to tackle all the sub-problems for identifying plausible and severe CMCs. However, they have not been integrated in a single coherent framework, which is one of the main challenges of this research.

Vulnerability analyses aim at finding weak infrastructures or critical situations in order to propose possible actions to decision makers for diminishing weaknesses and criticality. Consequently, vulnerability gauges have to be established to assist decision makers. An overall vulnerability index is necessary to compare different cases of transmission networks

---

or extreme weather events. More importantly, weak zones of the network have to be located to propose countermeasures to reduce the vulnerability.

To conclude, this vulnerability assessment taking into account space-time correlations of extreme weather events entails integration of existing concepts into a single framework. They have to be adapted, developed or created to handle interacting systems that have not been explicitly coupled previously. This systemic approach aims at a better understanding of the mechanisms jeopardizing the security of the electricity supply face to extreme weather events.

### **1.3 Objectives and scope of the research**

This research aims at establishing a methodology of vulnerability assessment for power transmission systems impacted by extreme weather events. The interactions of these two systems induce specific sets of plausible and severe CMCs, which are located in well demarcated areas. Few of them account for most of the vulnerability, which define the concept of major zones of vulnerability. Finally, countermeasures are proposed to reduce the vulnerability of these zones. The four main objectives of this research are detailed below.

- Determine the plausibility of CMCs
- Evaluate the severity of CMCs
- Locate major zones of vulnerability of power transmission systems
- Propose countermeasures for major zones of vulnerability

The development of the methodology undergoes several sub-objectives and constraints to assure coherence and originality.

First, power transmission systems and extreme weather events are modeled as scenarios. They take into account the complexities and uncertainties inherent in complex systems. Scenario-based modeling is a technique fostering discovery processes regarding the systems under investigation as well as non-linear thinking. It enables modifications and improvements when new information is available, and is a recommended technique, particularly when anticipating the possible future states of a system. However, scenario building is a time-consuming procedure limiting their number to a few.

Second, the evaluation of the plausibility of CMCs has to take into account the space-time correlations of extreme weather conditions, the geographic distribution of transmission lines and their physical resistance to weather exposure. This is a key sub-objective since most of the existing methodologies oversimplify spatiotemporal dimensions. The depth of modeling has to be associated with the final objective of proposing countermeasures for major zones of vulnerability. A model that is too simple would not correctly handle the spatiotemporal dynamics of CMCs. On the other hand, a model that is too complex would be intractable regarding available data and computational time.

Then, the vulnerability is assumed static or structural stemming from direct violation of security limits. It entails that dynamic phenomena of power transmission systems are not

---

taken into account. It is assumed, after CMCs, that the transmission system converges to a steady state functioning without further component disconnections regardless of the possible violation of security limits. Therefore, protection systems, operator maneuvers or subsequent cascading failures are not taking into account in the vulnerability.

Finally, countermeasures are proposed to improve the structural resilience of power transmission systems without explicitly considering other forms of constraints such as cost, acceptability or feasibility. Nevertheless, countermeasures have to follow guidelines which assure that they are not unrealistic. This research aims at offering possible countermeasures to decisions makers who are entitled to evaluate their suitability.

## 1.4 Conceptual framework of the methodology

This chapter introduces the main theories on which the vulnerability assessment methodology is based. First, the relationship between vulnerability and the security of the electricity supply is clarified and some standard analysis tools are presented. Second, the way of handling uncertainties inherent to interacting power transmission systems and extreme weather events is explained. Finally, light is shed on the added value of GIS for space-time vulnerability assessments.

### 1.4.1 *Vulnerability, security of supply and related analysis methods*

The concepts of vulnerability and the security of the electricity supply are closely related since they can be considered in a broad sense as antonyms. Put another way, the security of supply is not guaranteed in vulnerable electric power systems. For a more thorough comprehension, these terms need to be more precisely defined. Their definitions are manifold in the literature, though they have a common basis. The report on the vulnerability of the Nordic power system provides a pertinent statement (Doorman et al., 2004).

**Vulnerability:** “The vulnerability is an expression of the system’s lack of ability or reduced ability to withstand an unwanted situation, limit the consequences, and to recover and stabilize after the occurrence of the situation.”

On the other hand, the security of the electricity supply is guaranteed if it respects two principal criteria, the system adequacy and security. The North American electric reliability corporation proposes suitable definitions of these two criteria in (NERC, 2008).

**Adequacy:** “The ability of the bulk power system to supply the aggregate electrical demand and energy requirements of the customers at all times, taking into account scheduled and reasonably expected unscheduled outages of system elements.”

**Security:** “The ability of the bulk power system to withstand sudden disturbances such as electric short circuits or unanticipated loss of system elements from creditable contingencies.”

---

The adequacy can be understood as the ability of the bulk power system to continuously supply energy to users in normal conditions. Therefore, the access to primary fuels and a sufficient installed generation capacity is ensured to meet demand. Normal conditions also include overhauls and likely outages which can be encountered on a regular basis. The adequacy criterion is not relevant to this research since it involves extreme weather conditions.

The security is related to the ability of the bulk power system to minimize the consequences of unpredicted loss of several power plants or transmission lines. These situations are rare and have potentially disastrous results. Outages can be correlated by common causes such as droughts for reduced hydro generation or storms for overhead line outages. A total immunity to unpredicted losses is conceivable, but not likely to be achievable at a reasonable cost. A list of outages that a system should withstand without violating the security criterion is usually defined by official standards. Among international standards, the North American reliability standards (NERC, 2010) and the operation handbook of the ENTSO are two examples (ENTSO-E, 2009a). According to these definitions and in the context of extreme weather events, the security of the electricity supply is not guaranteed when weather-related disturbances are not withstood by the power system. In this case, the system is considered vulnerable. The first step of a vulnerability assessment consists of finding the conditions in which the security of the electricity supply is endangered. If the system under investigation is a power transmission system, plausible CMCs are those sought conditions. The next step is to understand how CMCs endanger the security of supply which lead to the appropriate methods to assess vulnerability. The concept of four system operating states proposed by Fink and Carlsen (1978) is a good start to answer this question, and the following schema is inspired by his work.



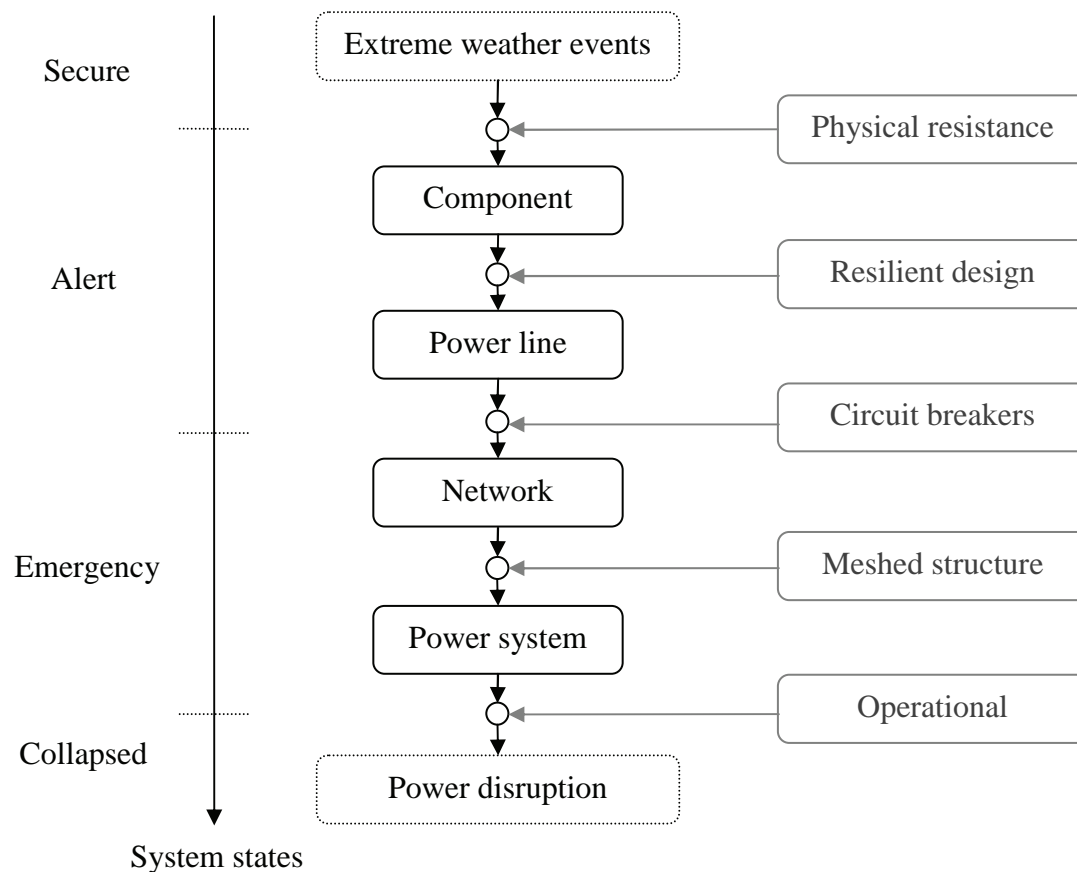


Figure 2: System operating states related to outages location

The schema shows the operation system states related to the location of outages in the power transmission systems caused by extreme weather events. Examples of barriers impeding outages are detailed on the right. Component malfunctions or damages entail an alert state, which signals a precursor for potential larger problems. If temporary malfunctions caused the disconnection of power lines, auto-reclosing circuit breakers are usually able to stop the creeping outages. On the contrary, lasting power lines unavailability can potentially trigger other outages in the network. It is worth mentioning that these states should be considered with fuzzy rather than strict borders. The meshed structure of power transmission systems has a limited resilience which can be overcome by a sufficiently high number of simultaneous outages. The electric power system is thus in an emergency state, which is the step just prior to power disruptions.

This bottom-up vision of outages creeping through the system allows illustrating the different analysis methods available. At the components and power line levels, classical reliability theory is able to cope with the modeling of outages mechanisms. From the network level, electric models of the system are necessary. These models are numerous as well as their ability to account for dynamical phenomena taking place in alert and emergency states. The task force for understanding, predicting, mitigating and restoring cascading failures gives a comprehensive review of the existing techniques in Baldick et al. (2009). Since the objective of this research aims at studying the static vulnerability, a steady-state modeling such as an AC power flow model used by contingency analysis is satisfactory. It computes

---

the state of the system in terms of the power flows and voltages provoked by single failures of elements, or CMCs as well. Therefore, transients or other dynamic phenomena are excluded from this steady state analysis. More sophisticated methods have been developed to take into account cascading failures and possible mitigation measures such as implemented in TRELSS, which is an industrial tool (Zhang, 2003).

Contingency analysis is a suitable method for quantifying static or structural vulnerability of power transmission systems. This leads to the identification of zones of vulnerability, which are very important in order to locate proper countermeasures. However, contingency analysis requires a list of CMCs triggered by extreme weather events, which has to be provided by other methods. Reliability theory allows identification of likely component failures exposed to extreme weather conditions, which can be modeled under GIS.

To conclude, structural vulnerability is only one component jeopardizing the security of the electricity supply. The elimination or reduction of zones of vulnerability is a way of improving the security of the electricity supply during extreme weather conditions. Structural resilience, the opposite of structural vulnerability, is a planning topic, which can prevent hazardous dynamical phenomena such as cascading failures.

#### *1.4.2 Handling of uncertainties*

Electric power systems are wide-scale complex infrastructures. They encompass hundreds of kilometers of power lines, thousands of power plants and consumers interacting together. The future development of these systems involves uncertainties. For example, the rise in consumption, new production infrastructures, and regulatory framework are not yet known. Complexity and uncertainty challenge any attempt of complete modeling. At the time of vulnerability analysis, these two features have to be addressed with the appropriate methods.

Uncertainty can be separated in two fundamental categories (PateCornell, 1996). The first one is the subjective or epistemic uncertainty, which stem from incomplete knowledge of the modeler (Ferson and Ginzburg, 1996). This uncertainty stemming from ignorance can usually be reduced by additional studies. In contrast, aleatory uncertainty arises from variability of underlying processes. This uncertainty is labeled objective since this variability is considered as a property of the object under study. In this case, no further investigation can reduce uncertainty. This taxonomy can be further expanded, such as in Klir and Smith (2001). The body of literature on the uncertainty modeling subject is important and still growing in complexity. However, the key point is to recognize these two different types of uncertainty occurring at the time of system modeling.

A priori, these two types of uncertainty are present in the modeling of electric power systems and extreme weather conditions. These uncertainties induce a tremendous number of plausible futures or states. The right methods have to be selected to cope with these difficulties without oversimplifying the problem. In this research, it is assumed that ignorance about the studied systems is far more prevalent than variability uncertainty. Indeed, the problem in the vulnerability assessment of present or future power transmission

---

systems impacted by extreme weather events encompasses an overwhelming interacting number of elements, which limits the possibility for a modeler to totally know these systems. Two approaches are preferred to deal with epistemic uncertainties related to this vulnerability analysis.

The first approach is constituted by scenario-based thinking or scenario-based planning dealing with plausible descriptions of prospective systems. This method allows building credible models of the world under conditions of uncertainty. Scenario-based thinking allows the structuring of flexible and complex long term plans, where scenarios are crafted based on a combination of many factors, which are likely to influence the system under scrutiny. Scenario-based thinking consists of the construction of scenarios, which are a consistent view of what the future might be, knowing it is not a prediction but only one possible future. This method copes with vague and fragmentary knowledge of reality (i.e a form of epistemic uncertainty). Scenario-based thinking has been used for decades for military intelligence, by experts in business strategies and in many scientific fields (Varum and Melo, 2010). The general methodology of scenario-based thinking is exposed, among other sources, in (Ringland, 2006). Adapted to this vulnerability analysis, the overall process can be summarized in the following points.

1. Define the objectives of the analysis
2. Identify relevant drivers for change and issues to address regarding the objectives
3. Establish a coherent framework for generating plausible and pertinent scenarios
4. Analyze scenarios and interpretations of outcomes

Two types of scenarios generated in this study are for power transmission systems and extreme weather events. The former contains all relevant parameters of the vulnerability analysis such as load flow models, spatial traces of overhead power lines, or mechanical resistance under weather related loads. This information is collected from electrical utilities or from grid operators. Scenarios of extreme weather events are spatiotemporal representations based on past events as measured by meteorological stations or computer-based simulations. By their way of construction, these scenarios are considered plausible. They are built based on available information found during a collecting stage, expert's knowledge or simply reasoning. The following table details some issues to address before the construction of power transmission systems and extreme weather events scenarios.

Table 2: Issues to address before scenario creation

**Power transmission systems**

**Extreme weather events**

Rise in consumption, new infrastructures of transmission, limit of the electric power system, new power plants, market liberalization, renewable and intermittent source of energy, ageing of infrastructures, regulatory framework, planning and operational rules,...

Which hazardous conditions to consider, effect of climate change, season/time of the analysis, number of scenarios, past or simulated events, source of data,...

The second approach relates to the subjective probability or Bayesian interpretation of the concept of probability. Subjective probability measures the state of knowledge (Jaynes, 2003) as opposed to the objective probability measuring a frequency. Subjective probability is used to quantify the degree of belief one has with respect to assumptions or statements, in our case, the probability of CMC occurrence. Indeed, they are not included in the power transmission systems scenarios. Space-time simulations evaluating their subjective probability to occur at a given time identify plausible CMCs. The evaluation of the probability of CMCs is based on reliability theory, which is a branch of statics. This theory has been successfully applied for decades in many engineering areas such as risk analysis, quality management or optimization of maintenance and operation. Reliability analysis provides a strong conceptual basis and decades of development in the power system field (Stanton, 1969).

In the rest of this document, subjective probability is mentioned as probability to simplify the writing. In the same way, plausible is used interchangeably with probable. Nevertheless, one has to keep in mind that plausibility has several other definitions (Van der Helm, 2006). In particular, one has to differentiate the meaning of plausibility given here to the one related to Dempster–Shafer theory a mathematical theory of evidence (Shafer, 2009).

In conclusion, epistemic and aleatory uncertainties should be recognized. The latter is due to the lack of knowledge or ignorance of the modeler, and the former is considered an inherent property of the system. This classification is not unique, although some argue that this distinction is pointless and only epistemic uncertainties should be considered (Winkler, 1996). In this research, the latter type is omnipresent. Consequently, two approaches dealing suitably with the lack of knowledge are used in this vulnerability analysis. A method based on scenarios is employed to model power transmission systems and extreme weather events. It allows non-linear thinking, modeling of plausible and prospective systems, readable updating of parameters and fostering of the learning process. However, plausible CMCs of transmission lines are derived from scenarios by simulations mostly based on reliability theory. Subjective probability quantifies the belief that a CMC occurs at a given time. It is worth mentioning that subjective probabilities respect the axioms of the classical objective probability theory. The former interprets randomness in nature into lack of knowledge for the modeler.

---

### 1.4.3 Geographic information systems

This chapter aims at succinctly presenting relevant concepts of GIS for this research. An introduction to this large field of studies and applications is exposed in many publications such as in (Harvey, 2008). GIS is designed to store, analyze, manage, and present spatial data. It is extensively used in numerous domains such as cartography, geography or territory planning. The potential applications are tremendous with the continuous rise in computing capabilities. The “S” of GIS refers to systems or sometimes to science depending on the context and authors. GIS does not refer directly to specific software as often thought. A paper map could be considered a GIS. Chrisman gives the following definition of GIS as well as how GIS is currently defined in scientific literature.

*“Organized activity by which people measure and represent geographic phenomena then transform these representations into other forms while interacting with social structures.”* (Chrisman, 1999)

From a more practical point of view, most of the current GIS are constituted by maps and databases implemented on computers. Maps are composed of layers, which represent different types of spatial data defined in a coordinate system. There are essentially three types of layer features including points, lines and areas. These geographic features are linked to their attributes containing relevant information. For example, a house can be modeled by a polygon linked to its ground surface and number of stories.

Topology is also an important characteristic of GIS. Topology describes how geographic features are related, such as a river and its banks. All this information is stored in (geo)databases. Data management systems control the consistency of the geodatabases to assure proper functioning even for large systems and frequently updated multi-users platforms. One of the key capabilities of GIS is the ability to perform analyses on geographic data. The list of analyses is long, but an overview is detailed below.

- Map retrieval, generalization, abstraction
- Layers overlay
- Data querying taking into account spatial information
- Measurements of length, surface and angle
- Digital terrain and network analyses

Standard analyses are built-in functionalities grouped in toolboxes as in the software used in this research, which is ArcInfo (ESRI, 2010a). For a brief but complete overview of GIS, the article of Cox and Grifford (1997) is appropriate. GIS presence has been growing for decades in many academic domains such as environmental sciences and ecology, engineering, computer science, geography or agriculture, and this trend is accelerating.

In the context of vulnerability assessment, GIS has a key role when spatial information comes into play. These assessments relate to natural or man-made related hazards such as seismic, air and water pollution, wildfires, and landslides. Nevertheless, very few

---

publications concern power transmission systems impacted by extreme weather events. One representative example of the recent publications on the subject is made when estimating the spatial distribution of outages due to hurricanes (Han et al., 2009). However, the dynamic of extreme weather events is not explicitly taken into account. In fact, dynamic is difficult to model in GIS because it is more oriented to the modeling of static phenomena. One explanation could be that the core business of GIS is dealing with static maps and analyses. GIS is widely spread in many scientific fields, however, vulnerability assessments related to electric power systems and GIS are not common. Moreover, the space-time dimensions cannot always be adequately handled by GIS. Therefore, the identification of CMCs taking into account space-time correlations is challenging.

In this research, GIS is used to model paths of transmission lines and extreme weather events which are well stored as maps or successive maps to simulate the passing of time. At the time of crafting these models, GIS is suitable or sometimes necessary for dealing with complex infrastructures or natural entities spreading on large scales. GIS enables the visualization and interaction with the models for fast and proper modifications. Nevertheless, the GIS environment is not explicitly used for space-time simulations. They are carried out in Matlab which has some built-in GIS capabilities. Although GIS allows sophisticated analyses, a temporal geographic information system could perform simulations that would be valuable in numerous fields.

## **1.5 Essential and original points of the research**

There are a number of essential points of this research, which are highlighted in the following paragraphs.

The vulnerability assessment is supported by scenario-based approach of power transmission systems and extreme weather events. This approach allows the modeling of complex systems subject to uncertainties. Scenario-based thinking allows the vulnerability assessment of future situations, which could be very different than those encountered in the past. Plausible scenarios of power transmission systems and extreme weather events can be built for any future timeframe, and for any imaginable power systems or weather conditions.

The level of vulnerability of electric power systems is measured by an aggregated index combining probability and severity indexes of CMCs. The probability is evaluated by space-time simulations taking into account the geographic distribution of transmission networks, the space-time correlations of extreme weather conditions, and the time dependent processes of power line failures and reconnection. The severity is related to exceeding security limits, namely transmission line current overloads and buses voltage deviations. The severity is evaluated by contingency analyses based on an AC power flow model taking into account the most important components of electric power systems such as power plants, transmission networks, transformers, security systems and loads.

The concept of matrix of vulnerability highlighting the major zones of vulnerability is derived from the aggregated index of vulnerability. Major zones of vulnerability are basically

---

a projection of the vulnerability index onto the infrastructures participating in CMCs and those which exceed security limits. Major zones of vulnerability identify the transmission infrastructures participating in the vulnerability to facilitate an effective search of countermeasures.

Countermeasures are proposed for major zones of vulnerability to reduce the vulnerability, and also aim to improve the structural resilience of power transmission systems by adding or modifying power lines, and/or changing network topology. These countermeasures provide complementary alternatives to existing development plans of electric power systems.

The evaluation of CMCs probability taking into account the dynamic of interactions of transmission infrastructures with extreme weather events is certainly an original point. This would not have been possible without the use of GIS combined with simulations supported by reliability theory. This combination is rare in the scientific literature, at least for the vulnerability assessment of large scale systems.

Furthermore, the geographic model of transmission lines is coupled with its electric model. It allows the calculation of relevant states variables of electric systems to evaluate structural vulnerability. The traditional network planning tool of contingency analysis is used to evaluate the severity of CMCs. However, the set of plausible CMCs is either issued from deterministic or probabilistic methods that do not take into account the space-time correlations of extreme weather events, geographic distribution of overhead transmission lines or their physical resistance. Consideration of these three points provides a more realistic vulnerability assessment during extreme weather events.

## **1.6 Organization of the thesis**

This core of this thesis is divided into five chapters as detailed below.

Chapter 2 discusses the three most relevant approaches of existing methodologies of vulnerability assessment. Strengths and weaknesses of the three approaches are underlined to allow critical analysis. Key deficiencies are highlighted to formulate a methodology overcoming some of their common weaknesses.

Chapter 3 exposes the methodology starting with an overview of its structure. After that, scenarios of power transmission systems and extreme weather events are defined, as well as their associated models. Next, probability and severity indexes of CMCs are formed to allow the formulation of the aggregated vulnerability index. Major zones of vulnerability are then formalized starting with this vulnerability index. A procedure for searching suitable countermeasures is then detailed.

Chapter 4 crafts the power transmission systems and extreme weather events scenarios for the application of the Swiss power transmission systems impacted by thunderstorms. Two periods of time have been taken into account for evaluating the evolution of vulnerability, namely the summer season 2006 and 2018. The power transmission systems scenario 2018 involves some plausible modifications added on the 2006 scenario, which is built on the

---

actual states recorded at this time. Two plausible extreme weather events scenarios are built respectively on a past event and a simulated one.

Chapter 5 presents the results of the vulnerability analysis of the two power transmission systems scenarios impacted by the two extreme weather events. Emphasis is placed on the 2018 scenario undergoing the simulated thunderstorms. The temporal evolution of vulnerability is revealed as well as major zones of vulnerability.

Chapter 6 proposes a more resilient alternative to the 2018 scenario. This alternative aims at drastically reducing the vulnerability located in the major zones of vulnerability without creating new ones. The efficacy of the alternative is discussed in terms of vulnerability reduction and feasibility.

Chapter 7 concludes the thesis with an overview of the main findings, contributions and limitations, as well as take-away points for future research.



---

## 2 State of the art

### 2.1 Introduction

This chapter reviews a selection of recent articles related to vulnerability assessments during extreme weather conditions. These articles focus on distribution or transmission networks impacted by adverse or extreme weather events. This presentation aims to obtain a clearer view of the major advantages and drawbacks of each class of the current approaches found in literature. They are sources of inspiration at the time of developing a new methodology to meet the objective of this research.

To facilitate the analysis, the focus has been particularly centered on the evaluation of probability of common mode contingencies (CMCs) taking into account space-time correlations and the effect of these CMCs on the security of the electricity supply. The methods to assess the effects of adverse or extreme weather to the security of the electricity supply can be divided into three groups with different approaches.

### 2.2 Presentation and analysis of the three main approaches

First, Billinton's approach evaluates the worth of reliability in normal and adverse weather conditions. The name of this group refers to a scientist from University of Saskatchewan who first proposed this approach, and numerous articles have been produced citing this work. The methodology is fully explained in his well know book (Billington and Wenyuan, 1994). This methodology consists of multi-states models of power lines, describing their behavior which involved two possibilities, either in service or failed. A Monte-Carlo simulation combined with a load flow model assesses reliability by aggregating indexes such as expected energy not supplied. This methodology fully integrates relevant components of electric power systems as well as their plausible behavior in terms of reliability.

In Billington et al. (2002), annual failure rates of three weather models are compared. They distinguish themselves by their ability to differentiate normal, adverse and extreme weather. It is shown that not considering these three types of weather leads to optimistic estimation of failure rates. In Billington and Singh (2006), single, two and three state weather models are applied to a distribution system. Expected cost and energy not supplied are compared among the three models. This simple application shows that single and two state models are highly optimistic, and should not be used to estimate realistic indices when adverse and extreme weather is prevalent. In these two papers, uncertainties about characteristics of weather and power line resistance are neglected. Li et al. (2009) incorporated fuzzy technique in the reliability assessment of transmission systems. Traditional methods and fuzzy methods lead to the same mean values of reliability indices. However, the fuzzy method provides better insight regarding the uncertainties inherent to

---

transmission systems. All methods presented above do not take into account the temporal properties of extreme weather conditions. Alvehag et al. (2008) modeled time dependent failure and repair rates by non-homogenous Poisson processes applied to a distribution system during high wind conditions. The annual distribution of these conditions is taken into account as well as time varying loads. It was found that costs of service interruption and energy not supplied are increased when temporal properties of severe weather conditions are modeled. In this case, severe weather coincides with high winter consumption, resulting in the primarily drivers of these costs.

In this approach, reliability worth is assessed during normal, adverse and extreme weather conditions. Monte-Carlo simulations are performed to mimic the actual behavior of the system related to the level of consumption and the states of power line. These lines can be in two states, either in or out of service. Transitions between these two states are driven by failure and repair rates. At the time of simulation, they are driven by the intensity of weather mentioned above. This approach can assess reliability of complex electric systems in terms of various valuable indices. Nevertheless, it has one salient flaw when assessing reliability during extreme weather conditions, namely, it does not take into account space-time correlations of weather events. Failure and repair rates are based on past data which has been averaged and does not take into account space-time information. Extreme weather conditions are rare, so it is unlikely to find extreme events in databases. These events are also highly variable in time, space and intensity, suggesting the next extreme event could be very different than those previously experienced. Electric systems also evolve over time, and thus, new infrastructures are without data.

The second approach takes advantage of data sets of damages related to specific extreme weather events. This statistical learning approach draws inferences between actual damages and explanatory variables. Guikema (2009) presents an overview of methods underlying this approach as well as their limitations. A generalized linear mixed model is implemented to forecast the number of hurricane and ice storms related to electric power outages in Liu et al. (2008), Han et al. (2009). This model is based on a generalization of least squares regression containing random effects following a normal distribution. Prediction of infrastructure damages at a town level could provide relevant information for supporting power companies before natural disasters strike. However, only physical damages to distribution infrastructures are predicted for a given extreme weather event. Their effects to the security of electricity supply cannot be evaluated because no model of electric systems is involved. This lack is corrected partially in Winkler et al. (2010), where a topological network fragility analysis is performed. However, it does not take into consideration power flows because it aims to compare performance of different network topology when impacted by hurricanes. Not surprisingly, highly meshed networks are less vulnerable than tree-like topologies. It is worth mentioning that GIS is used in the three articles to build spatial models of the system.

The second approach is recent, among others, because of the large amount of data and heavy calculations required. It is yet to be applied to hurricanes in the southern part of the USA where they are extremely severe, and not so rare. Therefore, a large amount of data is available especially for distribution systems, which are more fragile than transmission systems. In areas where extreme weather conditions are not as likely to occur, or where electric systems are well adapted to the natural environment, data is certainly lacking.

---

The third and last approach investigated is based on space-time weather event simulations. It consists of super-imposing a succession of weather event maps over the territory containing vulnerable infrastructures. Then, their exposure is transformed into expected losses via damage functions. This approach is already in use to estimate insurance losses related to natural catastrophes such as hurricanes or earthquakes. A GIS based hurricane hazard assessment system is detailed in Huang et al. (2001) for the southwestern United States. The final outcome is a map of the rate of expected annual damage for a given hurricane. It is based on records of past hurricane characteristics. However, this method can also be applied to future weather conditions taking into account climate change. State of the art global climate models are coupled with a probabilistic operational insurance model in Schwierz (2010). This approach has not been thoroughly applied to electric power systems, except in Brostrom (2007). An ice storm is simulated over two overhead power lines of the Swedish transmission network. These two lines are divided in segments to which a vulnerability model relating the ice load to failure rate is applied. Historical storms, including severe winds and precipitation, have been used for the simulation as well as a modified past storm to create a possible extreme ice storm. Time dependent ice load and rate of failure have been carried out to determine segments more likely to fail. Unfortunately, only two power lines of the network have been investigated. Therefore, the effects of ice storms on the security of the electricity supply cannot be assessed.

This approach is able to model space-time correlations of extreme weather events. GIS are necessary to manage spatial data covering countries or even continents. Simulations allow numerous complex processes to be taken into account, taking place in vulnerability assessments during extreme weather conditions. However, research still has to be carried out to link possible damages or power line failures to the ability of electric power systems to perform their tasks.

## **2.3 Summary**

In summary, current approaches do not simultaneously take into account space-time correlations of extreme weather events and electric models of the power systems. They focus on either the simulation of power systems without really considering extreme weather events, or they focus on prediction of overhead power line outages without considering the consequences of the outages. Billinton's methodology cannot accurately take into account space-time correlations of extreme weather events, but it does a good job of modeling electric power systems. Purely statistical methods require outages data that are usually not available in case of rare and extreme weather conditions. Moreover, only physical damages to infrastructures are predicted, which impair the vulnerability evaluation of electric power systems. However, statistical methods take into consideration complex spatial correlations as the third approach. It is also able to determine the effects of extreme weather events on parts of transmission infrastructures such as segments of transmission lines. However, electric power systems are not yet fully integrated in the simulations.

To conclude, these three approaches have advantages and drawbacks inspiring a novel

---

methodology of vulnerability assessment during extreme weather conditions based on simulations. It is able to fully integrate space-time correlations and geographic distributions of overhead power lines to identify plausible CMCs. The core of the vulnerability assessment can then be performed by contingency analyses to derive indices of vulnerability as inspired by the first approach. Finally, countermeasures can be identified to reduce vulnerability.

---

## 3 Methodology of the vulnerability assessment

*This chapter describes the methodology employed to assess the vulnerability of power transmission systems induced by extreme weather events. First, the general framework and context of the methodology is set. Second, the scenarios of electric power systems are defined as well as scenarios of extreme weather conditions. Then, the method for identifying plausible common mode contingencies is described. Afterward, metrics are derived to evaluate the overall level of vulnerability and to highlight major zones of vulnerability. Finally, the procedure for finding appropriate countermeasures is explained in order to reduce the vulnerability.*

### 3.1 Introduction

As shown in Chapter 1.1, extreme weather conditions are rare but can have significant impacts on the security of the electricity supply. One of the most vulnerable parts of electric power transmission systems is its networks, which can be divided into two sub-networks. First, the distribution network composed of cables and overhead power lines at lower voltage levels. This network distributes electricity from very high voltage networks or local productions to end-consumers. Distribution networks are usually the place of frequent but small electric power disruptions, primarily because of their extensive length and unmeshed structure. These networks are also sensitive to weather conditions when constituted of overhead power lines. They are susceptible to extreme weather events because mechanical resistance is limited for economical reasons. Cabling of distribution power lines is recognized as a good way to protect them against harsh weather conditions for reasonable additional cost. Therefore, cabling has been undertaken on a wide scale basis in most of European countries (COM, 2003).

On the other hand, the transmission network is mainly constituted by a lattice of overhead power lines of high voltages, typically more than 220 kV. They are the bulk transfer of electricity from large power plants to substations connected to distribution networks. Transmission networks are used to exchange energy among countries and span over continents. This network is strategic because its malfunction could impact millions of people. The growth of modern societies relies on the high reliability of this network, so when outages occur at this level of voltage, power disruptions can take place on large scales (Sundell et al., 2006). They may start with insignificant outages leading to large disturbances by a succession of cascading failures (Makarov et al., 2005). This phenomenon is highly unpredictable once it initiates, and everything all possible measures should be taken to avoid entering this emergency state. The IEEE PES task force provides a comprehensive review of the phenomenon (Baldick et al., 2008). Extreme weather conditions can damage overhead transmission lines even if it is much less likely than for distribution power lines. Unfortunately, massive cabling of transmission networks does not yet seem economically reasonable and involves a multitude of concerns (OFEN, 2009a). Therefore, careful planning

---

of the network structure is needed to minimize the likelihood of large power disruptions.

In common practice and most academic literature, simultaneous outages are considered as independent failures even during extreme weather events (Li, 2005). This assumption is very optimistic because it underestimates the likelihood of coincident outages. Extreme weather events exhibit strong spatiotemporal correlations and impact large portions of transmission networks. Therefore, one has to consider CMCs instead of independent outages. The formers are critical because power transmission systems are usually planned and operated according to the N-1 security criterion (Willis, 2004). The identification of CMCs is not trivial since it involves large scale systems interacting in time and space. The actual level of sophistication of power system simulations and GIS can facilitate the search of plausible CMCs capable of endangering the security of the electricity supply.

Nevertheless, some barriers still impede the thorough search of probable and severe CMCs. Epistemic uncertainties, combinatorial complexity of the problem, and limited resources are the main obstacles. However, it is possible to identify some of the most probable and severe CMCs for some well defined scenarios of power transmission systems and extreme weather events. Although all possible situations are not covered, a partial solution is better than none, so simplifications are introduced to formulate a tractable problem.

First, many phenomena regarding the interactions of power transmission systems with extreme weather events can be discarded if they do not inconsistently deter the evaluation of CMCs probabilities. Second, the delicate modeling of possible operators' actions or cascading failures can be avoided by considering a static or structural vulnerability (Mao et al., 2006). In this case, the vulnerability stems from exceeding static security limits provoked by plausible CMCs. On the other hand, the conjunction space-time correlations of an extreme weather event and some potential weakly structured zones of a power transmission system are likely to result in some delimited zones of vulnerability. These zones, or at least the most vulnerable ones (i.e. major zones of vulnerability), require planning measures to reinforce their structural resilience.

Consider two types of measures to reduce structural vulnerability, the first of which acts on the plausibility of CMCs. For example, mechanical reinforcements of pylons would decrease the likelihood of failures. The second measure can be undertaken to minimize the consequences of CMCs. For example, expanding the N-1 security criterion to N-X would increase the structural resilience. Nevertheless, all these measures could be deemed excessive in the case of mature power systems. More than 60 years of experience have led to a fairly good trade-off between security of the electricity supply and infrastructure costs. Within the next decade, no technological breakthrough is expected to alter this point. However, careful planning of the network structure is deemed appropriate to significantly reduce vulnerability without excessive costs (Gomes, 2004). Structural modifications are costly and probably unjustifiable for the sole reason of minimizing vulnerability, consequently, they should be integrated in network development plans. Massive investments in transmission networks are likely to be revealed within the next few decades, so this is a great opportunity to combine network developments and reduced vulnerability during extreme weather conditions. At the planning stage, several alternatives of development exist. The existing planning rules and criteria can be updated to take into account issues raised by the deleterious effects of extreme

---

weather conditions, which result in electric transmission systems which are structurally less vulnerable.

## 3.2 Overview of the methodology

The methodology is composed of four main stages. The first stage pertains to the definition of the scenarios of power transmission system (SPTS) and extreme weather event (EWE) as well as their underlying models. The power transmission systems scenario is presented in Chapter 3.3 and the extreme weather events scenario in Chapter 3.4. The evaluation method of common mode contingencies (CMCs) probability and severity are exposed in Chapters 3.5 and 3.6, respectively. The overall vulnerability quantification and the identification of major zones of vulnerability (MZV) are detailed in Chapter 3.7. Finally, the method for identification of countermeasures is provided in Chapter 3.8.

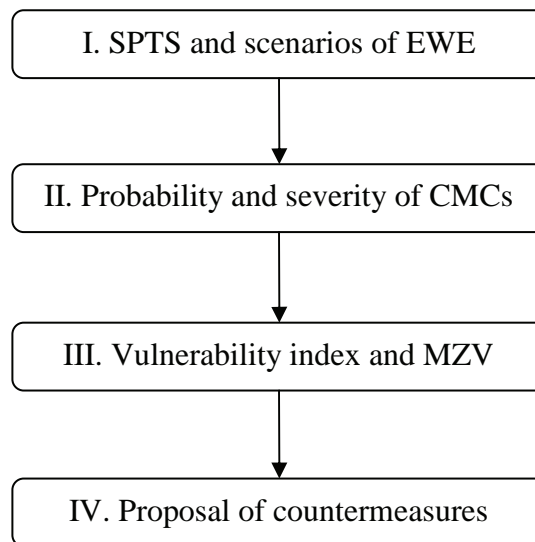


Figure 3: The four main stages of the methodology

The first stage establishes the models of electric and weather systems. When applied to concrete cases, these models have to be adapted via their parameters to the problem at hand. The term of scenarios is particularly appropriate at the time of the application of the methodology since different instances of the same power system or weather conditions can be considered. The SPTS is composed of three models, namely the electric model, the geographic model and the reliability model. These models describe the relevant features of power transmission systems required for the evaluation of probability and severity of CMCs. A space-time modeling of the weather event under investigation composes the scenario of extreme weather event (SEWE). The structure of these models is applicable for the wide majority of real or imaginable power transmission systems and EWEs.

The second stage starts with the evaluation of the time-dependant probability of a set of CMCs. This set groups the combinations of power lines which are a priori the most likely to

---

fail. This probability is the results of temporal simulations of transmission line exposure to hazardous features of EWEs, such as wind or lightning strikes. Over the duration of EWEs the temporal and maximum probability of CMCs are primordial components of the vulnerability. This entails two vulnerability measures respectively for a given time or for the total duration of the EWE. These two types of probability are interchangeable in the mathematical formulation. Therefore, the term probability is indifferently used for one or the other type. The most probable CMCs are then set aside for the severity index evaluation by a contingency analysis. This index is a function of violation of security limits such as current overloads or inadmissible voltage deviations.

The third stage consists in the definition of a vulnerability index and the mathematical formulation of MZV via the concept of matrix of vulnerability. The vulnerability index is the sum over all CMCs of the product of their respective probability and severity. This index is similar to the common definition of risk. The absolute value of this index is not very practical partially because it relies on subjective probabilities. However, this vulnerability assessment seeks weaknesses of the infrastructures not an evaluation of risk level. The search of weaknesses is achieved by the concept of matrix of vulnerability which is a projection of the vulnerability index onto two dimensions, the transmission lines in CMCs and those which undergo violation of security limits. A zone of vulnerability groups together transmission lines in CMCs and undergoing violations of security limits which are the most related while discarding the less related. MZV are zones of vulnerability which are responsible of most of the vulnerability. They allow locating the salient weak parts of the system.

The last part is related to the reduction of vulnerability. It is assumed that the vulnerability has to be reduced by countermeasures able to reinforce the structural resilience of the network. These countermeasures should fit in the development plan of the electric system as a possible alternative. Imaginable types of countermeasures pertain to addition or modification of transmission lines or topology changes of the network. A strategy of vulnerability reduction is based on the analysis of the vulnerability causes of the MZV. Following the strategy, countermeasures are proposed respecting some guidelines fostering their suitability. Finally, the countermeasures are implemented in the SPTS and the vulnerability reduction is assessed. Countermeasures able to reduce drastically the vulnerability can be presented as suitable.



---

### 3.3 Models of the electric power transmission system

Three models are needed to support the three different aspects of SPTS.

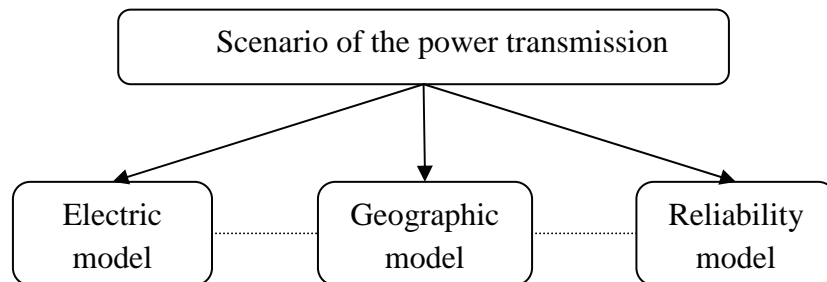


Figure 4: Scenario of the power transmission system and its three models

The electric model is based on an AC power flow model of the transmission system. The AC power flow model comprises the usual components of power transmission systems such as generators, loads, buses, transformers and power lines. This model allows power flow analysis, also named power flow simulation or load flow analysis, which determines voltage angles and magnitudes at buses, using voltages and power conditions for loads and generators. The voltage angles and magnitudes are then utilized to compute real and reactive power flows along power lines. This model is a non-linear and static model of electric networks. Contingency analyses use power flow analyses to evaluate the severity of CMCs.

The geographic model details the path on the ground of every overhead power line of the electric model. The paths are represented by lines divided into segments. Their middle point is the location where their exposure to weather is calculated. The geographic model is stored in a geodatabase accessible by GIS, and powerful built-in functionalities allow crafting, modifying, and visualizing the geographic model.

The reliability model evaluates the unavailability of overhead power lines due to its exposure to weather. The unavailability relies on two antagonist processes. First, the failure process, acting on segments, is a function of weather exposure and segment strength. Second, the reconnection process acts on transmission lines, represents the combined effects of automatic reclosing circuit breakers, operators' measures and fixing teams. This model is based on a continuous-time Markov chain.

#### 3.3.1 The electric model

The electric model defines and contains all data necessary to perform power flow analyses. It is the method used in contingency analysis which evaluates the severity of CMCs in chapter 3.6. Power flow analyses are extensively employed in the planning and operation of distribution and transmission systems. The main information obtained from power flow simulations is the active and reactive power transmitted through power lines, the branch

---

currents, and the magnitude and angle of voltages at buses. This analysis method allows computing the immediate steady-state operating point after disturbances such as CMCs. It is assumed that all the current and voltage transients vanish quickly without triggering any other outages. This static evaluation method is a crude approximation of the reality since the dynamic of the system is not taken into account. However, this tool has been used for decades at the planning and operation stage (Alguacil et al., 2009). Its relative simplicity allows the analysis numerous configurations of large systems in an acceptable time. The comprehensive review of Stott (1974) summarizes the abundant literature available in 1974 describing the different underlying methods of power flow analyses and their limitations.

Interconnected networks comprise thousands of elements such as buses and power lines. Specialized programs help the modeler handle the large amount of data and perform power flow analyses with several numerical methods in a user-friendly environment. In this research, the software *Neplan* (Busarello and Cott, 2010) is used to carry out power flow analysis. It allows the user to interact with electric elements, visualize the network schema, and perform analyses of SPTS for large scale systems. In general, these programs implement a standard AC flow model with some adaptations related to the depth of modeling and computing performance. Therefore, the remainder of the chapter is dedicated to the presentation of the standard inputs and output of power flow simulation while its mathematical formulation is detailed in Appendix 9.1

The electric model based on an AC power flow model includes the following types of elements: bus, transformers, generators, loads and lines. Different levels of modeling are possible. For example, buses, which represent substations, can be simply a busbar or a complex tangle of busbars, circuit breakers, protection and control equipments. Here, only passive elements are modeled to keep the complexity at a manageable level. However, these simplifications are compatible with the structural vulnerability analysis. The three-phase elements are represented in a single-line diagram since it is assumed the three-phase system is balanced and only three-phase outages are considered. The electric schema illustrates the elements retained with a color index indicating two levels of voltage.

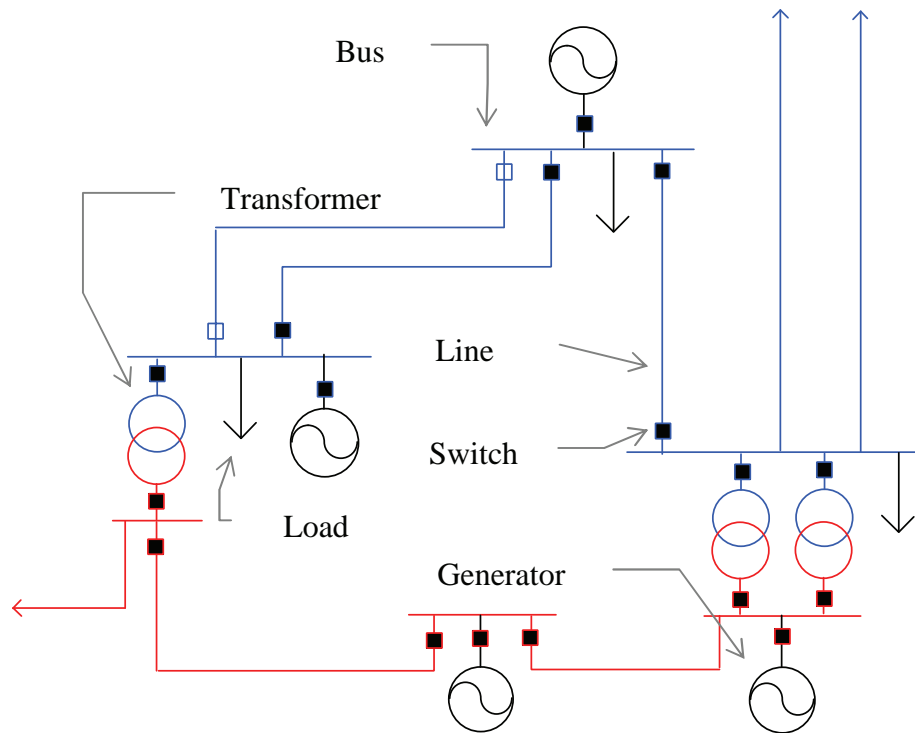


Figure 5: Illustration of the electric model

The buses connect together generators, loads, transformers and power lines. Buses are subject to limited deviations around their nominal voltage. Voltage deviations outside predefined boundaries are considered violations of security limits and in this case, the disconnection of essential equipment can take place. Elements are connected to a bus by a switch, which allows disconnecting of network elements. In this model, switches connect or disconnect at the same time the three phases of the element to simulate element maintenances and outages.

Generators represent power plants connected to buses. Their main parameters include the actual active and reactive power injected, minimum and maximum reactive power, preset voltage and types. There are three types of generators, which also determine the bus type. A PQ bus has generators that have a constant predefined active (P) and reactive (Q) power. In this case, the bus voltage is variable and determined after power flow analyses. The PV bus has generators with a constant predefined active power output. Their reactive power is adapted to force the actual bus voltage (V) to the preset voltage. When the reactive power exceeds its limits, the PV bus is changed into a PQ bus. Only a fraction of buses in transmission networks are PV type to keep the other buses voltage near their nominal value. PV generators are important elements keeping voltages within their security limits.

Finally, the slack bus SB serves as a reference for the angles of all other bus voltages. This bus is usually connected to a generator of large capacity since it is forced to compensate for the difference between the aggregated production and consumption, which include the active power losses of the power lines. Only one SB bus is usually required and should be located far from the region under investigation. Distributed slack buses are sometimes implemented to more realistically allocate the difference between production and consumption. Deo (2007)

---

offers a descriptions of the alterative modeling underlying power flow analyses. Loads are the opposite elements to generators. The former correspond to either large consumers or lower voltage networks. Primarily parameters for loads are the active and reactive powers withdraw from buses.

Transformers connect buses of different voltages. The main parameters are the resistance and leakage reactance at primary and secondary windings. The ratio of voltage between primary and secondary terminals is set by the ratio between the number of turns in the primary and secondary windings. This ratio can be adapted in tap transformers enabling voltage regulation.

Lines represent three-phase circuits of overhead power lines or cables connecting two buses. These circuits are characterized by an equivalent  $\Pi$  model giving a good approximation of their behavior for medium line length, namely less than 250 km. In this case, the branch resistance and reactance, the shunt capacitance and the maximum current are their main parameters. For long transmission lines, a model represented by an infinite series of two-port elementary components whose global behavior follows the telegraphers' equations must be considered (Aguet and Morf, 1990). The maximum current is related to the maximum temperature of the conductors after which plastic deformations happen possibly leading to outages and costly repair. The maximum current relies on environmental factors such as outside temperature and wind speed. In practice, the maximum current is set at a seasonal fixed value. A branch current surpassing the maximum current of a given power line entails an violation of security limits. Minor current overloads can be withstood a definite time based on the overload magnitude, while major overloads are likely to cause immediate disconnection of the power line.

The next table summarizes the main parameters ( $P_r$ ) and variables ( $V_r$ ) in most of the AC load flow models. The buses are identified by the indexes  $i$  or  $j$  belonging to the set of buses  $\mathcal{B} = \{1, \dots, N^b\}$ . Transmission lines are identified by their index  $l \in \mathcal{L} = \{1, \dots, N^l\}$ .

Table 3: Main parameters and variables required for power flow analyses

Element	Symbol	Label	Type
<b>Bus</b>	$V^i$	Voltage	Pr or Vr
	$V_{nom}^i$	Nominal voltage	Pr
	$V_{adm}^i$	Max voltage deviation	Pr
	$\theta^i$	Voltage angle	Vr
<b>Line</b>	$R^l$	Branch resistance	Pr
	$X^l$	Branch reactance	Pr
	$C^l$	Shunt capacitance	Pr
	$G^l$	Shunt conductance	Pr
	$I^l$	Branch current	Vr
	$I_{rating}^l$	Max current rating	Pr
	$P^l$	Active power	Vr
	$Q^l$	Reactive power	Vr
<b>Transformer</b>	$R_P^{i,j}$	Resistance at primary	Pr
	$X_P^{i,j}$	Reactance at primary	Pr
	$R_S^{i,j}$	Resistance at secondary	Pr
	$X_S^{i,j}$	Reactance at secondary	Pr
	$N^{i,j}$	Voltage ratio	Pr or Vr
<b>Load</b>	$P_L^i$	Active power	Pr
	$Q_L^i$	Reactive power	Pr
<b>Generator</b>	$P_G^i$	Active power	Pr
	$Q_G^i$	Reactive power	Pr or Vr
	$Q_{Gmin}^i$	Min reactive power	Pr
	$Q_{Gmax}^i$	Max reactive power	Pr
	$V_G^i$	Preset voltage	Pr
	$G_T^i$	Type PQ, PV or SB	Pr

At the time of application to a specific SPTS, the electric parameters are set to model the system under investigation. For real systems, electric utilities provide the basic data which can then be modified to suit the problem. Once the parameters are known, the equations of the AC power flow model are solved by numerical methods. A complete mathematical formulation can be found in Grainger and Stevenson (1994) in Chapter 9. Fundamental equations are presented in appendix 9.1. The model consists of a system of non-linear equations solved by the Newton-Raphson method (Kelley, 2003). It is an iterative method converging quickly to the root of a function. First, an initial guess of plausible bus voltage  $V^i$  and angle  $\theta^i$  is made. Then, voltage magnitude and angles are tweaked to eliminate the buses power mismatch. Line current  $I^l$ , active power  $P^l$  and reactive power  $Q^l$  are derived from bus voltages.

While evaluating the severity of CMCs by contingency analyses, power flow analyses are

---

successively performed by disconnecting the transmission lines included in each CMC. For each of them, violations of security limits stemming from current overloads of power lines and inadmissible voltage deviations of buses are identified.

Violations of security limits have two main consequence types. First, violations have a small magnitude and thus can be withstood by equipment until operational measures are taken. In the second case, some equipment fails or is disconnected due to higher violations, potentially leading to cascading failures and blackouts (Pourbeik et al., 2006). Unfortunately, the AC power flow model gives a static picture of the state of the system discarding transients responsible for power disruptions (Novosel et al., 2004). Some dynamics can be using a succession of pictures of the network, combining simulations of the possible actions of security devices and operators (Hardiman et al., 2004). However, the evaluation of the possible consequences of violations is not within the scope of this study since it aims at assessing static or structural vulnerability. Here, violations of security limits are considered as good indicators of vulnerability for identifying vulnerable zones and proposing planning measures.

### *3.3.2 The geographic model*

The probability of CMCs for overhead power lines are related to the space-time correlation of EWEs, in addition to the distribution of transmission networks over a territory. A geographic representation of the network is required to evaluate interactions between transmission lines and EWEs. The geographic model contains all relevant geographic information to virtually lay out the electric model on a map. The geographic model stores data from the reliability model and includes attributes linking it to the electric model. The geographic model is structured to allow its implementation under standard GISs.

Each overhead power line in the electric model must have a double in the geographic model. Although the three conductors of a circuit are spaced several meters apart and hung between 20 to 50 meters, only an averaging trace on the ground is required for the geographic model. The electric and reliability models both consider transmission lines as a single electricity carrier. In addition, the probability of CMCs is not sensitive to small horizontal displacements of a few meters. Therefore, the three-phase circuits of the electric model are represented by their projection onto a polygonal path stored in a path layer. A polygonal path, or sometimes named polyline in GIS, is a piecewise linear curve composed of a series of connected segments or also named vertices (Breslin et al., 1999). Paths are also represented by evenly spaced points stored in an exposure point layer. These points correspond to virtual transmission line segments where exposure to EWEs and calculation of probability failure are performed. Afterwards, these points are referred to exposure points. The path and exposure point layers are stored in a geodatabase containing geographic information as well as relevant characteristics of transmission lines, such as nominal voltage or name.

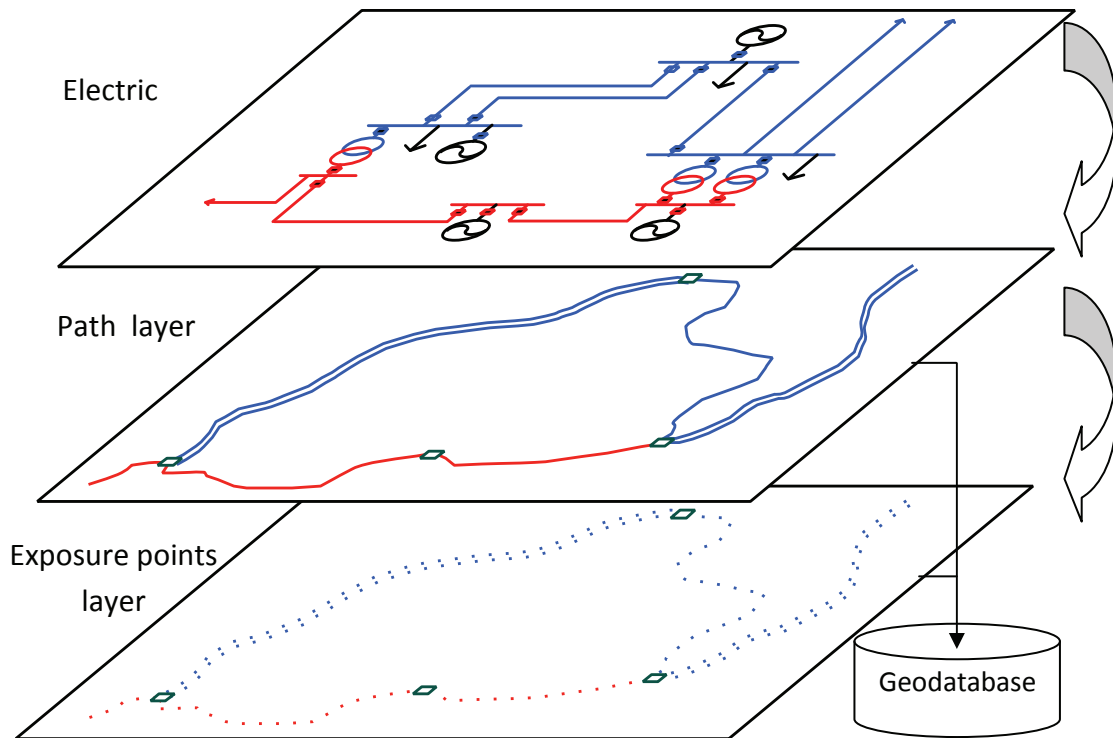


Figure 6: Two layers of the geographic model

The path layer is generally available at the electric utilities or at the system operator. However, their models do not always comply with the requirement that each transmission line of the electric model must have one unique trace in the geographic model. Moreover, different layer formats are likely since transmission networks are usually owned or operated by several utilities. The recourse to a GIS helps collect and process diverse geographic data to produce a coherent and unique model.

Several difficulties can arise when building the model. For example, each transmission line of the electric model must be linked to its counterpart in the geographic model with the same name or ID number. This could be tricky since those two models can have different abstraction levels, entails a tremendous effort of modeling especially for large networks. However, GISs have powerful functionalities that can solve most of modeling problems.

Due to spatiotemporal correlations of EWEs, power lines are not exposed with the same intensity at different locations. Line exposure to EWEs varies along its path, but this exposure and the strength of portions of transmission lines do not radically change over a reasonable distance. This fact leads to the division of continuous path into a discrete model represented by evenly-spaced exposure points. The distance between points can be variables but should not be too long or too short. An appropriate distance is a trade-off between the number of points influencing computing time and memory, and the level of detail needed to render the space-time correlations. A rule of thumb is that the distance between two exposure points should be a fraction of the spatial resolution of the EWE under investigation. Otherwise, information embodied in the EWE would only be partially taken into account. The number exposure point  $s$  for transmission line  $l$  is  $N_{seg}^l$ . All the exposure points of a specific

---

line belongs to  $\mathcal{S}^l = \{s \in \mathcal{S}^l \mid s \in [1, N_{seg}^l]\}$ .

The geodatabase stores two types of data. The first type regards all geographical information about paths and exposure points in a specific coordinate system. Paths are stored as a list of  $n^l$  connected points. These points and the exposure points are located in a Cartesian coordinate system by their three coordinates  $(x, y, z)$ . In most of the application, only the first two dimensions  $(x, y)$  are relevant. Other geographic coordinate systems could be more appropriate for large-scale transmission systems due to the ellipsoidal shape of the earth. The second type of data is attributes linked to layer features. For instance, each trace has an identifier connected to its double in the electric model. Each exposure point has attribute including segment length and parameters from the reliability model. The following table presents the mathematical form of the transmission lines path  $l$  and their exposure points  $s$ .

Table 4: Mathematical form of the features of the geographic model

Path of line $l$	$\mathcal{P}^l = \{(x_1^l, y_1^l, z_1^l), \dots, (x_{n^l}^l, y_{n^l}^l, z_{n^l}^l)\}$
Exposure point coordinates	$\sigma^{l,s} = (x^{l,s}, y^{l,s}, z^{l,s})$
Set of exposure points	$\mathcal{S} = \{\sigma^{l,s} \in \mathcal{S} \mid l \in \mathcal{L}, s \in \mathcal{S}^l\}$
Segment length	$d^{l,s}$
Reliability model parameters	$R^{l,s} = \{r_1, r_2, \dots\}$

This mathematical formulation is general and not related to any specific GIS. However, the formulation is compatible with GIS software used for this research, ArcInfo (ESRI, 2010b). Large geodatabases are supported and numerous of built-in toolboxes are available for this software. Its user interface allows many operations to be made without requiring coding skills. ArcInfo is a powerful example of GIS that simplifies geographic information processing.

The use of GIS in planning transmission networks is increasing, at least in academic literature, in particular when the objective is to find a suitable path (Monteiro et al., 2005) or rerouting overhead power lines (Luemongkol et al., 2009). GIS combined with the LIDAR technique is also utilized for vegetation management along right-of-ways (Mills et al., 2004). Nag and Sengupta (2008) review some applications of GIS to transmission networks. However, electrical models and geographical models are rarely integrated in the same framework. The methodology proposed here is thus quite novel.



---

### 3.3.3 *The reliability model*

The reliability model of the SPTS lays down a methodological framework aimed to evaluate the temporal unavailability of each transmission line. The reliability model is incorporated in the SPTS because this model is closely linked to the transmission lines of the electric model and the exposure points in the geographic model. The temporal unavailability is at the foundation of the evaluation of CMC probability developed in Chapter 3.5.

As with any model, the reliability model is also a simplification of the processes taking place in reality. When considering the modeling of the interaction between EWE and transmission lines, complexity and uncertainty issues arise. It would be pointless and vain to try describing every detail of the processes taking place during EWE. Moreover, the amount of data to collect, the development of the model, and the duration of the simulations would surpass any reasonable amount of resources allocated for this research. Therefore, the modeling must be strongly influenced by the objective of the vulnerability assessment, namely the identification of zones of vulnerability. This entails that estimation from subjective probability of transmission line failure leading to the discrimination of likely CMCs and unlikely ones is sufficient. The term subjective corresponds to the case where probability is a measure of certainty about a particular statement as opposed to the objective meaning related to frequency. Therefore, the concept of probability implemented here should not be interpreted as frequency, but as a means for ranking plausibility.

Most of the vulnerability assessments of power systems do not take into account spatiotemporal correlations. They strongly increase the probability of some CMCs while others are very unlikely to happen. For instance, Billington is one of the authors of an accepted reliability assessment (see Chapter 2.2). Without doubt, this method is appropriate when assessing large electric power systems during normal weather conditions. According to Li (2005), it reaches its limits during EWE because space-time correlations are discarded. The reliability model proposed here takes them into account, as well as the paths and physical strength of the overhead transmission lines.

EWEs are one of the main causes of CMCs. Therefore, the probability of CMCs has to take into account exposure to natural elements and the strength of transmission infrastructure. However, this probability is also affected by security equipment, action of operators and repair teams. Indeed, CMCs are alleviated in time depending on failure type. Intermittent failures last a very short duration of time such as most of the failures triggered by lightning, which are mitigated by reclosing breakers. Extended failures last until physical components are repaired, for instance after hurricanes. Blache and Shrivastava (1994) present a comprehensive classification of failure. Therefore, the probability of CMCs at a given time stems from failure processes and reconnection processes.

In the electric model, transmission lines are modeled as single electric links between buses. Partial failures of one phase cannot be analyzed by a standard AC power flow model. Therefore, it is assumed that transmission line failures are complete and thus comprise the failures of all three phases at the same time. Moreover, it is assumed that failure and reconnection processes are memoryless, (i.e. the future state of the transmission line only

depends on its current state disregarding all the previous states). This assumption is known as the Markov property (Brémaud, 2001b). On the whole, each transmission line has only two states, the functional (Up) and nonfunctional (Down) states. Over a small duration  $dt$ , the change from Up to down state is operated by failure processes whereas the opposite is handled by reconnection processes. This representation of transmission line states can be formalized by a time-continuous Markov process. Since the failure processes depend on weather conditions, which change over time, the Markov process is nonhomogeneous (Brémaud, 2001a).

Nonhomogeneous time-continuous Markov processes are not commonly implemented in reliability analysis (Zhang and Horigome, 2001). This is likely due to their complexity and lack of information about parameters. It implies the literature about this subject is theoretical and any application to a concrete problem is challenging. Therefore, it is proposed here to develop a simple but appropriate method tailored for the problem at hand.

The derivation of the time-dependent equations describing unavailability of any item such as transmission line starts with the following schema representing the two states and the possible transition during a duration  $dt$ .

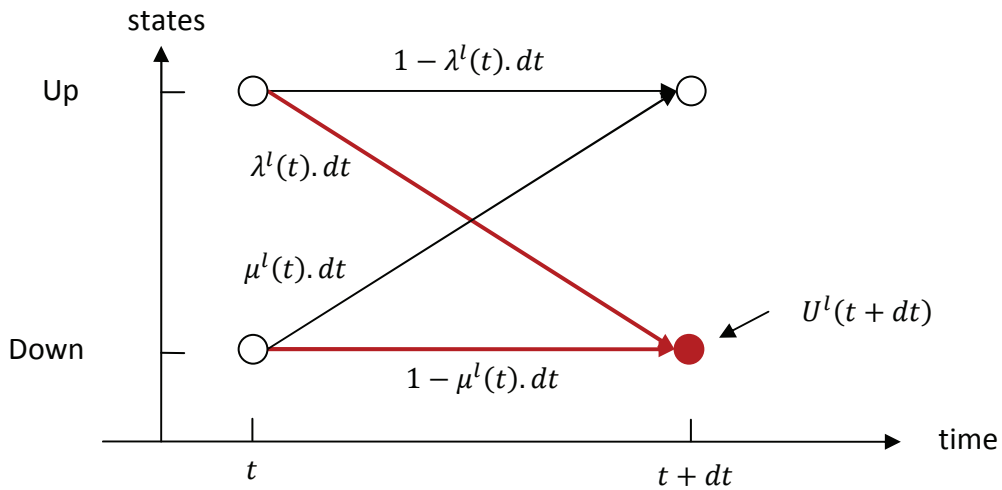


Figure 7: Transition in the two states model of power line  $l$

Formally, the state of a transmission line  $l$  at time  $t$  may be described by the state variable  $X^l(t)$ :

$$X^l(t) = \begin{cases} 1 & \text{if Up at time } t \\ 0 & \text{if Down at time } t \end{cases} \quad (3.1)$$

For a transmission line  $l$ , the probability of transition from any of the states at time  $t$  to any other states at time  $t + dt$  depends on the failure rate  $\lambda^l(t)$  and reconnection rate  $\mu^l(t)$ . rate of failure and reconnection of an item are defined by the following equations, (Rausand and Hoyland, 2004).

---


$$\lambda^l(t) = \frac{\text{Pr}(t \leq T < t + dt \mid T \geq t)}{dt} \quad (3.2)$$

$$\mu^l(t) = \frac{\text{Pr}(t \leq T^* < t + dt \mid T^* \geq t)}{dt} \quad (3.3)$$

Where  $T$  and  $T^*$  are, respectively, continuous random variables denoting the time to failure and to reconnection of the power line  $l$ . Equation (3.2) shows that the probability of moving from the Up state at  $t$  to the Down state at  $t + dt$  is equal to  $\lambda^l(t).dt$  as mention in the schema. According to the second axioms of probability, which stipulates that the sum of all possible events equals one, the probability of staying in the UP state is  $1 - \lambda^l(t).dt$ . The justification of the transition from the Down state is similar by taking into account equation (3.3). It is worth mentioning that in some textbooks, the rate of failure is called hazard rate or hazard function noted  $h(t)$  (Ascher and Feingold, 1984). In this case, the symbol  $\lambda$  is reserved for constant hazard rate.

By definition, the line unavailability  $U^l(t)$  is the probability being in its nonfunctional or Down state or  $X^l(t) = 0$ . Its complementary is availability  $A^l(t) = 1 - U^l(t)$ . From the schema above, the unavailability  $U^l(t + dt)$  is the result of only the two state transitions (red). Therefore, the unavailability can be expressed by the probability that the line is Up at  $t$  and does fail between  $t$  and  $t + dt$  or the line is Down at time  $t$  and is not repaired between  $t$  and  $t + dt$ .

$$U^l(t + dt) = \text{Probability } (X^l(t) = 1 \text{ AND } X^l(t + dt) = 0 \text{ OR } X^l(t) = 0 \text{ AND } X^l(t + dt) = 0)$$

Or formally

$$U^l(t + dt) = (1 - U^l(t)) \cdot \lambda^l(t).dt + U^l(t) \cdot (1 - \mu^l(t).dt) \quad (3.4)$$

$$\text{with } U^l(t = 0) = 0 \quad (3.5)$$

Rearranging some terms yields to

$$\begin{aligned} \frac{U^l(t + dt) - U^l(t)}{dt} &= \lambda^l(t) - \lambda^l(t).U^l(t) - \mu^l(t).U^l(t) \Rightarrow \\ \frac{dU^l(t)}{dt} &= \lambda^l(t) - (\lambda^l(t) + \mu^l(t)).U^l(t) = f(U^l(t), t) \end{aligned} \quad (3.6)$$

This differential equation describes the temporal evolution of the unavailability of any line  $l$  of the transmission network. Only the initial condition  $U^l(0)$  has to be given. It is assumed

that lines are all operational at the beginning of the simulation, i.e. equation (3.5). If the rates of failure and reconnection were constant, equation (3.6) would be a linear ordinary differential equation of first order with constant coefficient. Its solution could be easily found (Polyanin and Zaitsev, 2003). The time varying rate of failure and reconnection impede any analytical solution. In this case, numerical solutions are the only way out. Equation (3.6) can be numerically solved by the classical Runge-Kutta method (Rappaz and Picasso, 2000). It is a fourth-order method which means that the total error is proportional to  $h^4$ , where  $h$  is the stepsize (Iserles, 1996). At time  $t_{n+1} = (n + 1).h$  with  $n \in \mathbb{N}$ , the numerical estimate of the unavailability  $\tilde{U}^l(t_{n+1})$  is:

$$\tilde{U}^l(t_{n+1}) = \tilde{U}^l(t_n) + \frac{h}{6}(p_1 + 2p_2 + 2p_3 + p_4) \quad (3.7)$$

$$p_1 = f(\tilde{U}^l(t_n), t_n) \quad (3.8)$$

$$p_2 = f\left(\tilde{U}^l(t_n) + \frac{h}{2}p_1, t_n + \frac{h}{2}\right) \quad (3.9)$$

$$p_3 = f\left(\tilde{U}^l(t_n) + \frac{h}{2}p_2, t_n + \frac{h}{2}\right) \quad (3.10)$$

$$p_4 = f(\tilde{U}^l(t_n) + h.p_3, t_{n+1}) \quad (3.11)$$

The four factors  $p$  are estimated slopes of  $\tilde{U}^l$  at different times. The estimate (3.7) at  $t_{n+1}$  is the estimate at  $t_n$  plus a linear function of the step size and the weighted average of slopes. The Runge-Kutta method can be adapted to allow variable stepsize reducing computing time. For instance, Dormand and Prince (1980) provide a family of embedded Runge-Kutta methods with variable stepsize.

The evolution of the rate of failure still has to be defined, taking into account EWEs and the geographic model of Chapter 3.3.2. According to this chapter, transmission lines are divided into segments in series represented by their exposure point. One needs the following strong but plausible assumption to derive the rate of failure. That is to say, each segment fails independently from each other. It is plausible since segments of transmission lines are designed to avoid the propagation of mechanical or electrical outages to the adjacent segments. For instance, reinforced pylons are regularly placed among other pylons to stop the propagation of possible collapsing pylons. As mentioned on Modarres et al. (1999) page 198, the rate of failure of a system composed by independent components in series is the sum of its component rates of failure. The demonstration of this statement is given in Appendix 9.2. This rule applied to a power line  $l$  composed of  $N_{seg}^l$  independent segments gives:

$$\lambda^l(t) = \sum_{i=1}^{N_{seg}^l} \lambda^{l,s}(t) \quad (3.12)$$

---

Where  $\lambda^{l,s}(t)$  is the rate of failure for the segment  $s$  of the line  $l$ . This rate of failure is a function of the strength and the exposure to EWE of the segment. The term hazard function  $h$  found in academic literature corresponds well with this function. This function has no generalized formulation, it is strongly dependent on the type of EWE. For example, winter storms interact differently with overhead power lines than thunderstorms. The hazard function has to be explicitly defined at the time of the methodology application. However, parameters of strength or resistance noted  $r^{l,s}$  are in all cases required, as well as the exposure  $E(S^{l,s}, t)$  defined in chapter 3.4. These quantities can be vectors since they could contain more than one parameter. Resistance parameters are assumed constant during EWEs.

$$\lambda^{l,s}(t) = h\left(R^{l,s}, E(S^{l,s}, t)\right) \quad (3.13)$$

Regarding the reconnection processes, they are assumed independent of weather conditions, memoryless, and aggregated at the transmission line level. It requires that all the possible ways of reconnecting a line are lumped in a single process, which is not influence by weather conditions. This is a strong simplification because reconnection processes are certainly to some degree influenced by the intensity of weather along transmission line. In addition, rapid action of automatic security equipment is considered similar to slow repair of mechanical damages. In these conditions, the reconnection rate is constant.

$$\mu^l(t) = \mu^l \quad (3.14)$$

The only degree of modeling freedom is that each transmission line has its own rate of reconnection. A more realistic model of time-dependent unavailability should integrate more failures or reconnection modes acting on different parts of transmission lines. Although possible, this would extensively complicate the task of modeling and collecting data at the time of application. Time consuming Monte-Carlo simulations could be necessary to evaluate the unavailability. Therefore, the level of sophistication is deemed sufficient to fulfill the objective of identification of zones of vulnerability.

### 3.4 Scenario of extreme weather event

A SEWE is a spatiotemporal description of a plausible extreme weather event. It contains the exposure vector necessary to evaluate the hazard function defined by equation (3.13). The available source of data to build SEWE is not necessarily in the format required to implement the hazard function. Indeed, it is required that the exposure should be known at exposure points of all segments of all transmission lines at any time. To ensure compatibility between the requirements mentioned above and SEWE, they are transformed in space and time. First,

---

this chapter mathematically defines the required format of the exposure of segments of transmission lines and a possible representation of SEWE. Then, a transformation method is proposed to interpolate SEWE into a usable format for the hazard function.

Each weather condition has hazardous features which influence the likelihood of outages and thus the hazard function. For instance, hazardous features of hurricane are wind speed and direction. For thunderstorms, lightning strikes and their characteristics such as location of impact or peak current are example hazard features. To define the hazardous feature  $\eta$  which is a particular threat for the physical integrity of power lines, a total of  $N^E$  hazardous features are formally described by a vector field of exposure, represented by the vector-valued function  $E$ . This field is defined for the set  $\mathcal{Y}$  constituted by the set  $\mathcal{S}$  of exposure point  $\sigma^{l,s} = (x^{l,s}, y^{l,s}, z^{l,s})$  augmented with the set of positive time  $\mathcal{T} = \{t \in \mathcal{T} \mid t \in \mathbb{R}^+\}$ .

$$E: \mathcal{Y} \rightarrow \mathbb{R}^{N^E}$$

$$\text{With } \mathcal{Y} = \mathcal{S} \times \mathcal{T} \quad (3.15)$$

$$E(\sigma^{l,s}, t) = E(x^{l,s}, y^{l,s}, z^{l,s}, t) = \begin{pmatrix} \eta^1 \\ \dots \\ \eta^{N^E} \end{pmatrix}$$

The exposure is defined in a Cartesian coordinate system as an example. This coordinate system is appropriate to represent small portions of the earth. In other cases, other coordinate systems would be preferred.

SEWE are built from sources of exposure data provided by weather stations or numerical simulations. These sources produce discrete numerical data in space at sites  $d$  and times  $k$ . For instance, weather stations are distributed over a territory at some specific locations recording meteorological data at the typical rate of minutes to hours (Suter et al., 2006). Numerical simulations offer estimates of meteorological conditions at fixed points of a grid at variable time rates (Schättler et al., 2009). Therefore, exposure data of SEWE must be interpolated to the four coordinates of the set  $\mathcal{Y}$ .

To define the data source of exposure, the vector-valued function  $W$  represents vector field of data from weather stations or numerical simulations. It is defined for the set  $\Psi$  constituted of the set  $\mathcal{D}$  of the coordinate of the sites  $\delta^d = (x^d, y^d, z^d)$  augmented with the set  $\mathcal{K}$  of discrete times  $k$ .

$$W: \Psi \rightarrow \mathbb{R}^{N^E}$$

$$\text{With } \Psi = \mathcal{D} \times \mathcal{K} \quad (3.16)$$

$$W(\delta^d, k) = W(x^d, y^d, z^d, k) = \begin{pmatrix} \eta^1 \\ \dots \\ \eta^{N^E} \end{pmatrix}$$

The vector field  $W$  must be transformed to estimate the exposure at the element of the set  $\mathcal{Y}$  of (3.15). A comparison among numerous existing interpolations methods is performed in

---

Dobesh et al. (2007). Their performance and complexity vary over a long range. A method cannot be proposed in general since their performance is related to the type of weather condition under investigation. For instance, an inverse distance weighting interpolation of wind speed recorded by distant weather stations could lead to large errors due to specific local conditions, especially in mountainous regions. Interpolation methods can be splinted into two main categories, the deterministic and the statistics. The latter is part of the field of statistic and more specifically geostatistics. It is based on statistical methods, which represent spatial distributions taking into account spatial autocorrelations. Kriging methods are well known interpolation techniques, which are part of the geostatistics field (Cressie, 1993). Deterministic methods are simpler and faster at the price of accuracy losses. They are preferred here, since the speed of calculation is an important criterion because interpolations have to be made at every time step of the availability calculation of equation (3.4).

It is proposed to perform time and spatial interpolations successively. However, methods exist to consider time as an additional coordinate to carry out spatiotemporal interpolation in one batch (Li and Revesz, 2004). The sequence of interpolations is as follow:

First, an temporal interpolation of  $W(\delta^d, t)$  from  $W(\delta^d, k)$  is performed by an interpolant  $TI$ .

$$\widehat{W}(\delta^d, t) = TI(W(\delta^d, k^i)) \quad (3.17)$$

For instance, a linear interpolation is quick and easy, even if its accuracy could be limited for a long duration.

$$\widehat{W}(\delta^d, t) = W(\delta^d, k^i) + (W(\delta^d, k^j) - W(\delta^d, k^i)) \cdot \frac{t - k^i}{k^j - k^i} \quad (3.18)$$

Where  $t \in [k^i, k^j]$  and with  $k^i$  and  $k^j$  are respectively the discrete times just before and after  $t$ . Then,  $\widehat{W}(\delta^d, t)$  is spatially interpolated by the interpolant  $SI$  from  $\delta^d$  to the element of set  $Y$ .

$$\widehat{E}(\sigma^{l,s}, t) = SI(\sigma^{l,s}, \widehat{W}(\delta^d, t)) \quad (3.19)$$

The interpolant  $SI$  is problem specific and should be selected taking into account the space-time characteristics of the weather condition under investigation. Possible  $SI$ s include nearest-neighbor, natural neighbor, linear and bilinear or inverse distant weighting. The latter is presented hereunder. Gilgen (2006) gives an overview of existing methods.

The inverse distance weighting interpolation allow the estimation of an unknown exposure  $\widehat{E}$  at  $\sigma^{l,s} = (x^{l,s}, y^{l,s}, z^{l,s})$  by a weighted sum of the known exposure  $\widehat{W}$  at neighboring points  $\delta^d = (x^d, y^d, z^d)$ . The weight  $w(\delta^d)$  is inversely proportional to the distance between the unknown and the known point. The power factor  $p$  is a real number. It influences the weights

---

giving more importance to close points when  $p$  is higher.

$$\hat{E}(\sigma^{l,s}, t) = \frac{\sum_{d=1}^N w(\sigma^{l,s}, \delta^d) \cdot \widehat{W}(\delta^d, t)}{\sum_{d=1}^N w(\sigma^{l,s}, \delta^d)} \quad (3.20)$$

$$\text{With } w(\sigma^{l,s}, \delta^d) = \frac{1}{\|\sigma^{l,s} - \delta^d\|^p} \quad (3.21)$$

The SEWE containing the spatiotemporal data  $W(\delta^d, k)$  is readily stored in a geodatabase like the geographic model of Chapter 3.3.2. For each time  $k$ , a layer of the EWE supports all the points  $\delta$  at which the values of the exposure  $W(\delta^d, k)$  are known. The GIS coupled with this geodatabase greatly facilitate the interpolation. Indeed, most GIS programs have toolboxes implementing the standard SIs mentioned above. Moreover, the data of the geographic model, such as the exposure point of the set  $\mathcal{S}$ , are directly available through the same geodatabase. The use of GIS ensures the visualization of the data to detect errors, a suitable means of storage of multidimensional data, several methods of interpolation and a common framework for diverse geographic models. The next schema illustrates the procedure for interpolating a weather data from a SEWE to the exposure point  $\sigma^{l=1,s=6}$  at time  $t$ .

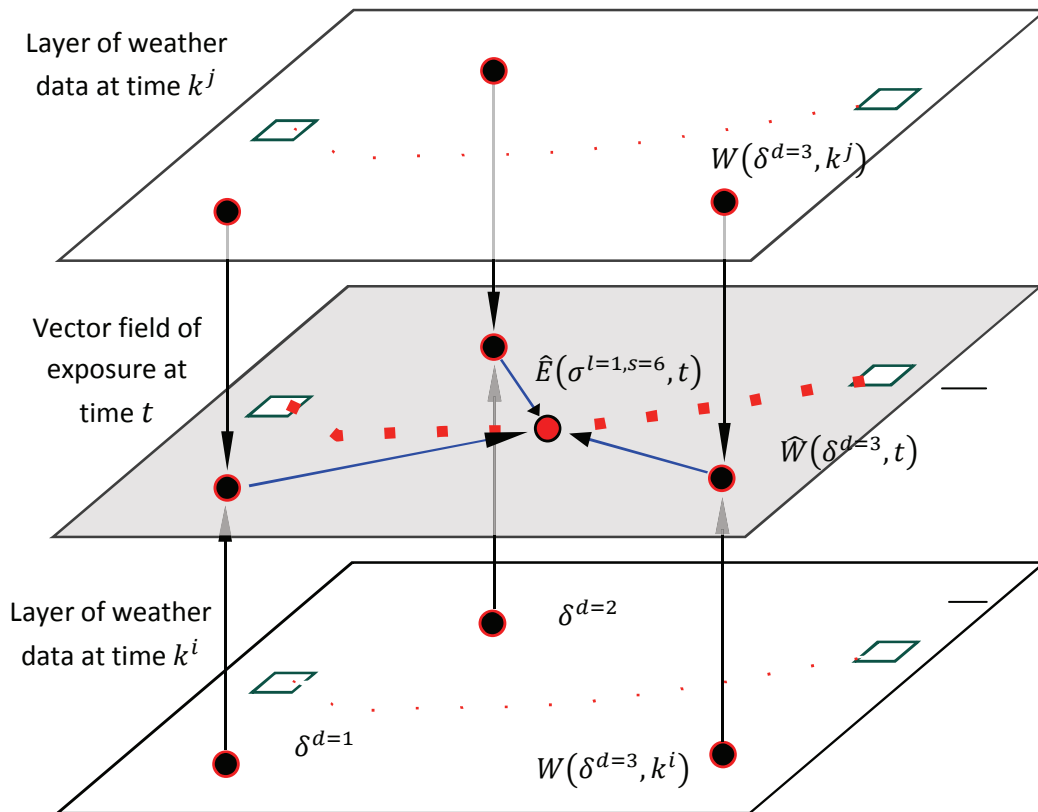


Figure 8: Example of interpolation from 3 weather stations to a segment

The SEWE is represented by the two white layers containing the data of weather station or



numerical simulations at time  $k^i$  and  $k^j$ . Three black points  $\delta^d$ , with a known exposure, are represented in addition to the red exposure points  $s = 6$  of transmission line  $l = 1$ . The black arrows show the  $TI$  as defined by (3.17), whereas the blue arrows represent the  $SI$  as defined by (3.19).

### 3.5 Probability evaluation of plausible common mode contingencies

This chapter aims at searching a set of plausible CMCs and evaluates their probability. The severity of CMCs is evaluated afterwards by a contingency analysis in Chapter 3.6. The tremendous number of possible CMCs combined with finite computing resources imply that the evaluation of their probability and severity has to be restrained to a more tractable number. Therefore, only the transmission line with the highest unavailability are retained by a screening method prior to their combination forming plausible CMCs. Afterwards, the calculation of the time dependent CMCs probability is performed assuming that transmission lines fail independently. Finally, the maximum probability of each CMC during the simulation is set aside to condense the temporal probability by a single key value. The schema hereunder shows the main steps implemented in this chapter.

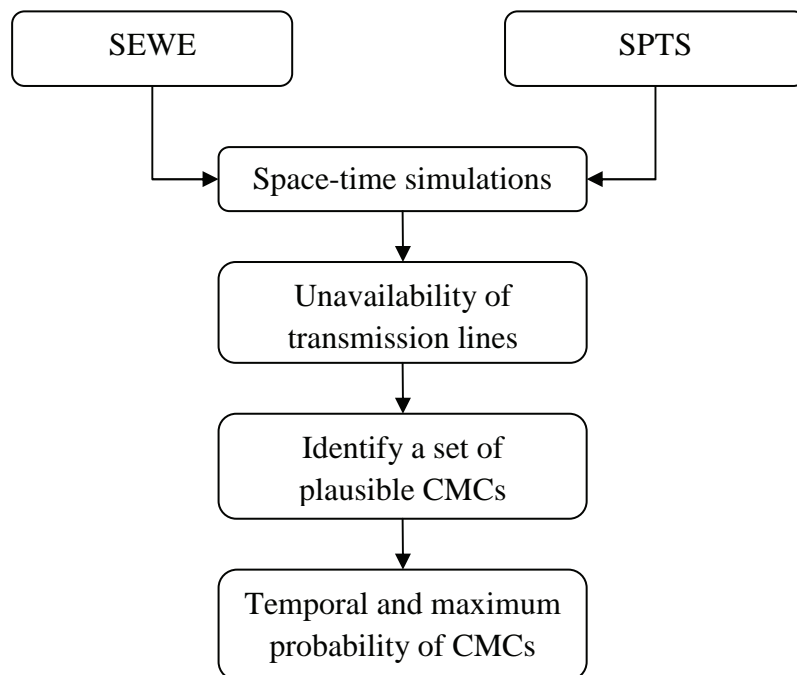


Figure 9: Overview of the probability evaluation CMCs

The temporal unavailability of transmission line  $l$  is given by equation (3.6) of the reliability model. It is likely that only a part of the network is significantly impacted by SEWE. It entails that some transmission lines are more unavailable than others during

---

weather events. It is assumed that the most plausible CMCs are combinations of transmission lines, which exhibit highest unavailability during weather events. This assumption allows setting a screening method to identify a set of plausible CMCs. It begins with the calculation of the maximum unavailability of each transmission lines  $l$  during SEWE.

$$\hat{U}^l = \max_t [U^l(t)] \quad (3.22)$$

All power lines with an  $\hat{U}^l$  above a certain threshold  $U^T$  are deemed likely enough to fail to generate plausible CMCs. This inclusion criterion is certainly not unique and can be further developed. However, it is a good trade-off between simplicity and performance in practice. The threshold is determined by the following method, named cumulative sum screening.

- 1) Find the bijective function  $C(l) = l'$  map the index  $l$  to the new sorted index  $l'$ . The transmission lines are sorted by decreasing order of unavailability.

$$\text{Find } C(l) = l' \text{ such as } \hat{U}^{l'} \geq \hat{U}^{(l'-1)} \quad (3.23)$$

- 2) Calculate the cumulative sum  $F(l')$  of  $\hat{U}^{l'}$ .

$$F(l') = \hat{U}^{l'} + \hat{U}^{l'-1} \quad (3.24)$$

- 3) Choose a cumulative sum threshold percentage  $\alpha$ . Find the transmission line  $l^T$  having a cumulative sum the nearest to  $\alpha$  of the sum of all  $\hat{U}^l$

$$\text{Find } l^T \text{ such as } \left| \hat{U}^{l^T} - \text{sum}_{l'} [\hat{U}^{l'}] \cdot \alpha \right| \text{ is minimum} \quad (3.25)$$

- 4) Identify the threshold  $\hat{U}^T$

$$\hat{U}^T = \hat{U}^{C^{-1}(l^T)} \quad (3.26)$$

- 5) Finally, compose the set  $M$  containing the most unavailable transmission lines

$$M = \{l \mid \hat{U}^l \geq \hat{U}^T\} \quad (3.27)$$

The cumulative sum method enables the combination of the most unavailable transmission lines to form CMCs, discarding the lines insignificantly contributing to the total unavailability. It is very effective for screening, especially when a fraction of the network is strongly impacted by a SEWE. This is usually the case in real situations where space-time correlations cause concentrated spots of intense activity. Nevertheless, other screening methods could be as effective or even more effective in specific weather conditions or

---

network topologies.

Then, all possible  $m$ -combinations of the line indexes included in  $M$  are performed to form a set  $\Gamma^m(c)$  of plausible CMCs. The multiplicity  $m$  is the number of transmission lines present in a particular CMC, while  $c$  is the  $c^{th}$  CMC of multiplicity  $m$ . The complementary set  $\bar{\Gamma}^m(c)$  contains the rest of line indexes not belonging to  $\Gamma^m(c)$ . The number of element  $N_{cmc}^m$  of  $\Gamma^m$  is found by the binomial coefficient.

$$N_{cmc}^m = card(\Gamma^m) = \binom{n^M}{m} = \frac{n^M!}{m!(n^M - m)!} \quad (3.28)$$

$$\text{Where } n^M = card(M) \quad (3.29)$$

The number  $N_{cmc}^m$  of elements of the sets  $\Gamma^m$  for a given multiplicity  $m \geq 3$  can become intractable when  $n^M$  is large. In this case, threshold  $\alpha$  of the screening method is diminished to limit the number of plausible CMCs. The enumeration of the element of set  $M$  to generate plausible CMCs is a method reaching its limits for large networks extensively impacted by EWEs. In this case, Monte-Carlo simulations treating the problem as a real experiments could used instead of analytical methods (Billington and Wenyuan, 1994). Anyhow, high multiplicity CMCs should not be plausible for well devised and maintained networks. Therefore, the upper bound  $N^m$  of multiplicity is likely to be limited to 3 or 4 in practice.

At a given time, the probability  $P_m^c(t)$  of facing a CMC  $\Gamma^m(c)$  is the probability that lines in  $\Gamma^m(c)$  are unavailable whereas the rest of the lines in  $\bar{\Gamma}^m(c)$  are available.

$$P_m^c(t) = \left[ \bigcap_{l \in \Gamma^m(c)} P(X^l(t) = 0) \right] \cap \left[ \bigcap_{l \in \bar{\Gamma}^m(c)} P(X^l(t) = 1) \right] \quad (3.30)$$

If one assumes transmission lines fail and are reconnected independently of each other, is the temporal probability of CMCs is :

$$P_m^c(t) = \prod_{l \in \Gamma^m(c)} U^l(t) \cdot \prod_{l \in \bar{\Gamma}^m(c)} (1 - U^l(t)) \quad (3.31)$$

The assumption of independence of transmission lines excludes all direct causal relations among lines. For example, this may be the case when a conductor of a three-phase circuit is damaged and falls on another circuit. On this occasion, conditional probabilities should be used.

Instantaneous probability  $P_m^c(t)$  is not the best metric for evaluating the plausibility of

---

---

severe CMCs. The violation of security limits entailed by CMCs can be withstood without damages up to a certain point. In the case of power line overloads, currents above the maximal rating are often tolerable for several minutes. Conductor temperatures augment within a few minutes allowing operators to take alleviating measures. It is worth mentioning that cascading failures can happen directly after CMCs occur. However, it is assumed that lasting CMC are more critical. Therefore, an average probability  $\bar{P}_m^c(t)$  during a centered window of duration  $T^W$  is deemed more appropriate than the instantaneous one.

$$\bar{P}_m^c(t) = \frac{\int_t^{t+T^W} P_m^c(t) \cdot dt}{T^W} \quad (3.32)$$

This probability evolves with time, reaching peaks and troughs. It is far too much information for assessing vulnerability on a global basis. The temporal information regarding CMC probability is not relevant in this case. The maximum average probability  $\hat{P}_m^c$  during the simulation period is more appropriate since it focuses only on the highest probability peak.

$$\hat{P}_m^c = \max_t[\bar{P}_m^c(t)] \quad (3.33)$$

### 3.6 Severity assessment

The severity of plausible CMCs for a given SPTS is assessed on the basis of a contingency analysis. It is a familiar method in network planning and static security assessment. This analysis is based on an AC power flow model of the network in appendix 9.1.3. The two main output of contingency analysis are the intensity of branch current along transmission lines and voltage magnitude at buses. In sound electric power systems, these two electric measures are maintained within security boundaries. In steady-state conditions, currents must be kept below its maximum value in order to limit the temperature of conductors below their maximum allowable temperature. Voltage at buses must also be kept around the nominal voltage to avoid tripping of electric components. CMCs can provoke exceeding of these boundaries because most of the networks are planned to withstand only single outages. The following conditions on the current of power line  $l$  and the voltage of bus  $i$  must be respected to consider the electric power system in a normal state. Currents and voltages are complex numbers whose units are respectively ampere and kilo-volt. Only their magnitude is constrained.

$$|I^l| < I_{rating}^l \quad (3.34)$$

$$\hat{V}^i = \frac{|V^i - V_{nom}^i|}{V_{nom}^i} < V_{adm}^i \quad (3.35)$$

Where  $I_{rating}^l$  is the absolute rating branch current and  $V_{adm}^i$  the maximum admissible deviation of bus voltage expressed as a percentage of the nominal voltage. The deviation outside the security limits are transformed into severity indexes. It measures the plausibility of elements direct tripping due to exceeding security limits. By construction, the severity index is bounded between 0 and 1. The lower limit coincides with CMC involving no current or voltage exceeding. The upper limit corresponds to a severe situation where the element undergoes major exceeding leading to its disconnection from the network because of security systems or physical damages. The relation between current overloads, voltage deviations and severity is assumed linear as illustrated hereunder.

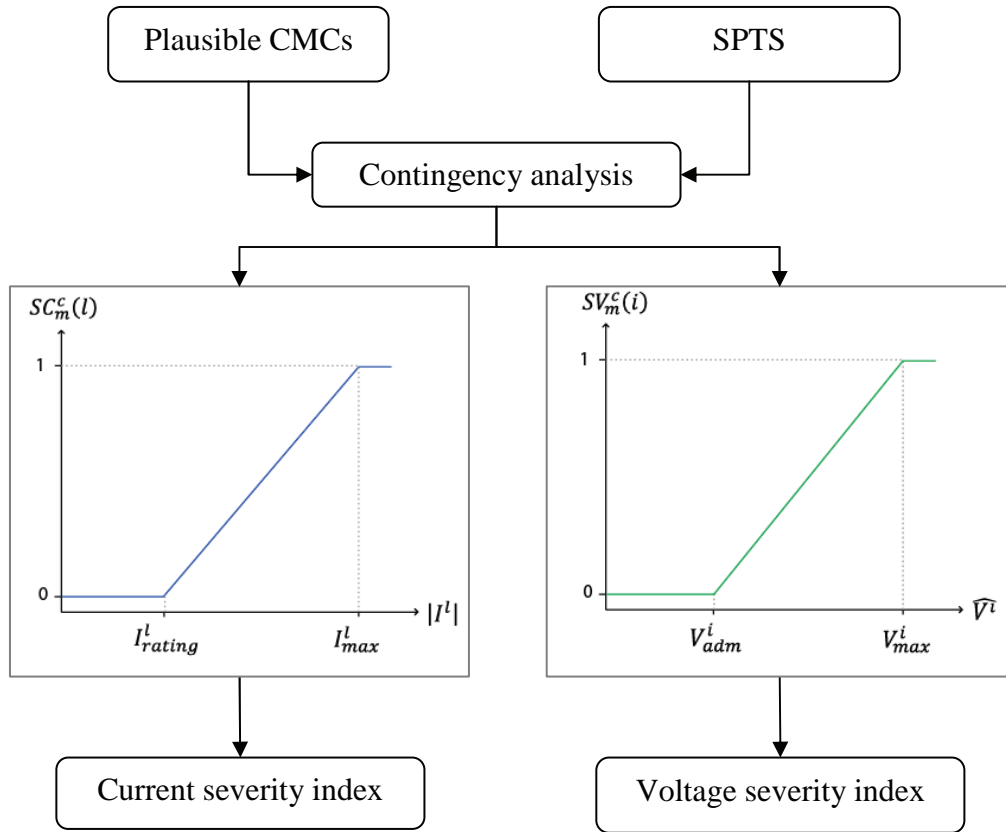


Figure 10: The two components of the severity index

The severity of each CMC from the set of  $\Gamma^m$  is measured by two indexes. First, the current severity index  $SC_m^c(l)$  is related to the branch current of line  $l$ .

$$SC_m^c(l) = 0 \quad \text{if } |I^l| \leq I_{rating}^l \quad (3.36)$$

$$SC_m^c(l) = \frac{|I^l| - I_{rating}^l}{I_{max}^l - I_{rating}^l} \quad \text{if } I_{rating}^l < |I^l| < I_{max}^l \quad (3.37)$$

$$SC_m^c(l) = 1 \quad \text{otherwise} \quad (3.38)$$

Where  $I_{max}^l$  is assumed to be the current leading for sure to the disconnection of the line  $l$ . Second, the voltage severity index  $SV_m^c(i)$  is related to the voltage of bus  $i$ .

$$SV_m^c(i) = 0 \quad \text{if } \hat{V}^i \leq V_{rating}^i \quad (3.39)$$

$$SV_m^c(i) = \frac{\hat{V}^i - V_{adm}^i}{V_{max}^i - V_{adm}^i} \quad \text{if } V_{adm}^i < \hat{V}^i < V_{max}^i \quad (3.40)$$

$$SV_m^c(i) = 1 \quad \text{otherwise} \quad (3.41)$$

Where  $V_{max}^i$  is assumed to be percentage of the nominal voltage which leads for sure to the partial or total disconnection of all the elements connected at the bus  $i$  such as loads, generators, transformers or transmission lines.

Both of the severity indexes do not take into account further disconnections known as cascading failures. Their complex dynamic is still not fully understood, although several modeling attempts have been made as mentioned in (Duenas-Osorio and Vemuru, 2009).

The partial composite index of severity  $\tilde{S}_m^c(l, i)$  is calculated for each CMC of  $\Gamma^m(c)$  as the weighted average of the current severity index of the power line  $l$  and voltage severity index of the bus  $i$ . Both terms are normalized by the number of element susceptible to fail. In the case of current severity index,  $N^\ell - m$  lines could be potentially overloaded above  $I_{max}^l$ . Regarding the voltage severity index,  $N^{\hat{b}}$  can undergo a voltage deviation greater than  $V_{max}^i$ .

$$\tilde{S}_m^c(l, i) = \frac{w^1}{N^\ell - m} \cdot SC_m^c(l) + \frac{w^2}{N^{\hat{b}}} \cdot SV_m^c(i) \quad (3.42)$$

$$\text{Where } w^1 + w^2 = 1 \quad (3.43)$$

The total composite index of severity  $S_m^c$  is the sum of the partial one over all power lines  $l$  and busbar  $i$ .

$$S_m^c = \sum_{l=1}^{N^\ell} \sum_{i=1}^{N^{\hat{b}}} \tilde{S}_m^c(l, i) = \frac{w^1}{N^\ell - m} \cdot \sum_{l=1}^{N^\ell} SC_m^c(l) + \frac{w^2}{N^{\hat{b}}} \cdot \sum_{i=1}^{N^{\hat{b}}} SV_m^c(i) \quad (3.44)$$

The normalization introduced in (3.42) combined with the condition (3.43) impose that the total composite severity index, or just the severity index  $S_m^c$ , is bounded in the interval  $[0,1]$ . The two weights change the influence of current overloads or voltage deviations on the severity index and ultimately on the vulnerability index. Both types of severity index can be treated separately by setting one of the weights to one and the other to zero.

### 3.7 Vulnerability quantification

The proposed metric of vulnerability has two major properties. First, vulnerability stems from probable and severe CMCs. These two factors must both be present to threaten the security of supply. Therefore, the vulnerability induced by a given CMC is assumed to be the product of its probability by its severity as defined Chapters 3.5 and 3.6. This definition of vulnerability is similar to the popular risk definition (Varadan and van Casteren, 2009). Second, vulnerability is extensive. Namely, the vulnerability of a set of CMCs is the sum of the vulnerability of each CMC. These two properties are at the base of the vulnerability index and are presented in the following subchapters.

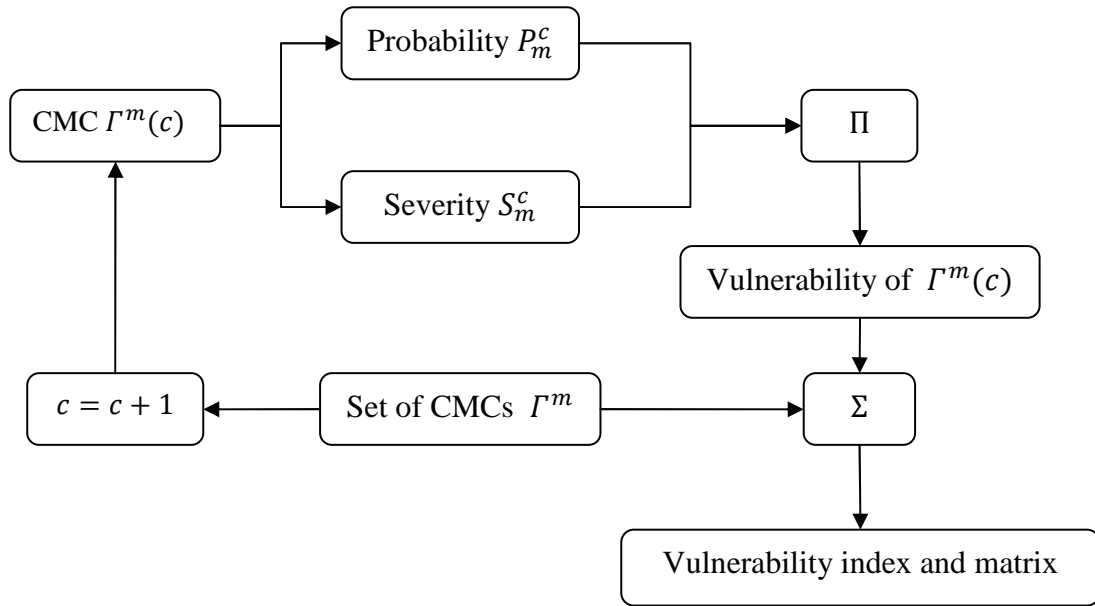


Figure 11: Overview of the vulnerability quantification

#### 3.7.1 Vulnerability indexes

The vulnerability index represents the overall vulnerability of a STPS impacted by a SEWE. It is defined as the sum of the vulnerability induced by each CMC of the set  $\Gamma^m$ . The individual vulnerability stemming from each CMC is simply the product of its probability  $\bar{P}_m^c(t)$  or  $\hat{P}_m^c$  by the composite index of its static severity  $S_m^c$ . Two indexes are derived for the two types of probability. The temporal probability  $\bar{P}_m^c(t)$  combined with  $S_m^c$  leads to the temporal vulnerability index denoted by  $V(t)$ .

$$V(t) = \sum_{m=1}^{N^m} \sum_{c=1}^{N_{cm}^m} \bar{P}_m^c(t) \cdot S_m^c \quad (3.45)$$

This vulnerability index describes the temporal evolution of vulnerability. Peaks of vulnerability occur when extreme weather impacts vulnerable zones of the power system. This index permits to highlight the periods of vulnerability for a better understanding of the source of vulnerability.

The aggregated vulnerability index  $V$  has the same form as (3.45), but the maximum probability  $\hat{P}_m^c$  is used instead of the temporal one.

$$V = \sum_{m=1}^{N^m} \sum_{c=1}^{N_{cm}^m} \hat{P}_m^c \cdot S_m^c \quad (3.46)$$

This vulnerability index aggregates the vulnerability induced by each of the CMC present in the set  $\Gamma^m$ . This index allows the comparison of vulnerability levels of combinations of SPTS and SEWE. The absolute value of vulnerability is difficult to interpret and likely to be very small due to low probabilities of CMC expected in a real system. On the contrary, the difference in vulnerability indexes among combinations of SPTS and SEWE allow their ranking on a vulnerability scale. SPTS with a lower vulnerability index guaranties better security of supply, and can be designated as better alternatives for future development of the electric system.

The aggregated vulnerability index has to be used with caution, because the vulnerability assessment is partial and limited to a subset of all possible CMCs. Only a minority of all possible CMCs are taken into account. Indeed, a screening method is required to select some of the most probable CMCs from the tremendous number of all possible CMCs. It entails that the set  $\Gamma^m$  is not necessarily the same for different SPTS and SEWE due to the screening method. This is a serious bias impairing the use of this index for ranking. In order to rank and compare different combinations of SPTS and SEWE, a common set  $\Gamma^m$  should be utilized for all simulations.

The vulnerability comparison index  $V^c$  allows gauging vulnerability against a scenario of reference. This scenario could represent a SPTS undergoing no particular extreme weather conditions where most of the plausible contingencies have no common modes. The ratio of vulnerability is transformed by the logarithm to base 10 to facilitate its interpretation in terms of order of magnitude.

$$V^c = \log_{10} \left( \frac{\hat{V}}{\hat{V}^{ref}} \right) \quad (3.47)$$

The vulnerability  $\hat{V}^{ref}$  of the reference scenario is derived from the procedure described in Chapter 3.5. However, temporal unavailability  $U^l(t)$  of power lines is replaced by their average unavailability  $\bar{U}^l$  in normal weather conditions. The aggregated indexes of vulnerability are normalized by the number of CMC of each multiplicity to avoid biases induced by different numbers of CMC for each combination of scenarios. The normalized index of vulnerability  $\hat{V}$  can also be scaled by the probability  $P^e$  of the SEWE if this



information is available. This allows different levels of plausibility of SEWE to be taken into account. This probability is set to one for the scenario of reference, and also in other scenarios where there is insufficient information.

$$\hat{V} = P^e \cdot \sum_{m=1}^{N^m} \frac{1}{N_{cmc}^m} \sum_{c=1}^{N_{cmc}^m} \hat{P}_m^c \cdot S_m^c \quad (3.48)$$

The vulnerability comparison index allows evaluation to be performed to determine whether the level of vulnerability is sufficiently high to justify the search of countermeasures. When  $V^c$  is close to zero, it would mean the vulnerability level during a SEWE is in the same order of magnitude as in normal weather conditions. In this case, countermeasures would not be easily justified. On the contrary, a  $V^c$  above one would indicate that countermeasures should be envisaged, and the necessity would continue to rise along with the comparison index.

### 3.7.2 Matrix of vulnerability

The vulnerability index is of little use at the time of identifying suitable countermeasures to reduce vulnerability. The vulnerability matrix addresses this problem by locating the vulnerable zones of the network. This matrix decomposes the vulnerability index into two dimensions. The first is the transmission lines included in CMCs, and the second is the transmission lines undergoing violation of security limits. This matrix can be seen as a cause to consequences diagram, which is a convenient way to characterize and locate the root of vulnerability. This matrix simplifies the complex relations between CMCs and violations of security limits projecting them onto network infrastructures such as transmission lines and buses. Two types of matrix are required to properly describe vulnerability. First, the aggregated matrix of vulnerability  $M^V$  characterizes the relations between CMCs and violations as follows:

$$M^V = (v^{k,l,i}) = \sum_{m=1}^{N^m} \sum_{c=1}^{N_{cmc}^m} \hat{P}_m^c \cdot \tilde{S}_m^c \cdot \gamma(k, m, c) \quad (3.49)$$

$$\text{Where } \gamma(k, m, c) = \begin{cases} \frac{1}{m}, & k \in \Gamma^m(c) \\ 0, & \text{otherwise} \end{cases} \quad (3.50)$$

$$\text{With } k \in \mathcal{C} = \{1, \dots, N^\ell\}, l \in \mathcal{L} = \{1, \dots, N^\ell\}, i \in \mathcal{B} = \{1, \dots, N^b\} \quad (3.51)$$

The element  $v^{k,l,i}$  of the three dimensional matrix has the coordinates  $(k, l, i)$ . The coordinates  $k$  and  $l$  represent transmission lines and  $i$  the buses. The first dimension is the lines included in CMCs, which cause violations of security limits. The other two dimensions

are respectively the violations of security limits for current overloads and voltage deviation. The term  $\tilde{S}_m^c$  is the partial composite index of severity as defined by (3.42). The function  $\gamma$  projects equally the vulnerability of each CMC  $\Gamma^m(c)$  onto the power lines  $k$  belonging to  $\Gamma^m(c)$ .

One interesting property of the matrix  $M^V$  is that the sum of its elements over its three dimensions is equal to the aggregated vulnerability index  $V$ . Appendix 9.3 details the demonstration.

$$\sum_{k=1}^{N^\ell} \sum_{l=1}^{N^\ell} \sum_{i=1}^{N^\ell} v^{k,l,i}(t) = V \quad (3.52)$$

This equation shows that the matrix of vulnerability  $M^V$  is a projection on its three dimensions of the vulnerability index without loss of information. In theory, the matrix of vulnerability  $M^V$  is appropriate to identify suitable countermeasures. In practice, its three dimensions are a burden. Two dimensional matrixes are much more convenient when it comes to representing them. This can be accomplished easily by setting one of the weights for  $w^1$  or  $w^2$  of the partial composite index of severity at zero and the other at one. In this case, current overload and voltage deviations are treated separately.

The matrix of vulnerability has the following form when only the current overloads are taken into account.

$$M^V = (v^{k,l}) = \sum_{m=1}^{N^m} \sum_{c=1}^{N_{cmc}^m} \hat{P}_m^c \cdot \frac{SC_m^c(l)}{N^\ell - m} \cdot \gamma(k, m, c) \quad (3.53)$$

$$\text{When } w^1 = 1 \text{ and } w^2 = 0 \quad (3.54)$$

The matrix of vulnerability is simplified as follows when only voltage deviations are taken into account.

$$M^V = (v^{k,i}) = \sum_{m=1}^{N^m} \sum_{c=1}^{N_{cmc}^m} \hat{P}_m^c \cdot \frac{SV_m^c(i)}{N^\ell} \cdot \gamma(k, m, c) \quad (3.55)$$

$$\text{When } w^1 = 0 \text{ and } w^2 = 1 \quad (3.56)$$

All developments detailed here have been presented for the aggregated matrix of vulnerability using the maximal probability  $\hat{P}_m^c$ . Similarly, the temporal matrix of vulnerability is formed by replacing  $\hat{P}_m^c$  by the temporal probability  $\bar{P}_m^c(t)$ . This matrix characterizes the temporal evolution of the relations between CMCs and violations of security limits. It is useful to picture the causes of vulnerability at a time of particular interest (such as peaks of vulnerability) as in the application of Chapter 5.2.2.

---

### 3.7.3 Zones of vulnerability

The matrixes of vulnerability link transmission infrastructures in CMCs to infrastructures enduring their severe consequences in terms of violation of security limits. These matrixes are helpful in locating vulnerable zones by visually examining them. However, their size can be cumbersome in certain cases, and their level of detail is too high to allow a quick understanding of the causes of vulnerability and also for the search for measures to reduce the vulnerability.

For this purpose, the elements of matrixes of vulnerability are aggregated in  $N^z$  zones of vulnerability. They group the transmission lines in CMCs and the power lines and buses enduring violations of security limits, respectively. Elements that are strongly linked are in the matrix of vulnerability while in the same zone of vulnerability, whereas elements that are poorly related should be in separate zones. Elements contributing negligibly to the vulnerability can be discarded to simplify the search of pertinent zones of vulnerability. The following paragraphs explain a method for identifying these zones.

The set  $Z^p$  contains the indexes of transmission lines and buses of the  $p^{\text{th}}$  zone. The number of zones  $N^z$  is an initial estimate corresponding to a plausible number of zones. The set  $Z^p$  is defined as the Cartesian product of subsets containing indexes of the transmission lines and buses. The set  $C^p$  contains indexes of transmission lines included in CMCs while  $L^p$  and  $B^p$  indexes transmission lines and buses enduring violations of security limits.

$$Z^p = C^p \times L^p \times B^p \quad (3.57)$$

Where

$$\begin{aligned} C^p \cap C^q &= \emptyset, \quad L^p \cap L^q = \emptyset, \quad B^p \cap B^q = \emptyset \\ \forall p, q \in [1, N^z] \text{ and } p &\neq q \end{aligned} \quad (3.58)$$

And

$$\bigcup_{p=1}^{N^z} C^p = C, \quad \bigcup_{p=1}^{N^z} L^p = L, \quad \bigcup_{p=1}^{N^z} B^p = B \quad (3.59)$$

Conditions (3.58) imply that subsets  $C^p$  and  $C^q$  are disjoint. Conditions (3.63) imply that the union of all  $C^p$  contain all elements of  $C$ . These conditions are also valid for the subsets  $L^p$  and  $B^p$ .

Measures of vulnerability also have to be defined. First, the zonal vulnerability index is the sum of vulnerability stemming from any sets  $C^p$ ,  $L^q$  and  $B^r$ .

$$V^{p,q,r} = \sum_{k \in C^p} \sum_{l \in L^q} \sum_{i \in B^r} v^{k,l,i} \quad (3.60)$$

According to (3.52), the sum of all components of the matrix of vulnerability  $M^p$  equals the vulnerability index  $V$ . Given the conditions (3.58) and (3.59), the sum of each zonal vulnerability index  $V^{p,q,r}$  over all subsets  $\mathcal{C}^p$ ,  $\mathcal{L}^q$  and  $\mathcal{B}^r$  is also equal to  $V$ .

$$\sum_{p=1}^{N^z} \sum_{q=1}^{N^z} \sum_{r=1}^{N^z} V^{p,q,r} = \sum_{k \in \mathcal{C}} \sum_{l \in \mathcal{L}} \sum_{i \in \mathcal{B}} v^{k,l,i} = V \quad (3.61)$$

The vulnerability index  $V$  can also be decomposed into two separate components, the intra zone overall vulnerability and the inter zones overall vulnerability:

$$V = V_{\text{intra}} + V_{\text{inter}} \quad (3.62)$$

$$V_{\text{intra}} = \sum_{p=1}^{N^z} V^{p,q,r} = \sum_{p=1}^{N^z} V^p \quad \text{such as } p = q = r \quad (3.63)$$

$$V_{\text{inter}} = \sum_{p=1}^{N^z} \sum_{q=1}^{N^z} \sum_{r=1}^{N^z} V^{p,q,r} \quad (3.64)$$

$q \neq p \quad r \neq q$

A portioning of the matrix of vulnerability in zones of vulnerability is defined as optimal when the intra zone's overall vulnerability is maximal. According to (3.62), an optimal portioning also leads to a minimized inter zone's overall vulnerability. Therefore, the transmission line and bus indexes are distributed into the subset  $\mathcal{C}^p$ ,  $\mathcal{L}^p$  and  $\mathcal{B}^p$  to maximize the intra zone overall vulnerability  $V_{\text{intra}}$  or minimize  $V_{\text{inter}}$ .

Distribute all  $k$  to  $\mathcal{C}^p, l$  to  $\mathcal{L}^p, i$  to  $\mathcal{B}^p$  (3.65)

Such as  $V_{\text{intra}}$  maximized or  $V_{\text{inter}}$  minimized (3.66)

With  $k \in \mathcal{C}, l \in \mathcal{L}, i \in \mathcal{B}$  and  $p \in [1, N^z]$  (3.67)

The choice of optimization algorithm is not unique and is left to the modeler as well as the number of zones of vulnerability  $N^z$ . By experience, the modeler is able to find near optimal portioning in a few minutes by hand. However, automatic techniques could be used to automate this process. It is not guaranteed they would be better than a manual method when taking into account the duration of development and implementation of the method.

---

Each zonal vulnerability index  $V^{p,q,r}$  is an elementary brick of the system vulnerability. The zonal vulnerability ratio  $V_{\text{ratio}}^{p,q,r}$  gauges the importance of each of those bricks as a percentage of the vulnerability index  $V$ .

$$V_{\text{ratio}}^{p,q,r} = \frac{V^{p,q,r}}{V} \quad (3.68)$$

This ratio is fundamental when searching for countermeasures. Zones of vulnerability ( $p = q = r$ ) with the highest ratio are those in which countermeasures must preferentially be implemented. After, these zones are named major zones of vulnerability (MZV). This concept aggregates the outcomes of complex space-time calculations in a natural way. It facilitates the search for countermeasures and can be easily illustrated by matrixes or maps. An example of matrix and zones of vulnerability is provided in Table 15 and the zonal vulnerability ratio in Table 16 of Chapter 5.2.1.

All developments here are detailed for the zonal vulnerability index using matrix of vulnerability  $M^V$ . Likewise, the time-dependent zonal vulnerability index is formed by replacing  $v^{k,l,i}$  by its temporal counterpart  $v^{k,l,i}(t)$ .

### 3.8 Proposal of suitable countermeasures

Vulnerability is an inherent property of real complex systems. It is difficult to imagine perfectly designing invulnerable systems as vast as transmission networks, especially when they are subject to a continuously changing environment. However, reduction of vulnerability is an achievable objective, and after identifying of MZV, countermeasures can be proposed to diminish the vulnerability, subject to certain constraints.

Extreme weather conditions are by definition rare and exhibit varying space-time patterns entailing two major points. First, countermeasures should be effective during extreme weather events and useful during normal weather conditions. That is, their acceptance will be higher if they are justified in more cases than simply situations that are unlikely to occur. Second, countermeasures are meant to reduce vulnerability regarding only a few SPTS and SEWE. In an ever changing environment, these scenarios are at best a fraction of all possible scenarios. It is hard or even impossible to evaluate a priori if the proposed countermeasures will be helpful during their useful lifetime. There is no silver bullet for reducing the vulnerability of electric power systems, but it is believed that an educated guess is far better than a random one.

The process of identifying suitable countermeasures is not straightforward because it is an open world problem. This process produces resilient alternatives to the development plan of SPTS. At the planning stage, the knowledge and skills of the modeler are of great importance. However, the modeler must be guided in the search for countermeasures by a well defined process.

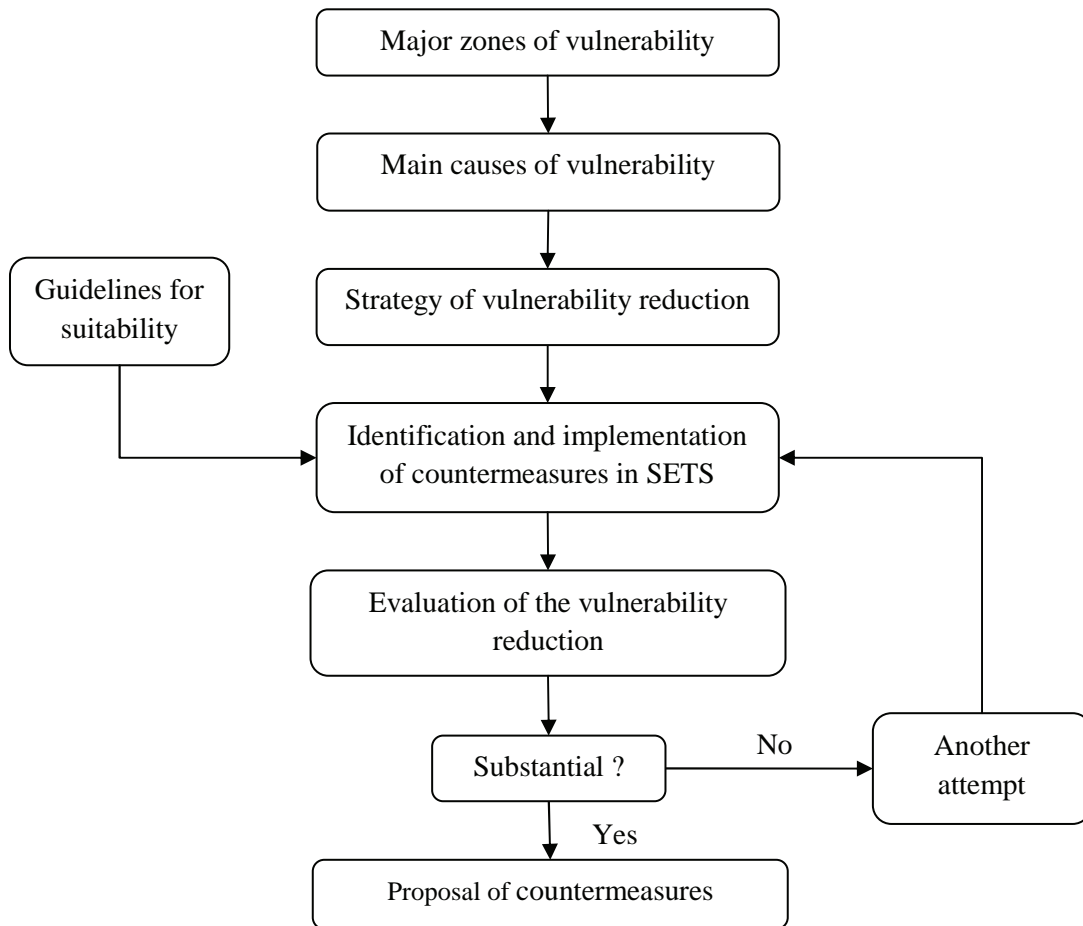


Figure 12: Methodology for suitable countermeasures proposal

The search for countermeasures begins with the identification of MZV by the zonal vulnerability ratio from Chapter 3.7.3. CMCs causing MZV are potential threats to the security of the electricity supply. These contingencies are analyzed to determine the most threatening, which could initiate cascading failures or potentially lead to islanding of whole regions (Kumbale et al., 2008). The main causes of vulnerability are then inferred based on those hazardous CMCs. This stage also requires the intervention of the modeler's expertise. For example, main causes could be lack of transmission line redundancy or bottlenecks. After, a strategy is developed to alleviate the main causes of vulnerability. Here, a strategy refers to a set of guidelines directing the search for countermeasures. For example, a strategy could consist of connecting large power plants to high capacity 380 kV interconnection lines to relieve the 220 kV network.

Subsequently, the strategy leads to the identification of suitable countermeasures, which are implemented in the STPS. They are for instance new power line construction, network topology changes or augmented capacity transfer of power lines. Countermeasures are conditioned to the following qualitative guidelines for suitability.

- 
- Technical feasibility
  - Usefulness during normal weather condition
  - Principle of parsimony of resources
  - Proportionality to the level of vulnerability
  - Compatibility with regulations and society acceptance
  - Effectiveness at reducing vulnerability

First, the technical feasibility constraint is deemed fulfilled if countermeasures are not impractical, such as construction of superconducting cables over high alpine summits. Second, CMCs must be useful not only during extreme weather events, but also during normal weather conditions. Extreme weather events are by definition rare, and CMCs endangering the security of the electricity supply are even rarer. Countermeasures would not be economically justified if they were only valuable in situations unlikely to occur. Therefore, countermeasures must be integrated as alternatives to development plans of transmission networks. Third, the parsimony principle aims at saving human and material resources and matching them with the level of vulnerability. For example, it would be inappropriate to triple all power lines of a network to reduce the vulnerability due to lightning. Furthermore, the compatibility of countermeasures with regulation and social acceptance is crucial. This has been a major burden for the construction or modification of power lines over the past few decades in many countries. Electromagnetic pollution of overhead power lines in addition to the visual impact on the environment need to be minimized for transmission lines to be erected within a reasonable timeframe (OFEN, 2009b). Finally, countermeasures must be effective in reducing vulnerability, although no absolute level is required. This list of guidance principles can be further extended, but are deemed satisfactory for addressing the current search for countermeasures. Kiessling et al. (2003) present a comprehensive overview of the issues mentioned before related to the planning and the construction of overhead power lines.

The last point on the list is quantitatively evaluated by simulating countermeasure effects on the vulnerability index. Practically, the countermeasures are implemented in the SPTS and the calculation of the vulnerability index from Chapter 3.7 is carried out. The results of the simulations are then analyzed and interpreted to determine vulnerability reduction. Countermeasures significantly influencing the vulnerability are accepted as good alternatives to the development plan of the power system.

Although no quantitative objective is required, the proposed countermeasures are able to reduce the vulnerability subject to a list of qualitative guidelines. This is compatible with the objective of the vulnerability assessment, which aims to suggest relevant measures to improve the security of supply. This methodology is not meant to draw definitive conclusions about what must be done, but rather screen suitable actions from possibilities according to a fully described methodology. A thorough examination of countermeasure suitability can take place subsequent to this screening process.





---

## 4 Definition of scenarios for the application to thunderstorms

*This chapter demonstrates the building of plausible scenarios of power transmission system and extreme weather events, which model two extreme thunderstorm events. The first is constructed with data from past events recorded by sensors. The second is a simulated event of six cells crossing Switzerland. The scenarios of power transmission systems model the Swiss electric power system interconnected to the continental Europe transmission network. These scenarios are situated in 2006 and 2018 to study the evolution of vulnerability induced by the construction of new infrastructures of transmission and production. The parameters of the underlying electric, geographic and reliability models are estimated based on currently available information.*

### 4.1 Context

The vulnerability assessment methodology from Chapter 3 is applied to thunderstorms impacting the overhead power lines of the Swiss transmission network. Thunderstorms have been chosen because of their capacity to cause common mode contingencies on transmission networks and because of their complex space-time correlations. In the past, several blackouts have been triggered by lightning striking transmission lines. For example, the Brazilian blackout of 1999 was initiated by thunderstorms disconnecting 440 kV lines leading to a maximum loss of load of 24 GW for a few hours (Gomes et al., 2004). A list of blackouts triggered by thunderstorms is found in Knight (2001), Chapter 6. Lightning is by far the most hazardous feature of thunderstorms regarding very high voltage lines. Precipitation and strong wind are also present during thunderstorms. However, they do not have as significant of an impact as lightning.

Thunderstorms exhibit complex space-time patterns, which are ideal to illustrate the methodology. Moreover, thunderstorms are likely to be more intense and/or frequent due to global warming as mentioned in of IPCC (2007), Chapter 12. Actual climate evolution over the next few decades is debatable, and the prediction of a well-respected institution like IPCC must even be handled with care.

The Swiss transmission network includes 220 kV and 380 kV lines passing over the Swiss territory. This network is connected to the European transmission network stretching all over Europe and connecting large power plants to load centers. Within the next few years, the Swiss electrical power system will change. According to the Swiss Federal Office of Energy, new transmission lines, topology changes and new power plants are planned to be built by the year 2018 (OFEN and ARE, 2001). According to the same source, the consumption is also predicted to rise at a rate of around 1.5% per year. The ongoing liberalization in Europe will modify the power flow patterns, especially between countries. The combined effects of power

system adaptations to increased consumption with the possible augmentation in extreme weather events could increase or change the zones of vulnerability.

## 4.2 Scenarios of extreme thunderstorm event

The scenarios of extreme thunderstorms events are a particular instance of scenarios of extreme weather event (SEWE) as defined in Chapter 3.4. The most hazardous feature of thunderstorms for transmission overhead power lines are lightning strikes. Other features such as wind or hail are usually not intense enough to provoke damages. Thunderstorms exhibit a very large range of space-time behaviors. A thunderstorm event can consist of a single cell to meso-scale convective systems of several cells (Schmid et al., 1997). Their direction, speed and striking rate vary significantly among events and within the same event. Thunderstorms are good candidates to illustrate the methodology of vulnerability assessment because of their complex space-time behaviors. To study the effect of this variability, two scenarios of thunderstorm events are proposed. The first scenario is based on the simulation of two groups of cells passing over Switzerland. The second is the more intense past events recorded by lightning sensors in Switzerland over the past ten years. These scenarios are based on cloud to ground lightning strikes, which are either collected by a lightning locating system or generated by computer simulations.

Table 5: Cloud to ground lightning parameters

Lightning strike n	$S^n = \{x^n, y^n, t^n\}$
Coordinate x of the strike n	$x^n$
Coordinate y of the strike n	$y^n$
Time at impact of the strike n	$t^n$

Each lightning strike is stored as a triplet of ground impact coordinates and time at impact. The coordinate reference system must be the same as for the geographic model of Chapter 4.3.2. The data is stored in a geodatabase of a GIS software (ArcInfo), which allows processing and visualization. These lightning strikes are used to evaluate the exposure of the transmission line segments defined in Chapter 3.4. The general methodology of this chapter is adapted to the case of thunderstorm events.

Lightning strikes are the results of spatiotemporal non-stationary processes driven by complex physical laws. Thunderstorm cells continuously move in space while their shape changes and their lightning rate evolves with time. It is not possible to fully reconstitute these processes from the sole resulting strikes. However, it can be reasonably assumed that the lightning strikes are the outcome of the homogenous Poisson process for a given surface and a small duration. This process generates a sequence of independent and identically distributed strikes in time and space (Box et al., 2008). It corresponds to the case of a thunderstorm cell

---

moving relatively slowly and much larger than the location under investigation. In these conditions, it is possible to approximate locally the ground flash density, which is the average number of strikes per unit of time and surface. This flash density is a pertinent measure of exposure influencing the failure process of transmission line segments.

Practically, the exposure  $E^{l,s}(t)$  at exposure points is measured by the ground flash density derived from the lightning impacts. This density is used by the reliability model to derived the rates of failure of segments of transmission line. Formally, the ground flash density is the number of lightning strikes  $N^Y = \text{card}(Y)$ , counted at a distance closer than  $d^E$  of the exposure point  $s$  of transmission line  $l$  of coordinates  $(x^{l,s}, y^{l,s})$ , divided by the surface defined by the circle of radius  $d^E$ .

$$E^{l,s}(t) = \frac{N^Y}{\pi \cdot d^E{}^2} \quad (4.1)$$

The lightning strike  $n$  belongs to the set  $Y$  if it fulfills the conditions  $C_1$  and  $C_2$ .

$$Y = \{n \in Y \mid C_1(n) = C_2(n) = 1\} \quad (4.2)$$

Where the conditions  $C_1(n)$  and  $C_2(n)$  are true if these inequalities are satisfied:

$$\sqrt{(x^n - x^{l,s})^2 + (y^n - y^{l,s})^2} \leq d^E \quad (4.3)$$

$$|t^n - t| \leq \frac{T^E}{2} \quad (4.4)$$

The first condition implies that lightning strikes belonging to  $Y$  must be at a maximum at Euclidian distance  $d^E$  of the exposure point  $s$ . The second condition imposes that lightning strikes belonging to  $Y$  must occur during the time window  $T^E$  centered in  $t$ . Therefore, the estimate of exposure in terms of ground flash density is a moving average of the number of lightning strikes occurring during  $T^E$ . The radius  $d^E$  and the duration  $T^E$  have to be appropriately set to properly sample the underlying Poisson process. If they are too short, no strikes will be counted, while the opposite will invalidate the assumption of a local Poisson process.

The figure hereunder illustrates the calculation of exposure  $E^{l,s}(t)$  for a specific scenario defined in Chapters 4.2 and 4.3. The exposure is calculated for the segment  $s = 11$  of the line  $l = 81$ , namely SMUEHL2A-SWATTE2A-1 (blue), of the Swiss transmission network 2018.

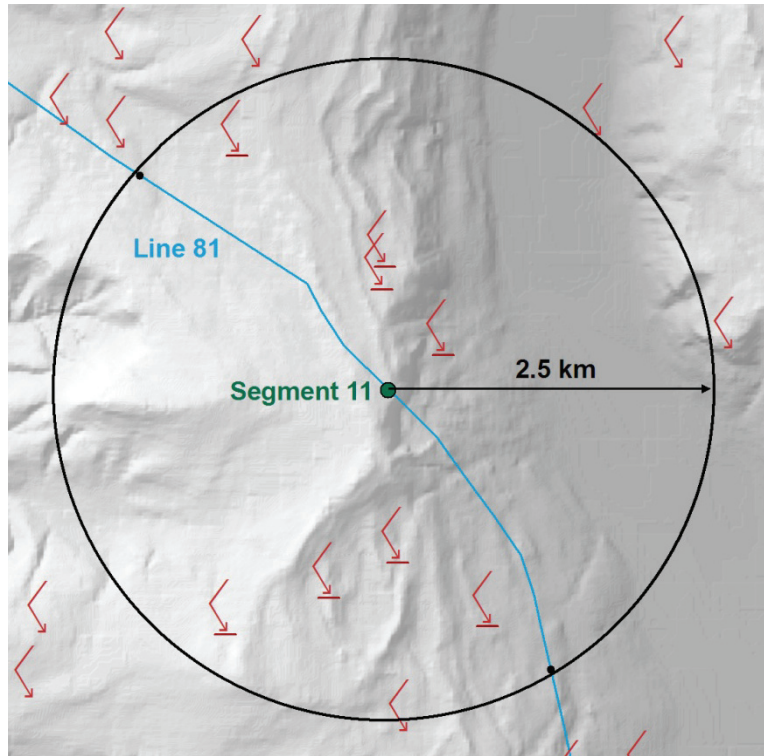


Figure 13: Illustration of segment exposure to lightning strikes

The black circle of radius  $d^E = 2.5 \text{ km}$  is centered on the exposure point of the segment 11 (green point). The red arrows represent lightning strikes during  $T^E = 7.5 \text{ min}$  centered in  $t = 213 \text{ min}$ . These parameters are equal to those used for the application, see Table 11. According to the figure, eight lightning strikes respect the condition (4.2). The calculation of exposure is therefore straightforward.

$$E^{81,11}(t = 213) = \frac{8}{\pi (2.5)^2} = 0.40 \left[ \frac{\text{strikes}}{\text{km}^2} \right] \quad (4.5)$$

#### 4.2.1 Simulated event of an extreme thunderstorm

This first scenario of an extreme thunderstorm event (SEWE 1) is based on one of the strongest and largest types of thunderstorm which can occur in Switzerland, namely mesoscale convective systems. They are usually comprised of several cells moving from the West-South to the East-North. They last a few hours and have strong lightning activity as mentioned in (Schiesser et al., 1996). The most intense of these convective systems can be considered as extreme events.

SEWE 1 has been simulated taking into account the important properties of mesoscale convective systems. This scenario is far from reproducing all the complexity of real events, but the simulation aims at showing the possibility to use SEWE that are not based on past data. It allows the assessment of vulnerability stemming from plausible weather events that could have occurred, which can be useful in case of events that have not been recorded

because they are rare or due to climate change.

The simulated SEWE 1 parameters are reported in Table 6. They are assumed plausible and extreme. The Schiesser et al. (1995) article contains precious information about mesoscale convective systems in Switzerland, and this article greatly inspired the parameters of SEWE 1.

Table 6: Definition of SEWE 1 parameters

	Group 1				Group 2	
	Cell 1	Cell 2	Cell 3	Cell 4	Cell 1	Cell 2
Initial position X [km]	516.153	529.857	462.3	464.888	680.099	715.629
Initial position Y [km]	106.137	73.145	86.34	23.403	92.94	80.759
Direction [°]	50	50	50	50	73	73
Speed [km/h]	60	60	60	60	40	40
Radius [km]	12.5	12.5	12.5	12.5	12.5	12.5
Shape	circle	circle	circle	circle	circle	circle
Duration [h]	6	6	6	6	2	2
Flash rate [# /min]	14	14	14	14	14	14

The SEWE1 is composed of two groups of respectively four and two convective cells. Each of the groups has a vectorial speed, initial location and duration.

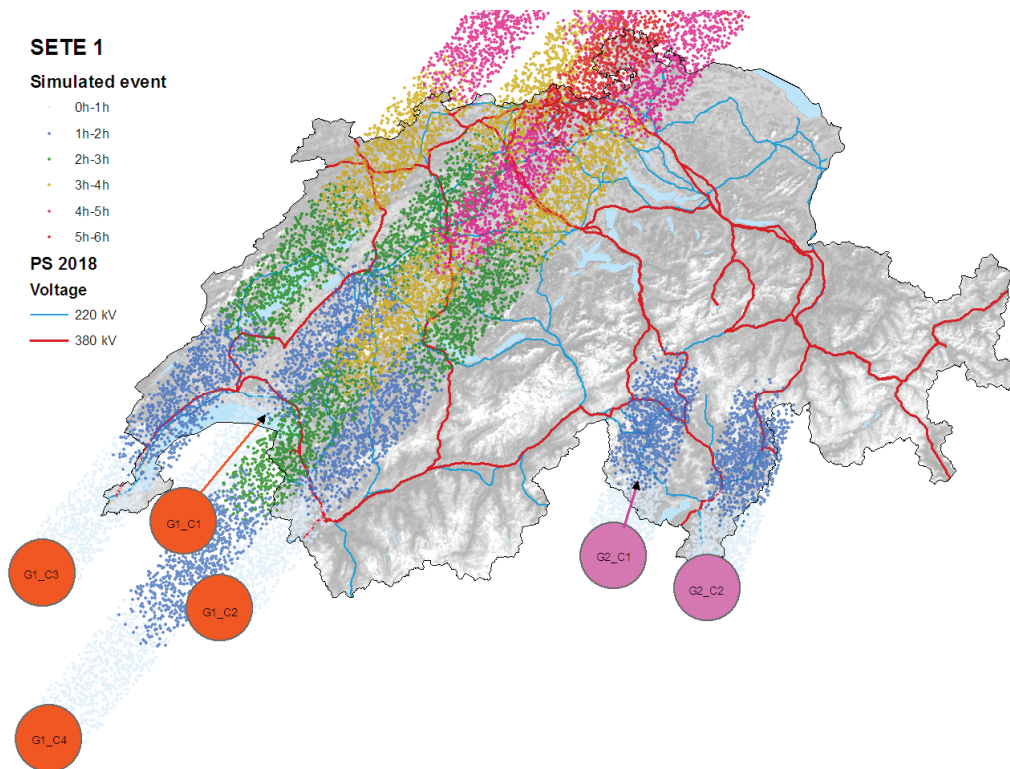


Figure 14: Illustration of SEWE 1

All the convective cells also have the same constant clouds-to-ground lightning rate.

Lightning strikes have been randomly generated in each cell taking into account their time-dependent path. The next map illustrates SEWE 1. The lightning impacts are colored according to their striking time within a range of one hour.

The number of lightning strikes reaches 23,603 after six hours. Among those, 5,652 were at less than 2.5 kilometers from an overhead power line of the electrical scenario of the plausible scenario 2018 (PS 2018) defined in Chapter 4.3. Appendix 9.4 exhibits more details of the SEWE 1. In particular, the lightning strikes at less than 2.5 km and the time-dependent number of strikes around the transmission lines of the PS 2018.

It is visually obvious that the SEWE 1 does not have all space-time correlations as in a real thunderstorm event. However, the SEWE 1 shares some properties real events, which occurred or could occur in the future. Zones of vulnerability which are still unknown could be disclosed by this simulated SEWE.

### 4.2.2 Real past thunderstorms event

SEWE 2 was recorded by a lightning detection system starting at 10 a.m. on June 27<sup>th</sup>, 2001. This event is the most intense found lightning strike database covering 10 years. The detection system is owned and managed by the company Meteorage providing georeferenced data of lightning strikes in Switzerland and other European countries (Finke and Kreyer, 2002). SEWE 2 lasted 24 hours with several peaks of activity (see Appendix 9.4). The sensors have sufficient average detection rate of 85% and an accuracy of 800 meters. The detection rate in the mountainous regions is certainly lower than 85%. These characteristics are largely sufficient for this application. The next map illustrates SEWE 2. The lightning impacts are colored according to their striking time within a range of four hours.

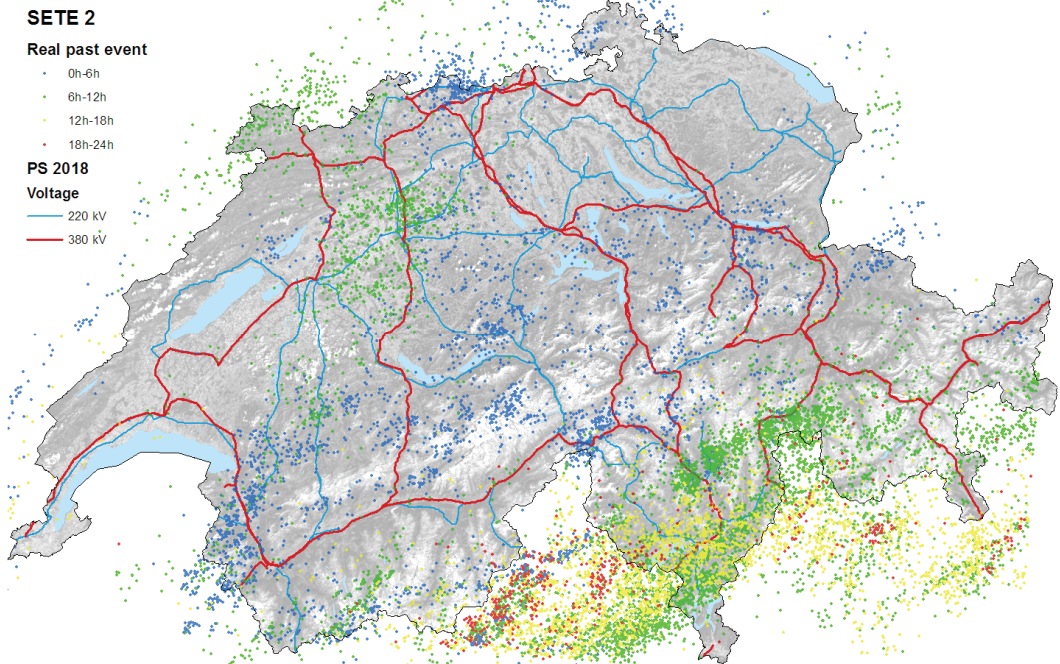


Figure 15: Illustration of SEWE 2

---

During the event, 14,067 lightning strikes were recorded and 5,354 were at less than 2.5 kilometers of the transmission line of the PS 2018. SEWE 2 is as intense in terms of strike number when compared to the simulated scenario SEWE 1, but lasted one day instead of six hours. SEWE 2 shows complex space-time correlations. The majority of the strikes are located in the southern part of Switzerland and in some limited zones in the northern part. The map of Appendix 9.4 shows lightning strikes at less than 2.5 km of power lines of the electrical scenario 2018.

### **4.3 Scenarios of the Swiss electric power system**

Two plausible scenarios of the Swiss electric power system are crafted for 2018. At this date, most of the transmission infrastructures mentioned in (OFEN and ARE, 2001) and new projects of hydro pumped-storage power plants stated by several Swiss electric utilities are expected to be operational. These two plausible scenarios (PSs 2018) are for the summer peak and off-peak periods. It is clear that the state of the system in 2018 will be different than those modeled in PSs 2018. The objective is not to predict the complete and true electric system, but rather plausible models are searched for this application.

The PSs 2018 are models of the system as described in Chapter 3.3 by the scenarios of the power transmission system (SPTS). It contains an electric, a geographic and a reliability model. The PSs 2018 are crafted from modified data of the system of 2006. Two SPTS in 2006, named reference scenarios (RSs 2006) have been built to serve as a basis for the PSs 2018. The latter are the central part of the vulnerability investigation. Nevertheless, the RSs 2006 are also investigated in order to draw some comparisons between 2006 and 2018. Care must be taken when comparing two different scenarios. Indeed, the set of probable common mode contingencies (CMCs) are not the same due to changes in the transmission infrastructures. Zones and levels of vulnerability are sensible based on the choices of these sets. The evolution of vulnerability between 2006 and 2018 could stem from either intrinsic changes in scenarios or from the differences between CMC sets. The interpretation of the vulnerability analyses must take this fact into consideration.

In the following subchapters, the RS 2006 and PS 2018 are described. They comprise two different electric and geographic models as well as a common reliability model.

#### *4.3.1 Electric model for RS 2006 and PS 2018*

The Electric Model is fully described in the methodology from Chapter 3.3, which is the central point of the severity assessment of the plausible CMC set. This model is compatible with the AC power flow model and contingency analysis calculations. The electric model is implemented for the Swiss transmission network connected to the continental European transmission network supplying around 450 million people. The Swiss transmission network

---

is without a doubt not an island, but rather imports, exports and transits of power flows through the Swiss borders are daily business (UCTE, 2008). The interconnection requires the inclusion of neighboring countries in the electric model. Therefore, it requires important resources to be built from scratch. Fortunately, this work has already been done and ready to use models are available at the TSOs. They consist of instantaneous pictures or “snapshots” of the state of the system at a given time in the format of a text file. The Swiss TSO Swissgrid has even provided a summer peak and off-peak snapshot of 2006. This data is confidential and cannot be disclosed. In the remainder of this research, a careful selection of information has been prepared to ensure there are no infringements regarding confidentiality clauses. Here is the list of data included in the snapshot.

- Time and date of the snapshot
- Buses name and their nominal voltage
- Active and reactive power injection from generators and loads
- Type of generators, i.e. PQ, PV, SB (including range of reactive power for PV)
- Resistance, reactance, capacitance and conductance of transmission lines
- Transformers and their electrical characteristics
- Power line and transformer current ratings
- Incident matrix connecting buses, power lines and transformers

The two RSs 2006 are based on the summer peak and off-peak snapshots. These two snapshots have been taken at 10:30h and 3:30h CET on July 19<sup>th</sup>, 2006. Snapshots represent particular cases of the system including power line maintenances, which are numerous during summertime. The transmission lines in maintenance changes from week to week if not day to day. A vulnerability analysis performed on these particular states would give particular vulnerability results. To have a better estimation of the intrinsic vulnerability, normative scenarios are considered. This means that all infrastructure overhauls are not taken into account and active elements are fully operational. Here is a summary of the modifications of the snapshots.

- All power lines under maintenance are reconnected
- All the hydro Swiss power plants are set to their maximum active power for the peak period
- Swiss hydro power plants are turned off and pumps are turned on at their maximum active power for the off-peak period

Transit flows at the Swiss borders also have to be adjusted to values close to what could be considered as plausible. Past transit flows are available from the website of the European network transmission system operators for electricity (ENTSO-E, 2010). Based on this information, it is assumed that Italy imports approximately 3 GW. This value is considered as fixed in all the scenarios. The transit flows have been adapted to satisfy the 3 GW export to Italy while ensuring plausible flows import or export to neighboring countries. These adjustments are performed by modifying the power generation of four nodes in France, Germany, Austria and Italy. These nodes are located near major areas of production and consumption.



In addition, a contingency analysis is performed on every element of the Swiss power system and the interconnection power lines to ensure that the RSs 2006 meet the N-1 criterion. In case of non-respect, minor changes of the power generation of critical power plants are carried out. The table hereafter summarizes the main characteristics of the RSs 2006 in terms of production, consumption, imports and border transits. These values have been confirmed plausible by experts from several Swiss electric utilities.

Table 7: Production, consumption and transit flows of RS 2006 for Switzerland

Period	Name	Import	Prod.	Cons.	CH->DE	CH->FR	CH->IT	CH->AT
Summer peak	RS SP 2006	-3097	8983	5887	213	267	2942	-325
Summer off-peak	RS SOP 2006	774	3158	3933	-1132	-2026	2954	-570

The power unit of the table is given in megawatts. Some relevant characteristics of the two 2006 are reported in Appendix 9.5.1.

The Plausible Scenarios (PSs) for 2018 integrate the new transmission and production infrastructures planned by 2018 for peak and off-peak periods. It is a modified version of the RSs 2006 taking into account 57 network modifications, and 7 new or upgraded power plants for additional power of 3.6 GW. The network modifications are mainly taken from the report of the transmission lines and supply security workgroup (OFEN and ARE, 2001). Parameters regarding the new power lines and transformers have been gathered from scenarios provided by two Swiss electric utilities, BKW-FMB and Alpiq as well as direct contacts with their collaborators. The loads are assumed to increase uniformly by 20% until 2018, which corresponds to a yearly rate of 1.5% (AES-VSE, 2006). The rest of the continental Europe transmission network has been kept as in the RS 2006. The PSs 2018 are only two plausible alternatives of the Swiss electric power system in 2018. This scenario includes the infrastructures, which have a possibility to be operational at this date. Details about this scenario are found in tables of Appendix 9.5.1. An electric schema of the PS 2018 is presented in Appendix 9.5.2, and it includes comments about changes made to turn the RS 2006 into the PS 2018.

During peak periods, all hydro power plants are at their full capacity. During off-peak, hydro power plants are off and the pumps are at their full capacity. This explains the high consumption and imports during the night. The N-1 criterion is met for both of the scenarios. Some productions have been lowered (-180MW) to satisfy this criterion. The export to Italy in 2018 is not yet known. However, the value of 3 GW assumed for 2006 is also plausible for 2018 despite the new transmission and generation capacities. Indeed, few new infrastructures are planned to increase capacity between Switzerland and Italy. During off-peaks, power is mainly imported from Germany and France to cover the national consumption including pumped-storage power plants. Indeed, the two countries dispose of extra generation capacity during off-peak hours, such as nuclear and coal-fired power plants. During peak hours, the Swiss surplus of production is distributed into 3 GW to Italy and the rest to Germany and France. It is worth mentioning that these border flows are physical and are not commercial

agreements. For example, power generated in France can flow through the German border. The following table summarizes the main characteristics of the PSs 2018 in terms of production, consumption, imports and border transits.

Table 8: Production, consumption and transit flows of PS 2018

Period	Name	Import	Prod.	Cons.	CH->DE	CH->FR	CH->IT	CH->AT
Summer peak	PS SP 2018	-5671	12711	7040	1412	958	2949	353
Summer off-peak	PS SOP 2018	2877	5478	6674	-2275	-2423	2940	-1119

Swiss off-peak consumption is almost as high as the peak. This is due to the construction of around 2.2 GW of pump-storage power plants. They store the affordable off-peak energy to produce high value peak energy. Therefore, their justification seems more economic instead of being related to security of supply. They require large off-peak imports, which could create congestion zones and thus vulnerable zones. This encourages the investigation and identification of off-peak periods, which are usually not critical in the summertime.

New power lines and network topology modifications are driven by new means of production, elimination of bottlenecks, adoption of new power flow patterns, rise in consumption, and better interconnectivity to neighboring countries. Uncertainties regarding the evolution of these drivers and the investments they require are significant. Therefore, the PSs 2018 are only possibilities, not predictions. Therefore, the PSs 2018 serve as an illustration of the vulnerability assessment methodology and should not be considered as actual forecasts of the future Swiss transmission network.

#### 4.3.2 Geographic model of RS 2006 and PS 2018

The geographic model contains the paths of the overhead power lines of the electrical model as defined in Chapter 3.3.2. The geographic data was provided by two Swiss electrical utilities (BKW-FMB and Alpiq) for the western part of Switzerland. The rest of the data was provided by the Federal Office of Topography by its model Vector 25 (Swisstopo, 2010). The reference coordinate system is the CH1903, which is the standard for official cadastral surveying, GIS applications and cartography in Switzerland. The peak and off-peak RS 2006 share the same geographic model. The paths of the overhead power lines pass approximately by the middle point of the pylons. The vulnerability assessment methodology does not require the same precision as in cartography (i.e. a few / ten meters away from the real position would not have significant consequences on the vulnerability). The following flowchart shows the construction process of the geographic model (GM) for the RS 2006.

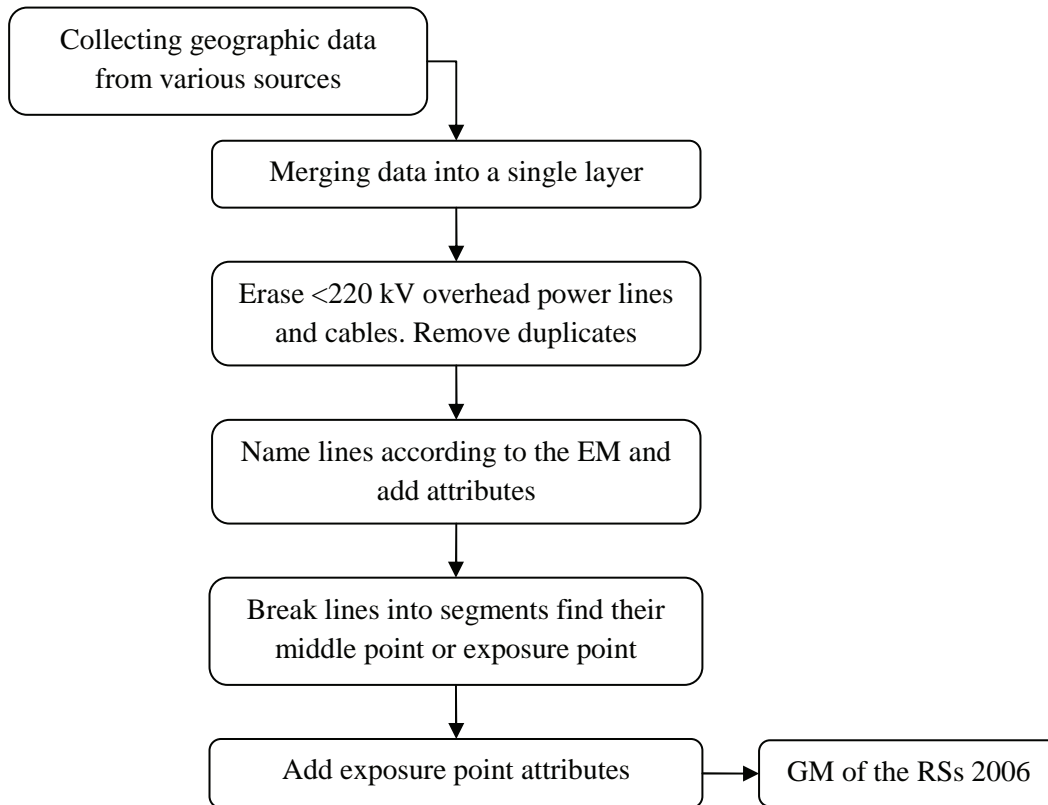


Figure 16: Building of the geographic model of the RSs 2006

The geographic model 2006 is quite easily built because all power lines of the electric model had at least one equivalent in the geographic data collected. Only the lower voltages networks had to be erased as well as cables. High voltage cables can be safely deleted because they are quasi invulnerable to extreme weather events and their total length is negligible compared to overhead lines.

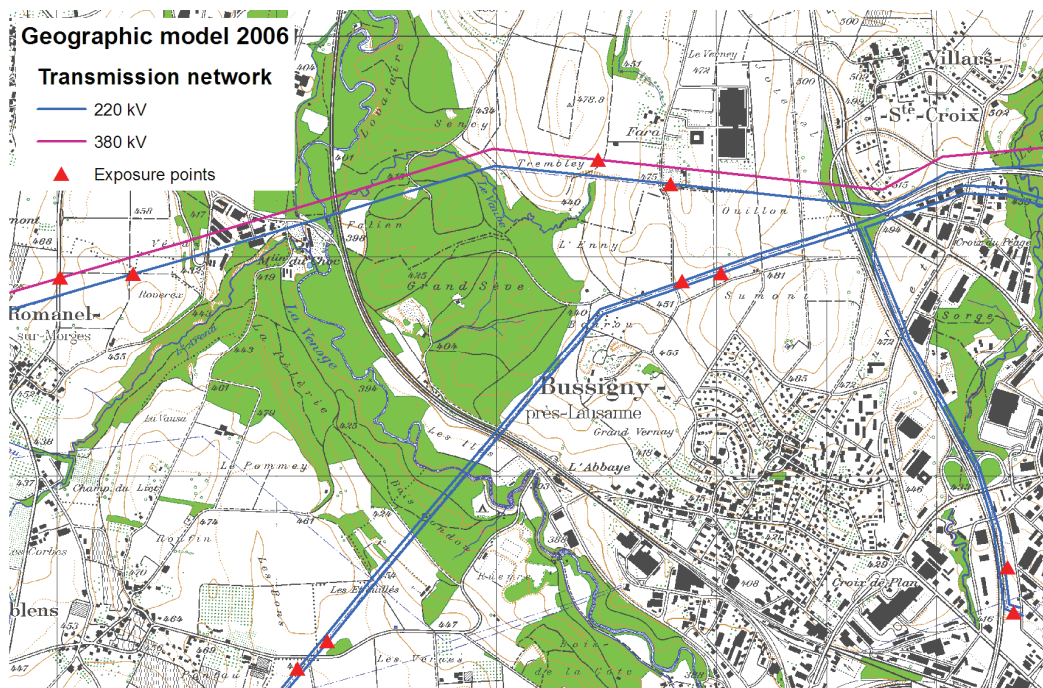


Figure 18: Zoom in the geographic model 2006

Here above, a map illustrates a zone of the geographic model 2006 by zooming in the region of Bussigny in the canton of Vaud. Power lines of 220 kV and 380 kV are shown as well as exposure points represented by red points evenly spaced at  $d^s = 2.5 \text{ km}$ . This map was generated by ArcInfo. This software was used to build the GMs.

The geographic model for the PSs 2018 is more difficult. According to electric model (EM), new lines must be added or modified. However, their path is not yet exactly known in totality. Information about paths are scattered in diverse documents and can change year after year. It is believed that the best has been done to find paths which are plausible considering available information. The following schema summarizes the crafting process of the geographic model 2018.

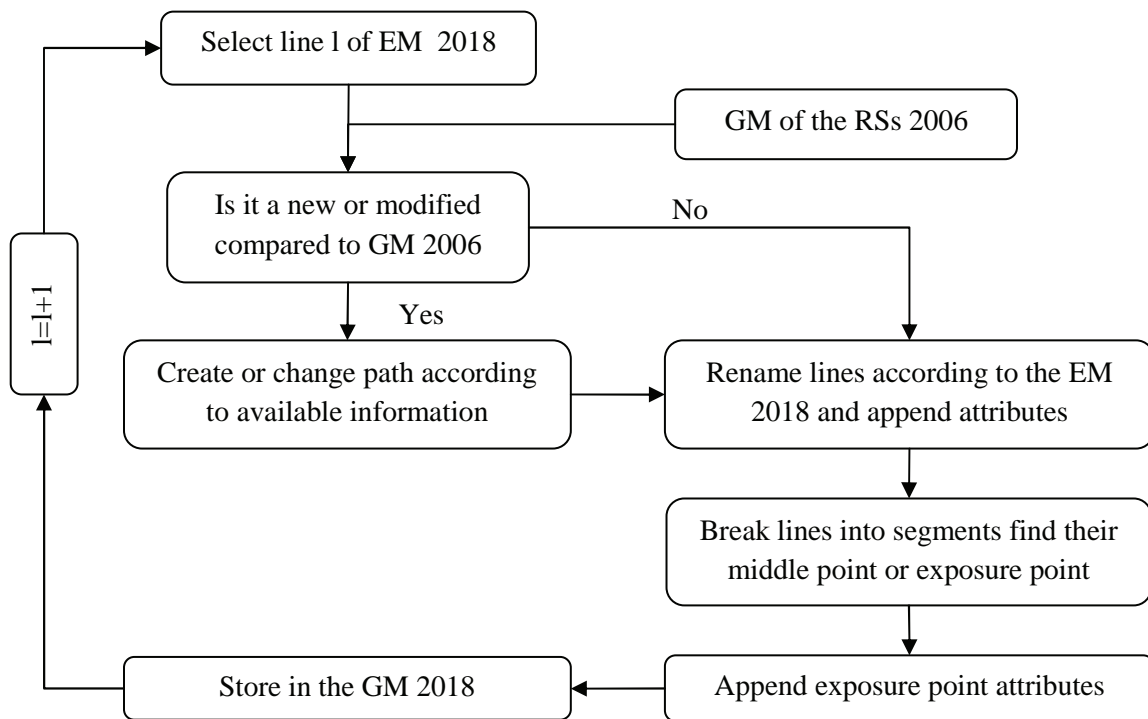


Figure 17: Building of the geographic model of the PSs 2018

Full maps of the geographic model 2006 and 2018 are detailed in Appendix 9.5.3 along with statistics of the geographic model and samples of lines and exposure points attributes.

### 4.3.3 Hazard function of the reliability model

The reliability model and the hazard function are formally described in Chapter 3.3.3. The hazard function  $h$  transforms the exposure  $E^{l,s}(t)$  of an exposure points  $s$  into the rate of failure  $\lambda^{l,s}(t)$  according to some resistance parameters  $R^{l,s}$ . By definition, the rate of failure is the probability  $P_f^{l,s}$  per unit of time  $dt$ .

---


$$\lambda^{l,s}(t) = h(R^{l,s}, E^{l,s}(t)) = \frac{Pr(t \leq T < t + dt | T \geq t)}{dt} = \frac{P_f^{l,s}(t)}{dt} \approx \frac{P_f^{l,s}(t, \Delta t)}{\Delta t} \quad (4.6)$$

Where  $T$  is a continuous random variable denoting the time to failure of the segment represented by the exposure point  $s$  of the power line  $l$ .  $P_f^{l,s}$  is the probability of the segment to fail between  $t$  and  $t + dt$  knowing it was operational until  $t$ .

The evaluation of  $P_f^{l,s}(t)$  in function of the exposure  $E^{l,s}(t)$  and the resistance factor  $R^{l,s}$  is derived from the next equation proposed by the handbook for improving overhead transmission line lightning performance (Phillips, 2004). The number of flashover  $FO(t, \Delta t)$  of a segment of transmission line is the product of the ground flash density by a lightning performance factor.

$$FO(t, \Delta t) = GFD(t, \Delta t) \cdot LPF \quad (4.7)$$

Where  $FO(t, \Delta t)$  is the average number of flashover during  $\Delta t$  around  $t$ ,  $GFD(t, \Delta t)$  is the average ground flash density during  $\Delta t$  around  $t$ , and  $LPF$  is the lightning performance factor equivalent to the resistance factor  $R^{l,s}$ . It is constitutive to the design of the segment including pylons, conductors, isolators and shield wires.

Flashovers designate short circuits between at least one phase conductor to the ground. They are due to direct lightning strikes on conductors or shield wires. Every flashover entails the disconnection of the line until reconnection by automatic reclosing breakers or manually by operators. De Conti et al. (2006) shed the light on the mechanism underlying flashovers due to lightning strikes.

According to Bessis (2007), if the number of occurrences of an event is very small, this number of occurrences is approximately equal to the probability of the event. Therefore, if the number of flashovers respects (4.9), it is approximately equal to the probability of failure .

$$FO(t, \Delta t) \approx P_f^{l,s}(t, \Delta t) \quad (4.8)$$

$$\text{If } FO(t, \Delta t) \ll 1 \quad (4.9)$$

The condition (4.9) must also be respected for another reason. Indeed,  $P_f^{l,s}(t)$  is defined for non-repairable items while the probability of failures, derived from the number of flashover  $FO(t, \Delta t)$ , is related to “repairable” items. According to Ascher and Feingold (1984), these two different types of probabilities are approximately equal when (4.9) is true.

The  $GFD$  is the number of lightning strikes  $S(t, \Delta t)$  during  $\Delta t$  in an area  $A$  around the segment. Therefore,  $GFD$  is equal to the exposure  $E^{l,s}(t, T^E)$  as implemented in equation (4.1).

$$GFD(t, \Delta t) = \frac{S(t, \Delta t)}{A} = E^{l,s}(t, T^E) \quad (4.10)$$

---


$$\text{with } T^E = \Delta t \quad (4.11)$$

Equation (4.7) combined with (4.8) and (4.10) yields to:

$$P_f^{l,s}(t, \Delta t) \approx E^{l,s}(t, \Delta t) \cdot R^{l,s} \quad (4.12)$$

Therefore, the rate of failure (4.6) is approximated by:

$$\lambda^{l,s}(t) \approx \tilde{\lambda}^{l,s}(t) = \frac{E^{l,s}(t, T^E) \cdot R^{l,s}}{T^E} \quad (4.13)$$

The rate of failure of segments is function of their exposure, their resistance factor, and the time window  $T^E$  of the sampling process of lightning impacts. Methods for evaluating the resistance factor  $R^{l,s}$  are has been thoroughly studied over the past 40 years. These methods requiring numerous parameters of transmission lines and time consuming simulations (Alberto Nucci, 2010). These methods are not well-suited at the time of resistance estimation of all segments of a large transmission network. Therefore, some simplifications are required and in this case, it is assumed all the segments of transmission lines of the same nominal voltage, i.e. 220 kV and 380 kV, have the same resistance factor per unit of length. These two voltages are considered separately because they significantly influence this factor.

$$R^{l,s} = d^{l,s} \cdot R^1 \quad \text{if } l \text{ is a 220 kV line} \quad (4.14)$$

$$R^{l,s} = d^{l,s} \cdot R^2 \quad \text{if } l \text{ is a 380 kV line} \quad (4.15)$$

According to (4.7), the resistance factor can be evaluated knowing the number of flashovers and the number of lightning strikes counted during  $\Delta t$  around  $t$  within a surface  $A$  around the segment.

$$R^1 \text{ or } R^2 = \frac{FO(t, \Delta t)}{GFD(t, \Delta t)} = \frac{FO(t, \Delta t) \cdot A}{S(t, \Delta t)} \quad (4.16)$$

The two resistance factors have been estimated for the year 2005. It is assumed they will not significantly change until the year 2018. The terms of equations (4.16) are calculated for an average segment of 1km for the 220 kV and 380 kV networks.

The number of lightning strikes  $S^{net}$  is estimated in a buffer zone of 2.5 km on each side of the transmission lines of the geographic model 2006. Then, this number is divided by the length of their respective network  $L^{net}$  in order to compute the number of strikes  $S$  for the average segment. Practically, the number of lightning strikes has been evaluated by ArcInfo and the Meteorage database for 2005 which includes the geo-referenced cloud to ground lightning over Switzerland (Meteorage, 2010).

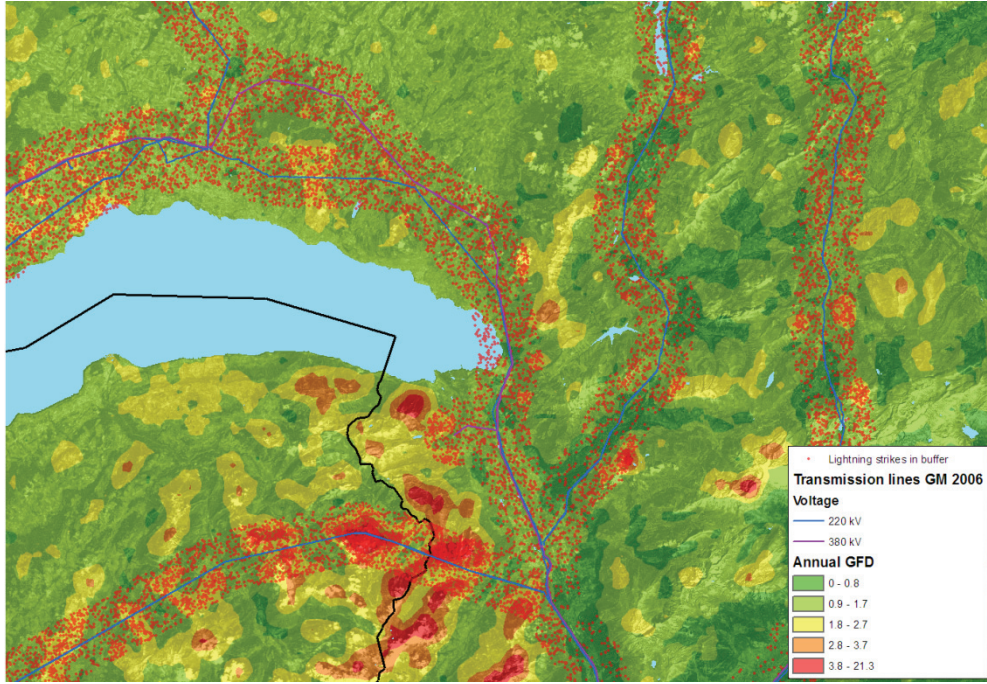


Figure 19: Evaluation of number of lightning strikes with ArcInfo

The number of flashover per kilometer is extracted from the annual statistics for 2005 of the Swiss transmission network (AES-VSE, 2005). The calculations of the resistance factors  $R^1$  and  $R^2$  are detailed in the table hereunder.

Table 9: Calculation of the resistance factors scaled to two reference segments

	Unit	220 kV lines	380 kV lines	Source
$S^{net}$	#	14356	7730	ArcInfo analysis
$L^{net}$	km	4406	1919	ArcInfo analysis
$S$	#/km	3.25	4.02	$S^{net}/L^{net}$
$A$	km	5	5	Buffer width
$GFD$	#/km <sup>2</sup>	0.65	0.8	$S/A$
$FO$	#/km	$1.6 * 10^{-2}$	$5.6 * 10^{-3}$	AES statistics
$R^1, R^2$	km	$2.4 * 10^{-2}$	$7.0 * 10^{-3}$	$FO/GFD$

Finally, the resistance factors of 220 kV and 380 kV segments per unit of length are:

$$R^1 = 2.4 * 10^{-2} \quad \text{and} \quad R^2 = 7.0 * 10^{-3} \quad (4.17)$$

These resistance factors are rough estimates of the true value of the actual segments, because available statistics about flashovers are aggregated at the network level. However, the order of magnitude of these values is sufficient to identify major zones of vulnerability.

---

The transmission line length and exposure to extreme weather events are more contributing than resistance factors to the probability of CMCs. As new data becomes available, these factors can be more precisely estimated.

#### 4.3.4 Reconnection rate of the reliability model

The reconnection process puts transmission lines back in service after flashovers. This process aggregates the actions of auto-recloser breakers, operator's maneuvers or physical repair. As mentioned in Chapter 3.3.3, this process is modeled by a constant rate of reconnection. In addition, it is assumed that the rate is equal for all power lines.

$$\mu^l(t) = \mu^l = \mu \quad (4.18)$$

A unique and constant rate of reconnection is a harsh simplification. In reality, automatic security systems are much faster at reconnecting lines than fixing teams. A variable and distinct rate of reconnection would increase the complexity of the model and would stumble on the limited available outages data. Indeed, they are generally not detailed enough to infer different rates of reconnection for each power line. In addition, a more detailed modeling would not necessarily lead to different conclusions about the existence of major zones of vulnerability.

The estimation of the rate of reconnection stems from statistical outage data. If they are sufficiently detailed, a mathematic model of the reconnection process could be fitted by a linear regression or other methods as described in (Gross, 2003). Unfortunately, the available statistics are too aggregated to perform the methods mentioned herein. Indeed, the annual statistics of the Swiss electric network only contain the initial number of disconnected transmission lines by lightning strikes and the number of lines still disconnected after three minutes (AES-VSE, 2005). However, it is sufficient to carry out an estimate of the reconnection rate since it is assumed constant in time.

A process with a constant rate of reconnection follows an exponential distribution (see Appendix 9.2. The probability of reconnection after  $t$  is given by:

$$U(t) = \Pr(T \geq t) = e^{-\mu \cdot t} \quad (4.19)$$

Where  $T$  is the random variable of time to reconnection of a transmission line. Applying the logarithm function on both sides of the equation yields to:

$$Y(t) = \text{Log}(U(t)) = -\mu \cdot t \quad (4.20)$$

Therefore, the reconnection rate  $\mu$  is the slope of  $Y(t)$ . This model can be fitted to actual data by a linear regression to estimate  $\mu$ . If only two values are available, the regression is



---

transformed in simple slope estimation.

$$\hat{\mu} = -\frac{\hat{Y}(t^1) - \hat{Y}(t^0)}{t^1 - t^0} \quad (4.21)$$

Posing  $N(t)$ , the number of lines still disconnected after  $t$  from statistical data. Assuming the ergodic hypothesis, the natural estimator of the probability of reconnection after time  $t$  is (UCTE, 2008, Brémaud, 2001a):

$$\hat{U}(t) = \frac{N(t)}{N(0)} \quad (4.22)$$

According to these reports for the years 2001, 2003, 2004 and 2005, 594 disconnections caused by thunderstorms have been reported, and 92 of them lasted more than three minutes.

Table 10: Number of outages caused by thunderstorms during four years

$t$ [s]	$N(t)$	$\hat{U}(t)$	$\hat{Y}(t)$
0	594	100%	0
180	92	15%	-1.87

The estimate  $\hat{\mu}$  of the rate of reconnection is straightforward applying (4.21) with the data from Table 10.

$$\hat{\mu} = -\frac{-1.87 - 0}{180 - 0} = 0.010 \quad (4.23)$$

Two assumptions are made for the reconnection rate. First, it is constant in time. It requires that there is no discrimination between fast automatic security systems and slow manual operations. The dynamics of the reconnection process are lumped into a single constant behavior. Second, each power line has the same rate of reconnection. It requires that short and long lines or aged and recent lines are reconnected at the same rate. These assumptions could have an impact on the results of the vulnerability assessment. However, simplifications are unavoidable to limit the complexity of the model. In addition, data is rare at this level of detail and confidential if existent. However, it is believed that the level of simplification is appropriate to this concrete case illustration.



---

## 5 Vulnerability assessment of the Swiss electric power system

*The vulnerability assessment is carried out for the scenarios of transmission systems impacted by the two extreme thunderstorm events defined in Chapter 4. The main objective of this chapter is the identification of major zones of vulnerability. First, the probability of plausible sets of common mode contingencies is evaluated by space-time simulations. Then, the severity of the most probable contingencies is assessed by contingency analyses. The vulnerability of the plausible scenario 20018 impacted by the simulated extreme thunderstorm event is fully analyzed with regards to temporal and aggregated vulnerability indexes in addition to the identification of major zones of vulnerability. Finally, zones of vulnerability are identified for the other combination of scenarios to allow the proposal of countermeasures in Chapter 6.*

### 5.1 Performing the simulations

#### 5.1.1 Main stages of the vulnerability assessment

To carry out the numerical simulations of the vulnerability assessment described in Chapter 3, four major stages are required. Stage A, the geographic models and the electric models of the scenarios of the power transmission system (SPTS) as well as the scenarios of the extreme weather event (SEWE) are crafted and implemented in databases as described in Chapter 4. The parameters of the reliability model are appended to the geographic models. In Stage B, the temporal unavailability of each transmission line is calculated by a numerical solving method. The most probable power lines to fail are combined amongst themselves to generate the set  $\Gamma^m$  of common mode contingencies (CMCs). Then, their temporal unavailability is computed according to Chapter 3.5. In Stage C, the severity of the most probable CMCs is evaluated by a contingency analysis presented in Chapter 3.6. In Stage D, the vulnerability indexes and matrixes are computed and major zones of vulnerability (MZV) are identified according to Chapters 3.7. The following schema shows in which programs the four stages are implemented.

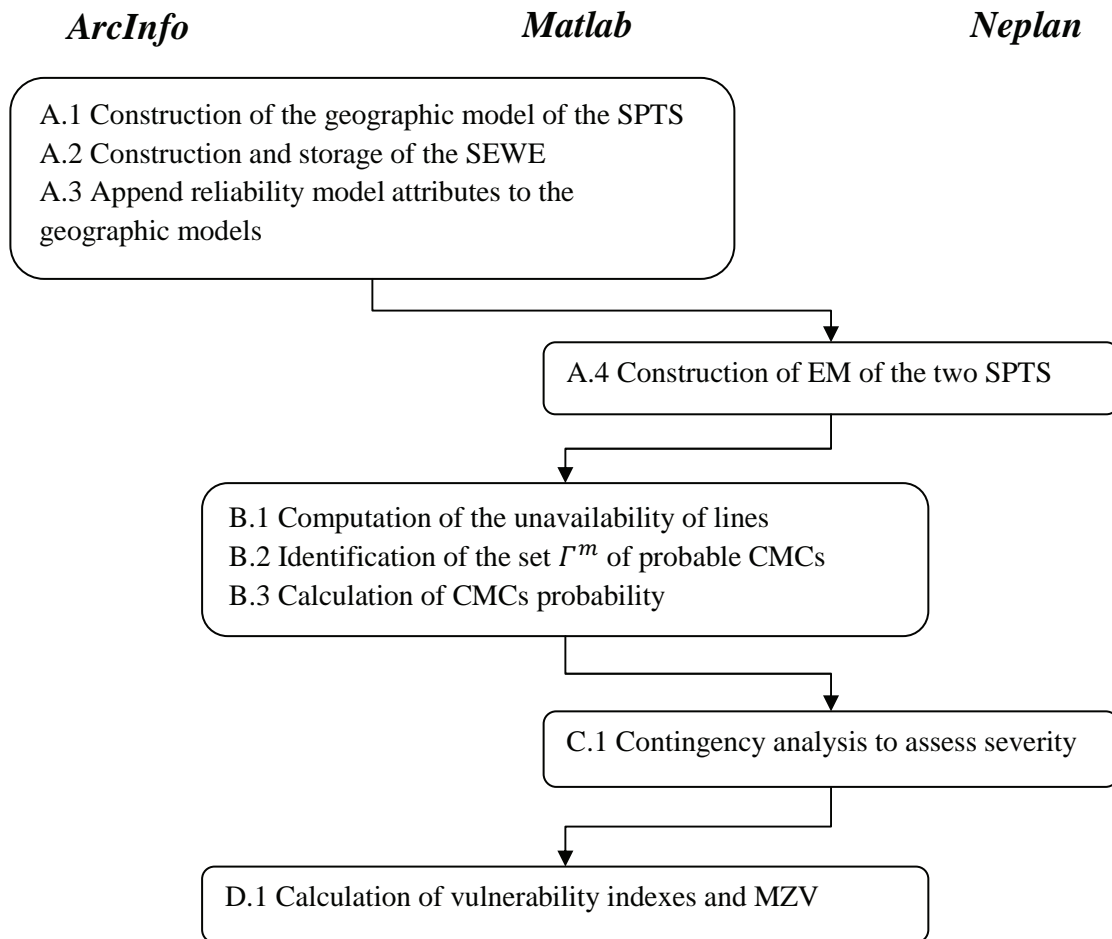


Figure 20: Stages of the simulations implemented in three software

The GIS software ArcInfo allows the processing, visualization and storing of the geographic models and scenarios of extreme thunderstorm events. Unfortunately, GISs are not made to conveniently handle time dependent problems. Consequently, the temporal unavailability is performed under Matlab, which can handle with great ease any numerical problems regardless of their dimensions. Matlab has a GIS toolbox allowing the loading of ArcInfo data and performance of basic functions. Matlab has enough GIS capabilities to carry out the required calculations of transmission line unavailability. In addition, Matlab assures the flow of data with the two other programs. Nevertheless, all the functions implemented in Matlab scripts could have been programmed in ArcInfo or in another GIS environment. This would require only some specific skills by the programmer. On the contrary, the construction of electric model and the contingency analyses could not have been performed elsewhere, except for in a fully dedicated software of power system analysis such as Neplan. Its advanced functions of editing and analyses are the results of years of development. Real electric networks require professional software for their modeling and analysis because of their complexity and size.

---

### 5.1.2 Parameters of the simulations

A few parameters related to discretization processes have to be set before carrying out the simulation. For example, computer-based simulations and SEWE require appropriate steps of discretization, which is often a trade-off between accuracy and calculation speed (Bossel, 1994). When steps are small, more details can be taken into account. However, steps of discretization cannot be too small for two main reasons. First small steps imply more memory and more calculations, which require higher computing resources. Second, there exists a lower limit where smaller steps do not imply a significant discretization error.

The geographical model from Chapter 3.3.2 is composed of lines divided into segments of length  $d^{l,s}$  represented by exposure points. The length cannot be too small because it would significantly augment the number of segments and thus the duration of the simulation. On the other hand, the length cannot be too large because the local variations of extreme weather events could not be taken into account. Since most thunderstorm cells are larger than 10 km, a segment length of 2.5 km is assumed to be a reasonable compromise. There is almost no risk that significant thunderstorms could pass between two exposure points of segments without being detected. On the other hand, a shorter distance would not be likely to grasp more information about the space-time correlation of thunderstorms, which have a finite spatial resolution.

In the calculation of the exposure as defined in Chapter 4.3.3, the influence distance  $d^E$  and size of the moving average window  $T^E$  has to be defined. Both of these parameters cannot be too small, otherwise too few lightning strikes would be detected and the evaluation of the exposure would not be representative of the actual thunderstorm. If these parameters are too large, the local space-time patterns of thunderstorms would be averaged. Again, the exposure would not be representative of the actual thunderstorm. To get a good representation, the length and duration should be smaller than the space-time scale of a thunderstorm cell. Most of the cells are larger than 10 km and they do not move faster 80 km/h or 1.3 km/min (Schmid et al., 1997). The influence distance  $d^E$  is set at 2.5 km, which is a fraction of a standard cell size. On the other hand, a 10 km wide cell with a speed of 1.3 km/min takes 7.5 min to entirely pass over a given point. It is proposed here to set the  $T^E$  at 7.5 min. If  $T^E$  was set radically below 7.5 min, the number of strikes detected could be too low to be representative. The exposure would peak at each lightning strike and be zero otherwise. If  $T^E$  was set drastically above this value, the space-time dynamic of thunderstorms would be averaged and thus lost. The estimate of the exposure from scenarios based on lightning strikes limits the space-time dynamic. Lightning strikes do not contain enough information to derive a smooth and complete exposure. However, it is often the only appropriate data available in the case of thunderstorms.

The differential equation (3.6) describing the temporal unavailability of transmission lines and the probability of CMCs of equation (3.31) are numerically solved under Matlab and its simulating platform Simulink. It allows the graphical modeling of systems and their constitutive equations. It provides a user-friendly environment to model complex systems in a natural way. The unavailability leading to the probability of CMCs is modeled by the following block diagram.

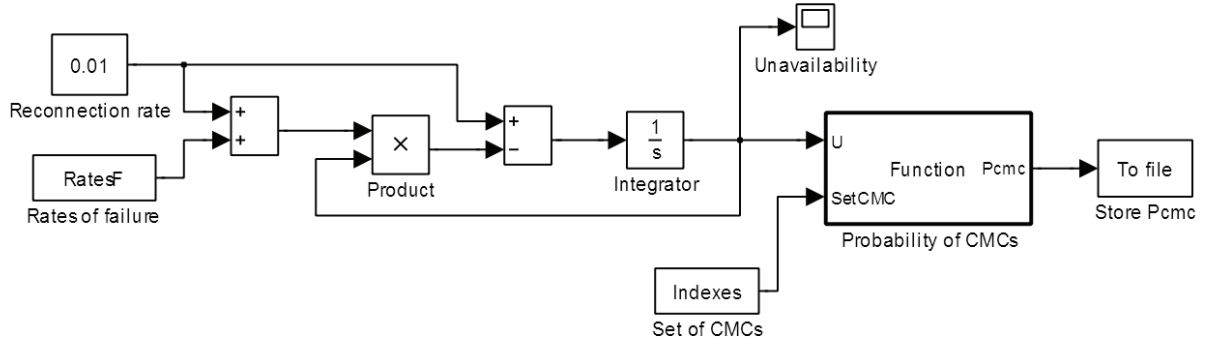


Figure 21: Numerical simulations of the unavailability under Simulink

This system of equations is numerically solved using a variable stepsize Dormand-Prince method which is an adaptation of the fourth-order Runge-Kutta method presented in Chapter 3.3.3. The stepsize  $h_{n+1}$ , where  $n$  is the time, is controlled by the maximum local error  $\delta$  (Dormand and Prince, 1980).

$$h_{n+1} = 0.9 * h_n \left( \frac{\delta}{\epsilon_{n+1}} \right)^{1/5} \quad (5.1)$$

Where  $\epsilon_{n+1}$  is the estimated error caused by the discretization. The error  $\delta$  has to be set to an appropriate value which is a trade-off between simulation speed and accuracy. After few numerical simulations, the temporal unavailability do not significantly change for  $\delta = 1E^{-11}$  which is retained for the rest of the vulnerability assessment.

Regarding the severity assessment from Chapter 3.6, three parameters must be set, i.e. the maximum current  $I_{max}^l$ , the maximum admissible voltage deviation  $V_{adm}^i$  and the maximum voltage deviation  $V_{max}^i$ . Chapter 2.3 of Knight (2001) helps to set credible limits for these parameters. First, the maximum current is the current entailing the disconnection of the three-phase circuit after several minutes. This maximum current is variable, but 140% of the rating current is credible. From the same reference, a deviation of 5% of the nominal voltage could already entail equipment disconnection at the bus, while 10% is certainly fatal for most of the equipment. It is worth mentioning that the designation of transmission lines as 220 kV and 380 kV lines is misleading since they are operated at 230 kV and 400 kV. Therefore, the voltage severity index is based in  $V_{nom}^i = 230$  or 400 kV .

Here is a summary of the main parameters set above.

Table 11: Definition of the main parameters of the simulation

Segment length	$d^S = 2.5 \text{ km}$
Influence distance of the exposure	$d^E = 2.5 \text{ km}$
Size of the moving average window	$T^E = 7.5 \text{ min}$
Maximum local error	$\epsilon_{n+1} = 1E^{-11}$
Maximum current	$I_{max}^l = 140\% * I_{rating}^l$
Actual nominal voltages	$V_{nom}^i = 230 \text{ or } 400 \text{ kV}$
Admissible voltage deviation	$V_{adm}^i = 5\%$
Maximum voltage deviation	$V_{max}^i = 10\%$

### 5.1.3 Simulations

The vulnerability assessment is performed on the reference scenarios 2006 (RS 2006) and plausible scenarios 2018 (PS 2018) impacted by the simulated and past extreme thunderstorm events. Some key figures of the four stages of simulations presented in Chapter 5.1.1 have to be shown before the results of the simulations.

Stage B involves the calculation of probability of CMCs of the set  $\Gamma^m$ . The number of CMCs is limited by the random access memory of the computer used. Only the most plausible CMCs are investigated according to a screening process. Indeed, the number of CMCs is rapidly growing with multiplicity  $m$ . For a given  $m \geq 3$ , the number of possible combinations exceeds the memory of recent desktop computers. Fortunately, as the multiplicity increases, the probability of CMCs becomes negligible. For this application to thunderstorms, the multiplicity  $m \leq 3$  has been considered credible. The number of CMCs investigated for peak and off-peak scenarios are similar.

Table 12: Maximum number of CMCs vs. investigated CMCs

SEWE	SEPS	#CMCs maximum			#CMCs investigated		
		m=1	m=2	m=3	m=1	m=2	m=3
SEWE 1	RS 2006	216	23220	1.7E+06	216	23220	43680
	PS 2018	252	31626	2.6E+06	252	31626	43680
SEWE 2	RS 2006	216	23220	1.7E+06	216	23220	43680
	PS 2018	252	31626	2.6E+06	252	31626	43680

SEWE	SEPS	# investigated/# maximum		
		m=1	m=2	m=3
SEWE 1	RS 2006	100%	100%	2.6%
	PS 2018	100%	100%	1.7%
SEWE 2	RS 2006	100%	100%	2.6%
	PS 2018	100%	100%	1.7%

For the multiplicity  $m = 1$  and  $m = 2$ , all possible CMCs can be investigated. On the contrary, only a fraction of the possible CMCs of multiplicity  $m = 3$  can be analyzed. Nevertheless, the large majority of uninvestigated high multiplicity CMCs is very unlikely. The CMCs investigated are among the most probable even if some could have been discarded.

The temporal unavailability of all investigated CMCs has been calculated and stored for further analysis. This simulation takes at most a few hours on a modern desktop computer, and the duration is reasonable when taking into account the number of CMCs. The number of investigated CMCs and the simulation duration could certainly be lower with improvements to the calculation algorithms.

Stage C involves the severity assessment by contingency analyses. Only the most probable CMCs of the set  $\Gamma^m$  undergo the contingency analysis based on an AC power flow model. The screening is performed according to the cumulative sum criterion with  $\alpha = 80\%$  as described in Chapter 3.5. The following table shows the ratio between the number of CMCs causing violations of security limits and the number of CMCs investigated.

Table 13: Selected results of the contingency analyses

SEWE	SEPS	# CMCs on investigation			# CMCs severe		
		m=1	m=2	m=3	m=1	m=2	m=3
SEWE 1	RS 2006	74	1760	2113	0	24	149
	PS 2018	87	2212	2999	0	24	331
SEWE 2	RS 2006	55	970	1459	0	8	10
	PS 2018	62	1260	1781	0	16	59

SEWE	SEPS	# severe/# investigated		
		m=1	m=2	m=3
SEWE 1	RS 2006	0%	1.4%	7.1%
	PS 2018	0%	1.1%	11.0%
SEWE 2	RS 2006	0%	0.8%	0.7%
	PS 2018	0%	1.3%	3.3%

Only the peak period of the RS 2006 and PS 2018 suffers from violations of security limits. The off-peak period apparently has sufficient margins to undergo CMCs without a problem. This is certainly due to the lower night consumption. As expected, single contingencies do not cause violation of security limits because of the N-1 criterion. Unsurprisingly, as the multiplicity increases, the ratio also increases. However, most of the investigated CMCs by the contingency analysis do not cause violation of security limits. Only current overloads have been caused by these CMCs, and no voltage deviation outside the limits has been identified. This is probably the consequence of PV generators constraining some buses voltage, the relatively low summer consumption and a fully operational network without overhauled transmission line.



---

Stage D is the core of the simulations as it relates to the vulnerability assessment (i.e. the indexes and matrixes of vulnerability as defined in Chapter 3.7). The calculations involved in this stage are quite straightforward and do not engage a significant amount of computing resources. These calculations have been carried out by Matlab scripts. The results of Stage D are presented in the next chapter.

#### *5.1.4 Sensitivity analyses*

Sensitivity analyses have been performed on the main parameters or calculation methods liable to influence the simulation results. First, AC power flow model has been replaced by its linear counterpart named DC power flow model (see Appendix 9.1.2). The DC model is at least five times faster to the detriment of accuracy. The index of vulnerability is systematically lowered by 10% to 20% compared to the AC model. This diminution stems from few CMCs whose severity is incorrectly evaluated. Although the loss of accuracy is tolerable on average, some severe CMCs could be neglected leading to inappropriate conclusions. Therefore, the DC model should only be used for screening the potential severe CMCs whereas the AC model numerically evaluates the level of severity.

For the maximum current, the admissible and maximum voltage deviation of Table 11, they have a moderate influence on the level of vulnerability. For example, a doubling of the maximum current lowered the vulnerability level by approximately 50%. On the other hand, the location and relative vulnerability of MZVs is not sensitive to these parameters as long they are uniformly revised among power lines and buses. It implies that comparison of levels of vulnerability among different transmission system scenarios has to be performed with the same set of those parameters.

The segment lengths have little influence on the simulation results as long as they are kept smaller than the space-time scale of thunderstorm cells. In this condition, smaller segment lengths only augment the number of exposure points, and thus, the computing time. Consequently, segment lengths should be just smaller than the space-time scale to ensure a fair trade-off between simulation time and accuracy. The influence distance of the exposure points and size of the moving average window are strongly linked with the space-time scale of thunderstorm cells. Their ratio should not be higher than the minimum space-time scale contained in the SEWE. Otherwise, overlapping zones of influence among exposure points would average spatiotemporal information.

## 5.2 Vulnerability assessment of the PS 2018 impacted by the SEWE 1

This chapter aims to identify major zones of vulnerability according to the metrics presented in Chapter 3.7. First, the aggregated index and matrix of vulnerability are presented to locate the MZV of the PS 2018 hit by the SEWE 1. Then, the temporal vulnerability index and matrixes are presented to get an idea of the vulnerability dynamic.

### 5.2.1 Identification of vulnerable zones

At this stage, the probability and severity of the all CMCs have been computed. The aggregated vulnerability index  $V$ , as defined by (3.46), is the sum over all CMCs and multiplicity of the product of the CMCs probability and severity. The table hereunder shows the intermediate vulnerability index for the different multiplicity of CMCs.

Table 14: Vulnerability index for the PS 2018 and the SEWE 1

$m = 1$	$m = 2$	$m = 3$	$V$
0	2.0E-06	1.0E-06	3.0E-06

Unsurprisingly, the vulnerability is zero when  $m = 1$  since the N-1 criterion guaranties no overload in case of single failures. On the contrary, CMCs of multiplicity 2 and 3 exhibit the same order of magnitude in vulnerability. Triple contingencies tested entail less vulnerability than double ones. This can be explained by the fact that only the most probable, but not all triple contingencies have been taken into account. On the other hand, their lower probability may compensate for their increased severity. The absolute value of the vulnerability index has a limited interest since it is hardly interpretable. Nevertheless, it is the foundation of the matrix of vulnerability and zonal vulnerability ratio (Chapters 3.7.2 and 3.7.3).

The matrix of vulnerability of the PS 2018 can be found in Table 15. Briefly stated, this matrix is the projection of the  $V$  on two dimensions. The first dimension (row) includes the transmission lines that are contained in CMCs. This dimension can be seen as the cause of violation of security limits. The sum of the columns is the vulnerability caused by each transmission line involved in CMCs. Since no voltage deviations have been noted, violation of security limits are only current overloads. The second dimension (column) includes the transmission lines that undergo overloads. This dimension can be interpreted as the consequences of the CMCs. The sum of the rows is the vulnerability consequent to each transmission line with violation of security limits. The map hereunder illustrates the projection of vulnerability to the transmission lines respectively involved in the CMCs and with violations of security.

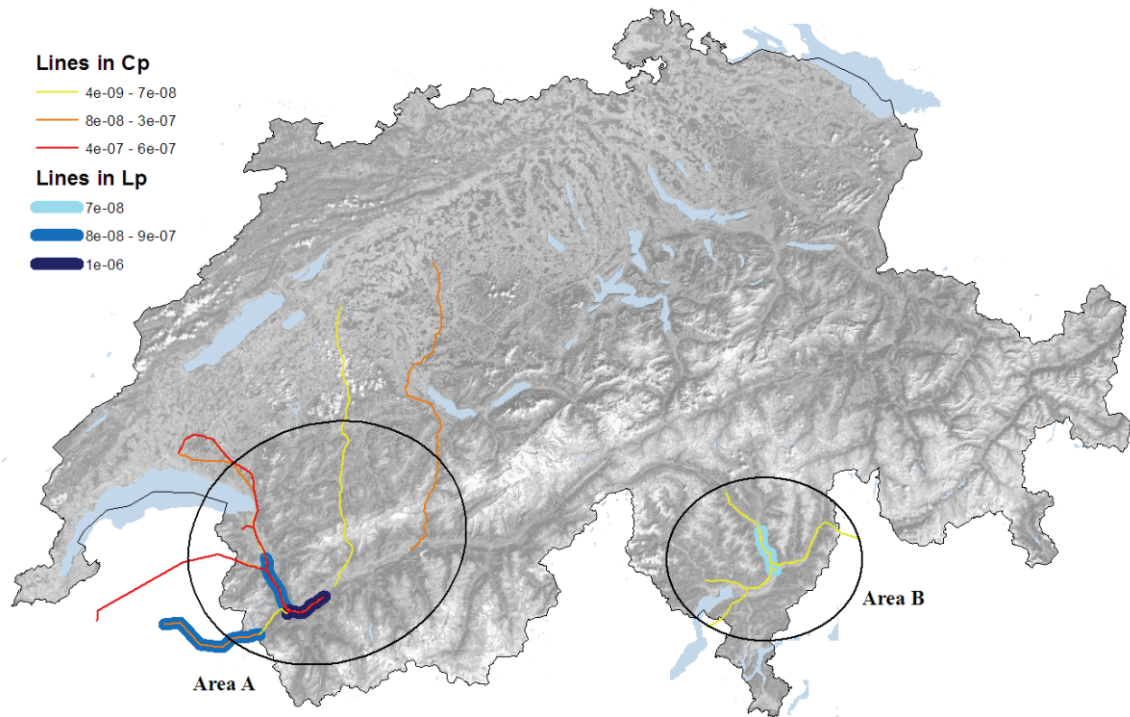


Figure 22: Map of the vulnerable areas of the PS 2018

The vulnerability seems visually concentrated into two geographic areas, and they are identified by the transmission lines inside their perimeter, which are contributing to the vulnerability. These areas are both situated in mountainous regions with high hydro production and a relatively low consumption. The area of vulnerability A stretches along the Rhône valley where more than 2 GW of hydro power plants are located. On the other hand, the area B lies in the canton of Tessin constituted by steep and narrow valleys scattered with multiple power plants of several hundred megawatts.

From the visual interpretation of Figure 22, the number of MZV is  $N^z = 2$  because the two areas of vulnerability seem independent. Therefore, they are good MZV candidates. In order to formally identify these MZV, the method described in Chapter 3.7.3 has been applied to this concrete case. The process of distributing transmission lines in the MZV has been performed manually. Indeed, the maximization of the intra-zonal overall vulnerability is obvious in this situation. The following matrix of vulnerability is formatted to present the transmission lines belonging to the set  $Z^p = C^p \times L^p$  of the MZV 1 and 2. The transmission lines index is replaced with their name to facilitate understanding.

Table 15: Matrix of vulnerability and MZV 1 and 2

	SBATIA2A-SRIDDE2A-1	SVALLO2A-FPRE.A2A-1	SBATIA2A-SS.TRI2A-1	SBIASC2A-SGORDU2A-1	Sum columns	
SBATIA1A-SCHAVA1A-1	3E-07	1E-07	1E-07		<b>6E-07</b>	$\mathcal{C}^1$
SCHAVA1A-SROMAN1A-1	3E-07	1E-07	9E-08		<b>5E-07</b>	
SS.TRI2B-SVEYTA2A-1	2E-08	6E-10			2E-08	
SROMAN2A-SVEYTA2A-1	2E-07	3E-08	1E-07		<b>3E-07</b>	
SVALLO2A-FPRE.A2A-1			2E-07		<b>2E-07</b>	
SS.TRI2A-FCOR.S2A-1	6E-09	1E-08			2E-08	
SROMAN2A-SS.TRI2A-1		1E-08			1E-08	
SBICKI1A-SCHIPP1A-1	1E-07	7E-10	2E-08		<b>1E-07</b>	
SBICKI2A-SCHIPP2A-1	5E-08	8E-10	1E-09		6E-08	
SGSTAA2A-SMUEHL2A-1	1E-08	6E-11	2E-09		1E-08	
SCHAMO2A-SMUEHL2A-1	7E-10	3E-10	6E-08		7E-08	
SRIDDE2B-FCOR.R2A-1	2E-07	1E-07	1E-07		<b>4E-07</b>	
SRIDDE2B-SS.TRI2B-1	1E-07	8E-09	4E-08		<b>2E-07</b>	
SBATIA2A-SS.TRI2A-1		4E-07			<b>4E-07</b>	
SBATIA2A-SVALLO2A-2			2E-08		2E-08	
SBIASC2A-SLAVOR2A-1				2E-08	0E+00	$\mathcal{C}^2$
SLAVOR1A-IMUSM11A-1	5E-09	3E-09	2E-10		9E-09	
SIRAGN2A-SSOAZZ2A-1	6E-09	4E-09	1E-09	2E-08	1E-08	
SMAGAD2A-SSOAZZ2A-1	7E-09	6E-09	2E-09		1E-08	
SGORDU2A-IMESM12A-0	5E-09	4E-09	1E-09		1E-08	
SAVEGN2A-SGORDU2A-1	3E-09	3E-09	7E-10		7E-09	
<b>Sum rows</b>	<b>1E-06</b>	9E-07	8E-07	5E-08	$\Sigma =$	3E-06
		$\mathcal{L}^1$		$\mathcal{L}^2$		3E-06

The first MZV  $Z^1$  is constituted by 15 transmission lines in  $\mathcal{C}^1$  (CMCs) and 3 lines in  $\mathcal{L}^1$ , while the second  $Z^2$  is composed of 6 lines in the set  $\mathcal{C}^2$  and 1 in the  $\mathcal{L}^2$ . The sets  $\mathcal{B}^p$  are empty since no overvoltage has been detected by the contingency analysis. The element of the matrix can be interpreted as the intensity of the link between lines included in CMCs and lines suffering from violations of security limits. The sum of the columns and rows allows the identification of the transmission lines most responsible for the violation of security limits and those most frequently undergoing violation of security limits, respectively. As demonstrated in Appendix 9.3, the sum of the matrix elements is equal to the aggregated vulnerability index of Table 14.

In general, the existence of MZV can be explained by two properties of weather and transmission systems. First, the limited range in space-time correlations of EWEs preferably causes failures of nearby transmission lines. Second, CMCs located in the same area are likely to provoke violations of security limits not far from this area due to the small electric distance. Therefore, CMCs triggered by thunderstorms are likely to be grouped in the same vulnerable area which entails an augmented probability of violation of security limits compared to independent contingencies. Discarding space-time correlations leads to an underestimation of vulnerability.

The zonal vulnerability ratio measures the aggregated link between transmission lines in  $\mathcal{C}^p$  and in  $\mathcal{L}^q$  as a percentage of the aggregated vulnerability index as defined by (3.68).

Table 16: Zonal vulnerability ratio

	$\mathcal{L}^1$	$\mathcal{L}^2$
$\mathcal{C}^1$	97%	-
$\mathcal{C}^2$	1%	2%

MZV 1 accounts for 97% of the vulnerability, while MZV 2 accounts for only 2%. Therefore, countermeasures should have priority in MZV 1. The clustering process into two zones is optimal or near optimal since the inter-zonal overall vulnerability stems from  $\mathcal{C}^2$  to  $\mathcal{L}^1$  at only 1%. This is the result of CMCs of multiplicity three taking place in the two MZV and causing violations of security limits only in MZV 1. This situation is the consequence of the rule underlying the vulnerability projection used in matrixes of vulnerability. It states that each transmission line in a CMC is equally responsible for the violation of security limits. This allocation could be improved by taking into account the actual effects of each single failure.

In a nutshell, the vulnerability of the PS 2018 impacted by SEwE 1 is mainly located in the MZVs 1 and secondly in MZV 2. Countermeasures should be proposed in priority to the most vulnerable Zone 1. In general, vulnerable areas refer to fixed geographic region, while MZV are related to transmission infrastructures and are scenario dependent. In the present case, the two MZV coincide by construction with the mountainous areas A and B. It is not surprising that the MZV are in this type of terrain since it fosters high hydro production, low consumption, and does not facilitate the development of the transmission network. Moreover, mountainous regions are prone to intense weather activity. The results presented here show the ability of the methodology to quantify the vulnerability and identify its sources.

### 5.2.2 Temporal analysis of the vulnerability

In the previous subchapter, the aggregated vulnerability index is used to identify the vulnerability of the PS 2018 hit by the SEWE 1. This index is timeless since it aggregates the maximum probability of each CMC. On the contrary, the temporal vulnerability index gives an image of the vulnerability  $V(t)$  at a given time as described by (3.45). It shows that

vulnerability is a temporal function of the dynamic of the SEWE, the paths of the transmission networks and the power flows. The temporal contribution of each CMC to the vulnerability comes from its time-dependent probability, defined by (3.32), since its severity derives from a unique SPTS. Therefore, the evolution of the vulnerability is linked to the sum of probability  $P_{CMC}(t)$  of having double and triple CMCs, which are potentially severe CMCs.

$$P_{CMC}(t) = \sum_{m=2}^3 \sum_{c=1}^{N^m} \bar{P}_m^c(t) \quad (5.2)$$

As shown in the following figure,  $P_{CMC}(t)$  is fluctuating over time. Peaks correspond to storms cells hitting larger portions of the network. The process of reconnection is clearly apparent. It limits the probability of CMCs and ensures a fully operable network once the SEWE 1 has passed.

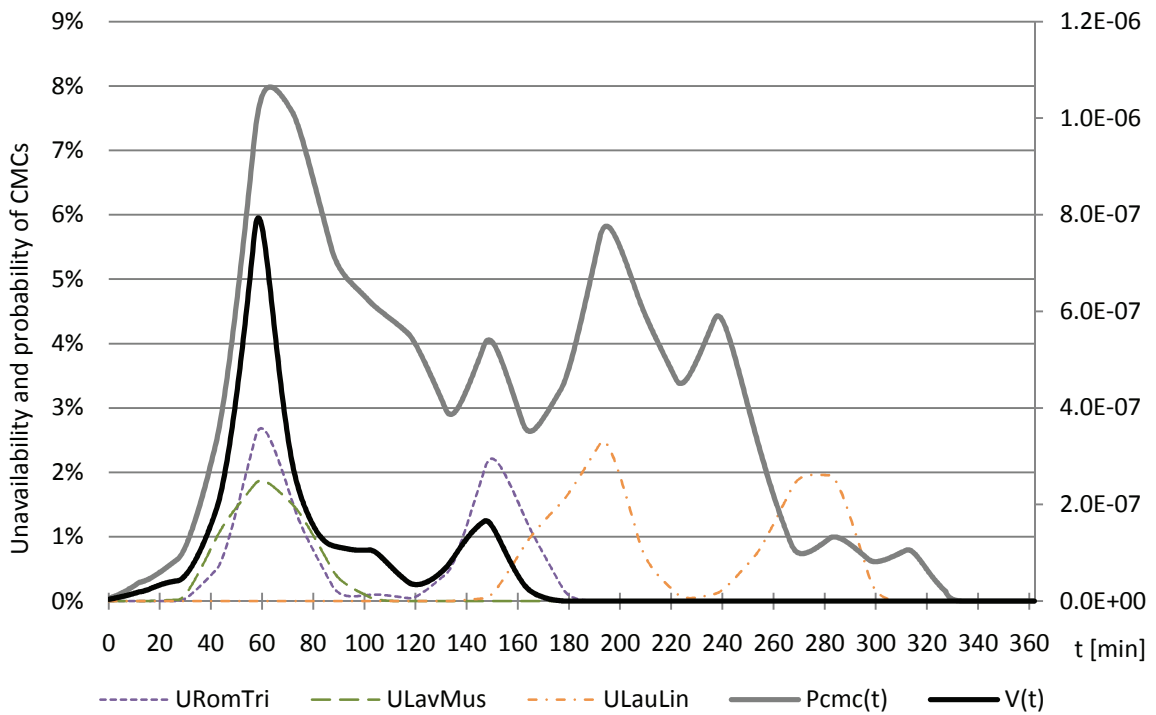


Figure 23: Temporal evolution of the vulnerability

The temporal unavailability of three lines from different regions is also represented in order to associate the temporal vulnerability with the regions exposure. The line Romanel to St-Triphon is located in Area A and its unavailability is denoted  $U_{RomTri}$ . The line Lavorgo-Musignano ( $U_{LavMus}$ ) is in Area B whereas the line Laufenburg-Lindenholz ( $U_{LauLin}$ ) is situated in the northern part of Switzerland.

Two peaks of vulnerability are detected centered at  $t = 60$  and  $t = 150$ . The highest is caused by cells G1\_C1, G1\_C2 impacting the Area A and cells G2\_C1 and G2\_C2 hitting Area B (see Figure 22). The second lower peak corresponds to the contact of cells G1\_C4 with Area A. The vulnerability sunk close to zero when none of the two vulnerable areas are impacted. At  $t = 200$ , a peak in  $P_{CMC}$  is caused by thunderstorm cells passing through the

north of Switzerland, which has a dense transmission network. However, this peak does not coincide with a surge of vulnerability since this part of the network is resilient to CMCs.

The cause of the first vulnerability peak is corroborated by the temporal matrix of vulnerability and the two MZV as detailed in the following table.

Table 17: Temporal matrix of vulnerability at 60 minutes

	SVALLO2A-FPRE.A2A-1	SBATIA2A-SRIDDE2A-1	SCHAMO2B-SGSTAA2A-1	SBATIA2A-SS.TRI2A-1	SBIASC2A-SGORDU2A-1	Sum columns	
SBATIA1A-SCHAVA1A-1	8E-08	2E-07	2E-09	3E-09		3E-07	$c^1$
SCHAMO2A-SMUEHL2A-1	1E-08	2E-09				1E-08	
SRIDDE2B-FCOR.R2A-1	1E-08	2E-07	2E-09	2E-09		2E-07	
SRIDDE2B-SS.TRI2B-1	7E-09	7E-09	2E-09	8E-10		2E-08	
SBATIA2A-SS.TRI2A-1	1E-07					1E-07	
SBIASC2A-SLAVOR2A-1	8E-09	2E-09			3E-08	4E-08	$c^2$
SLAVOR1A-IMUSM11A-1	8E-10	2E-10				1E-09	
SIRAGN2A-SSOAZZ2A-1					4E-08	4E-08	
Sum rows	2E-07	5E-07	5E-09	5E-09	7E-08	$\Sigma =$	8E-7
	$\mathcal{L}^1$				$\mathcal{L}^2$		8E-7

MZVs 1 and 2 at  $t=60$  are not composed of exactly the same transmission lines as those detected in Chapter 5.2.1. However, they are also situated in the same Areas A and B. It is not surprising since temporal vulnerability is a subset of aggregated vulnerability at a given time. The time dimension brings more information about the vulnerability. It is variable and some particular times are prone to severe CMCs endangering the security of the electricity supply.

Table 18: Zonal vulnerability ratio at 60 minutes

	$\mathcal{L}^1$	$\mathcal{L}^2$
$c^1$	89%	0%
$c^2$	1%	10%

The zonal vulnerability ratio for the two MZV indicates that MZV 1 is responsible for the majority of the vulnerability at  $t=60$ . Despite the simultaneity of the thunderstorms in the two areas, CMCs of  $c^2$  contributes insignificantly to the vulnerability of MZV 1. Therefore, these two zones can be considered as electrically distinct when it comes to the effects of

---

contingencies.

This example shows that vulnerability induced by an extreme weather event exhibits strong space-time correlations. Therefore, it is important to take these correlations into account when assessing vulnerability to propose effective countermeasures. The focus can be restricted to the fraction of the network showing signs of vulnerability.

These results are close to those obtained by the timeless analysis. The concept of time dependent vulnerability allows the modeler to have a better idea of the interaction between a SPTS and a SEWE as well as the capacity of the methodology. However, a timeless analysis presents aggregated values that are readily interpretable in order to propose countermeasures for the whole period of the SEWE and not just for a given time.

### 5.3 Vulnerability assessment of other scenarios

The search of vulnerable zones is more robust if they are not only based on one pair of electric and weather scenarios. Although, a quasi infinity of plausible cases exists, it is valuable to evaluate the sensitivity of the vulnerable zones to few other scenarios. Two other SPTS are investigated in this section in the same way as in Chapter 5.2.1. First, the RS 2006 is a plausible scenario of the 2006 summer peak period. This scenario aims at evaluating whether the two vulnerable Areas A and B of the PS 2018 are also present in the RS 2006. Second, the PS 2018 T is similar to the PS 2018, but the transit from Switzerland to Italy is lowered by 1500 MW. In this case, most of the electricity exported from Switzerland heads to its northern border, which includes France and Germany. This explores the effects of larger imports to northern Europe, which could take place when adverse weather conditions lower the production of large wind farms (EWIS, 2007). The SEWE 2 defined in Chapter 4.2.2 is mingled with the PS 2018 and RS 2006 to assess the vulnerability with a real past weather event. The PS 2018 T is only combined with SEWE 1 to inspect the vulnerability changes induced by the new transit flows.

In order to allow non-biased comparison of vulnerability levels for different scenarios, the vulnerability comparison indexes  $V^c$  have been computed based on the RS 2006 during normal weather conditions as described in Chapter 3.7.1. This scenario is based on three years of power line unavailability statistics for the Swiss transmission lines (AES-VSE, 2001-2003-2004). It is assumed that all transmission lines have the same average unavailability. More details about the data and calculations are found in Appendix 9.6.

The next table summarizes the simulations in terms of vulnerability indexes and zonal vulnerability ratio for the two MZV identified. They are located in the two vulnerable Areas A and B of Figure 22 related to the PS 2018 impacted by the SEWE 1. MZV and areas coincide for all combination of scenarios. Therefore, these terms are here rather interchangeable, even if MZV contain different sets of transmission line. The zonal vulnerability ratio  $V_{ratio}^{1,1}$  and  $V_{ratio}^{2,2}$  indicate the percentage of vulnerability attributable to, respectively, Areas A and B. The next column is the inter-area vulnerability ratio.



Table 19: Zonal vulnerability ratio focused on Areas A and B

		$V^c$	$V_{ratio}^{1,1}$	$V_{ratio}^{2,2}$	$V_{ratio}^{1,2} + V_{ratio}^{2,1}$
<b>SEWE 1</b>	<b>PS 2018</b>	3.9	97%	2%	1%
	<b>PS 2018 T</b>	3.9	100%	0%	0%
	<b>RS 2006</b>	4.2	95%	4%	1%
<b>SEWE 2</b>	<b>PS 2018</b>	3.4	72%	27%	1%
	<b>RS 2006</b>	2.8	0%	100%	0%

A first observation is that the vulnerability comparison index  $V^c$  of the SEWE 2 are lower than SEWE 1. This can be explained by the smaller number of lightning strikes of SEWE 2 in the vicinity of transmission lines leading to less probable CMCs. Second, all combinations of scenarios are several orders of magnitude more vulnerable than the RS 2006 submitted to normal weather. It shows the capacity of extreme weather events to endanger the security of supply.

It is worth mentioning that the probability of the two SEWE is assumed equal to one. It allows comparing scenarios regardless of their probability. However, it is sensible to consider these SEWE as having low probabilities of occurrence during a single year. In this case, the vulnerability comparison index would considerably be lowered. For example, a time of recurrence of 100 years leads to a probability of 0.01, which diminishes the vulnerability comparison index by 2 orders of magnitude. The vulnerability of investigated scenarios would still be several order of magnitude higher than the RS 2006, subject to normal weather conditions.

The PS 2018 T clearly has only one major MZV. Compared to the PS 2018, there is a transfer of vulnerability from Area B to A. It is not surprising since the transit to Italy, which passes mainly by Area B, is lowered to the detriment of the northern borders. The non-negligible power produced in Area A heads to the north instead of the south, which loading more transmission lines which are already vulnerable. This also explains the change of rate from 97% to 100% in Area A in addition to an augmentation of  $V$ . From this example, Area B seems sensitive to transit flow to the south, while Area A is sensitive to power flows to the north.

The PS 2018 impacted by the SEWE 2 has the same two vulnerable Areas A and B. Around one third of the vulnerability is located in Area B because the SEWE 2 is more intense in the southern part of Switzerland. The Area A still accounts for most of the vulnerability.

The past configuration of the network of RS 2006 also exhibits the two vulnerable Areas A and B. However, the results are very dependent on the SEWE. The most vulnerable area passes respectively from A to B for SEWE 1 to SEWE 2. These two weather scenarios do not reveal the vulnerability of the RS 2006 in the same way as the PS 2018. However, the two Areas A and B already existed in 2006.

To conclude, vulnerable Areas A and B account for the totality of the vulnerability in all

---

combinations of scenarios. These areas can be also considered as independent as demonstrated by the low value of the inter-areas vulnerability ration. The modifications of the network between 2006 and 2018 do not change the areas of vulnerability. The new transmission capacities are certainly balanced by the new pumped-storage power plants. The two areas are both located in mountainous regions, and they are good locations to erect dams and hydro power plants. At the same time, the population is limited by available land, which entails a relatively low consumption of electricity. Large amounts of power have to flow out of these regions to the main center of consumption through a limited number of power lines. Transmission lines have to follow natural paths such as valleys and passes. Apparently, these natural barriers contribute to vulnerability. It is harder to devise a resilient transmission network capable of withstanding CMCs. In these conditions, it is a challenge to find countermeasures capable of reducing the vulnerability at acceptable costs while respecting environmental regulations.

## 5.4 Conclusions

The probability and severity of sets of plausible CMCs of five scenarios of the Swiss electric power system have been computed to assess vulnerability. The probability is evaluated by space-time simulations of two SEWE impacting several SPTS. These simulations take advantage of the adequate environment offered by Matlab and its GIS functionalities. The severity is assessed by contingency analyses under Neplan for the most probable CMCs. In the end, a fraction of the most probable CMCs generate current overloads whereas no overvoltages were detected. Therefore, the methodology is able to screen the most relevant CMCs regarding vulnerability under extreme weather conditions.

Two major zones of vulnerability have been identified based on the index and matrix of vulnerability developed in Chapter 3.7. These zones of vulnerability exist in the scenarios of 2006 and 2018, which suggests that there is an exogenous underlying cause of vulnerability such as topography. Indeed, these zones are both situated in mountainous regions prone to thunderstorms combining high hydro production and limited natural paths for transmission lines. Despite the new transmission infrastructure in the PS 2018, the vulnerable areas do not disappear, undoubtedly because of the increased hydro production. Nevertheless, countermeasures can be envisaged to reduce vulnerability of these two major areas of vulnerability.

This application demonstrates that simulations of space-time correlations in extreme weather events combined with electric models of transmission systems leads to distinct and identifiable major zones of vulnerability. The vulnerability is thus located in space and also in time. The proposed methodology is able to reduce the complexity of system interactions to target countermeasures. The scenario-based methodology allows simulating any imaginable past or future situations, and this application is only an illustration of the methodology. It is applied to plausible scenarios of the Swiss power system, which are not predictions. However, it is believed that some results can be generalized and are able to shed light on vulnerable areas of the Swiss electric power system.

---

## 6 Proposal of countermeasures to reduce vulnerability

*This chapter aims at searching for countermeasures to reduce the vulnerability of PS 2018. First, the context in which countermeasures take place is clarified as well as the constraints applying to them. Second, the most hazardous major zones of vulnerability and its main underlying cause of vulnerability are identified to propose appropriate countermeasures. Finally, the reduction of vulnerability is assessed to judge the efficacy of the proposed countermeasures.*

### 6.1 Introduction

In Chapter 5.2, two vulnerable areas were identified for the plausible scenario 2018 (PS 2018). They also exist in the reference scenario 2006 (RS 2006) which suggest that these areas are constant over the years. The modifications to the transmission network brought to the PS 2018 do not reduce the vulnerability of these areas in case of thunderstorms. These changes aim at achieving different objectives leading to billions francs in investment within the next years. They are related to the connection of new hydro pump-storage power plants, while others permit a better interconnection to neighboring countries, the respect of the N-1 criterion or the mitigation of congestions. Some of these new infrastructures will not be operational in 2018 whereas other alternatives will be adopted. Knowing the important efforts already planned in upgrading the system raises the question of whether it is appropriate to reduce the vulnerability during rare extreme weather events.

In order to get more insight, a seminar was organized with experts from two Swiss electrical utilities (Alpiq and BKW) and the Swiss TSO (Swissgrid). The details of the discussion are confidential, but general outcomes can be disclosed without breaking confidentiality clauses. In a nutshell, it was acknowledged that the risk of disturbances during extreme weather events (EWEs) is moderate and the cost of countermeasures should be economically justified by a significant reduction in vulnerability. It requires that countermeasures to assure the security of supply during EWEs are at the lower end of the list of priorities. This point can be further developed.

First, security of supply during extreme weather conditions is only one dimension requiring investments in transmission networks. The rise in consumption and transit flows, the new intermittent sources of energy or aging infrastructures require urgent upgrades of the system. Resources including time, money and workforce are limited and they should be engaged in priority to urgent upgrades.

Second, the Swiss transmission network has been built, operated and maintained during more than 60 years without large blackouts due to extreme weather conditions. Standards of construction, planning and operation standards are the results of year of experience of a

---

mature industry. Little can be done without expensive countermeasures, which are difficult to justify if only aim is to squeeze out a residual risk of disturbances.

Nevertheless, vulnerability during extreme weather events could be lowered by a careful planning of the coming infrastructures. Their original purpose is to adapt the system to new conditions ensuring the security of supply during normal weather conditions. At the planning stage, several alternatives of development exist and those which lessen the vulnerability have an advantage. The electric system growth should also integrate the reduction of vulnerability during EWEs as a criterion. In this case, countermeasures should be considered as part of the normal development of the network.

Summing up, the purpose of planning the evolution of mature power systems is to adapt the existing infrastructure to its new changing environment. This resource consuming task is the main priority. Years of experience and practice already assure a high level of security of supply during extreme weather conditions. Nevertheless, the residual vulnerability can be reduced by a careful planning of the future network structure. One key point is that countermeasures must be useful during extreme and normal weather conditions. Countermeasures are integrated in development plans under a relevant set of constraints. Among acceptable expansion alternatives, the most resilient in case of extreme weather events should be selected to guaranty the security of electric supply.

## **6.2 Proposal of a more resilient alternative to the PS 2018**

The search of suitable countermeasures for vulnerable areas follows the method presented in chapter 3.8. First, the common mode contingencies (CMCs) of major zones of vulnerability (MZVs) 1 and 2 are categorized as low or high threats. CMCs are considered as low threats if they do not cause further equipment tripping such as transmission lines, transformers or power plants. On the contrary, high threats CMCs have the capacity of triggering further disturbances. This method screens the severe CMCs in function of their capacity of endangering the security of supply. In order to differentiate CMCs, a worst case approach is used consisting of a succession of contingency analysis disconnecting at each time the most overloaded transmission lines. If the disconnections lead to appearance of new overloads, the CMC is deemed as a high threat.

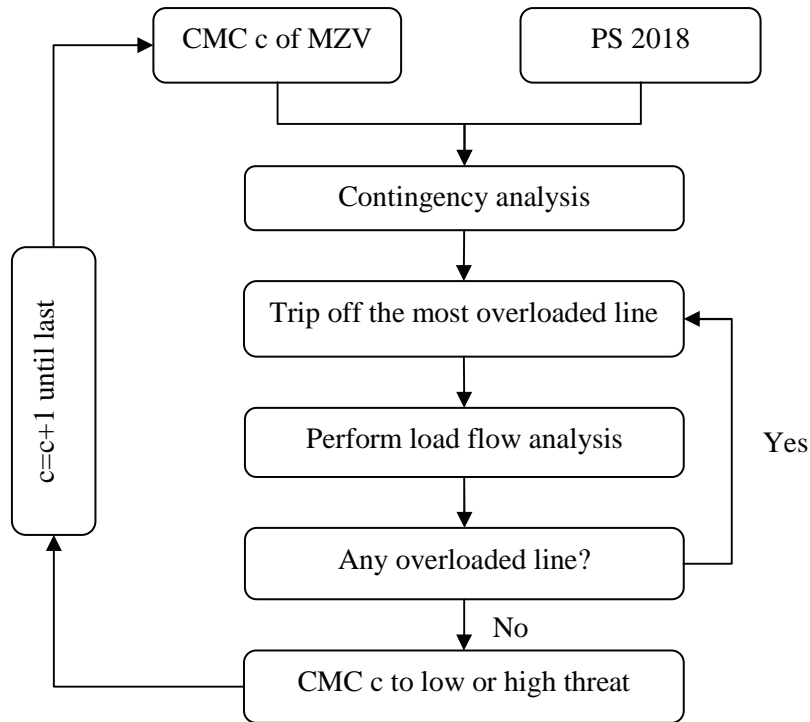


Figure 24: Categorization of CMCs potentiality to threaten the security of supply

Other methods take into account dynamical phenomena of equipment disconnection and the actions of operators and automatic security systems (Hardiman et al., 2004). However, the objective here is to focus on the few highly threatening CMCs to facilitate the understanding of the source of vulnerability. On the other hand, MZV with a significant proportion of highly threatening CMCs have the priority at the time of vulnerability reduction. This screening has been applied to the PS 2018 and its two MZVs induced by the SEWE 1 and 2.

Table 20: CMCs as low and high threats

		# total	# low threat	# high threat	#high/#total
SEWE 1	MZV 1	303	251	52	17%
	MZV 2	52	52	0	0%
SEWE 2	MZV 1	46	42	4	9%
	MZV 2	28	28	0	0%

The MZV 1 comprises 17% of high threat CMCs. This indicates that this zone should be considered as potentially threatening the security of supply in case of thunderstorms. On the contrary, the MZV 2 shows no high threat CMCs. If overloaded lines trip off, it entails no further disturbances. Even if this zone is vulnerable, it is deemed as a low threat to the security of supply. Moreover, the first zone concentrates most of the vulnerability, see Table 19. Therefore, the search of countermeasures should to be located in priority in the MZV 1.

The main cause of the vulnerability of the MZV 1 is certainly the high hydro production

---

with negligible local consumption which forces long distance transfer of the production. The augmented network capacity of this zone is balanced by supplementary generations in Chamoson and Vallorcine. The Figure 30 of Appendix 9.5.2 helps to locate these places. It is worth mentioning that transmission line maintenance has not been taken into account. It usually takes place in summertime when thunderstorms are likely. Maintenances are certainly a factor amplifying the vulnerability.

A first strategy could be the strengthening of capacity of the overloaded transmission lines in  $\mathcal{L}^1$  of Table 15. This entails the change of 68 km of three-phase circuits to allow more current to flow. The implementation of this strategy in the PS 2018 is rather simple. The capacity of the three lines of the MZV 1 is increased at least to the maximum current caused by the CMCs. The advantages are that no supplementary overhead power lines or circuits are built. However, the augmentation of capacity requires lengthy and burdensome administrative procedures. Besides, these costly alterations would not be particularly useful during normal weather conditions where CMCs are not likely. Therefore, this strategy does not seem a credible alternative to the PS 2018.

A more appealing strategy is the creation of supplementary paths of high capacity diffusing the hydro production to large centers of consumption. The objective is to drain out several hundred of megawatts, which can be adequately achieved by a 380 kV transmission line. In order to stick as close as possible to the guidelines of Chapter 3.8, the utilization of existing paths should be preferred. Two possible options could be an additional 380 kV circuit from Vallorcine to Cornier in France (SVALLO1A-FCORNI1A) to the existing 220 kV line or a line between Riddes and Rondissone in Italy. The second option is less appropriate since it requires at least the upgrading of a 220 kV line to 380 kV for more than 150 km while the first require an additional circuit on an existing path for less than 60 km. Furthermore, the shortest option directly connects the pumped-storage power plant of 600 MW in Vallorcine. An article published on the Alpiq website reports that a study is ongoing to evaluate the possibility to increase the installed capacity to 900 MW (ALPIQ, 2009). This augmentation of production capacity advocates in favor of the first option.

A plausible alternative scenario of development, namely PSA 2018, is implemented including the SVALLO1A-FCORNI1A line. Few electric parameters of this line are required to assess the reduction of vulnerability. This new 380 kV circuit is assumed to be mounted in parallel with the existing 220 kV line. From the geographic model, the length of this line is about 58 km. According to (Aguet and Ianoz, 2004), a plausible resistance and reactance for a 380 kV overhead line is respectively 0.02 and 0.3 Ohm/km. The maximum rated current is assumed as 1800 amperes, which corresponds to other transmission lines in the PS 2018.

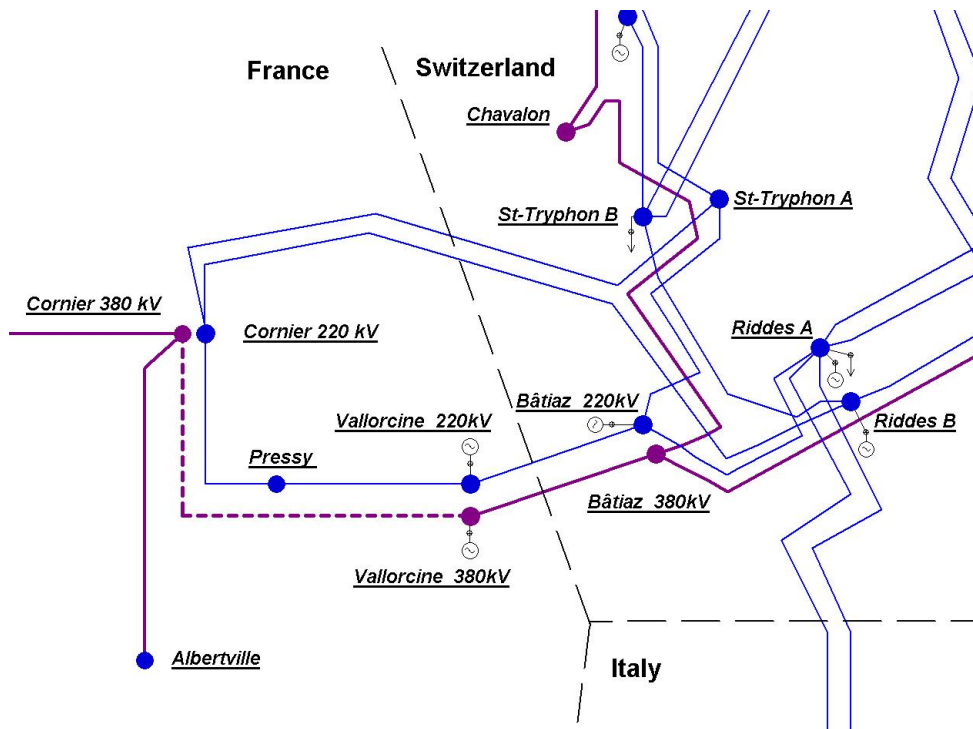


Figure 25: Additional 380 kV line to reduce the vulnerability of the area A

In this schema, 220 kV transmission lines are blue and the 380 kV are purple. The new 380 kV (dotted) line is a new link between Switzerland and France. This line closes the loop around the Lake Geneva with the already existing 380 kV line from Bâtiâz to Bois-Tollot. The substation of Cornier is connected to a major 380 kV north to south axe in France and also near interconnection lines between France and Italy. The SVALLO1A-FCORNI1A is a new link between the hydro production of Valais and some major consumption centers. According to load flow calculation, this line carries 550 MW to Cornier by locally diverting power flows. The parallel 220 kV line is unloaded of 150 MW while the line Bâtiâz to Bois-Tollot undergoes a reduction of 100 MW. The remainder of the power flows is mainly due to the increase by approximately 200 MW from Switzerland to France the power flow whereas the flows to Italy decrease of by approximately the same amount.

The SVALLO1A-FCORNI1A line is entirely located on the French territory. The proximity of the area A to the French or Italian borders raises the likelihood of binational measures which can seriously complicate their realization. The institution responsible of developing the transmission network in France is the transmission system operator RTE. Its agreement is necessary to envisage the installation of this transnational link. According to (OFEN, 2010), RTE considered negatively the construction of this line because they did not see its necessity. This opinion could change considering the augmentation of the installed capacity in zone A and the possible positive effect on vulnerability of the SVALLO1A-FCORNI1A line.

### 6.2.1 Reduction in vulnerability

The vulnerability of the PSCM 2018 is assessed in terms of aggregated vulnerability index  $V$  and the zonal vulnerability  $V^p$  for the two MZV 1 and 2. The inter and extra zonal vulnerability is grouped in  $V^{IE}$ . The same sets of CMCs of the PS 2018 are used in the PSCM 2018.

Table 21: Reduction of vulnerability by the SVALLO1A-FCORNI1A line

		$V^c$	<i>Absolut</i>				<i>Relative</i>		
			$V$	$V^1$	$V^2$	$V^{IE}$	$V^1_{ratio}$	$V^2_{ratio}$	$V^{IE}_{ratio}$
<b>SEWE 1</b>	<b>PS 2018</b>	3.9	3.0E-06	2.9E-06	5.9E-08	2.7E-08	97%	2%	1%
	<b>PSCM 2018</b>	-0.1	3.4E-10	0	3.4E-10	2.2E-13	0%	100%	0%
<b>SEWE 2</b>	<b>PS 2018</b>	3.4	4.9E-07	3.5E-07	1.3E-07	5.8E-09	72%	27%	1%
	<b>PSCM 2018</b>	1.6	9.2E-09	0	9.2E-09	0.0E+00	0%	100%	0%

The supplementation of the SVALLO1A-FCORNI1A line reduces the vulnerability by several orders of magnitude. For the SEWE 1, This line reduces the vulnerability by a factor of approximately 10'000. The vulnerability is comparable with the RS 2006 subject to normal weather conditions. The vulnerability of the MZV 1 vanishes while the one of the MZV 2 is drastically lowered. The inter and extra zone vulnerability also vanish. The vulnerability only stems from the hydro power plants in Biasca in Area B which is connected by three 220 kV lines. When two of the three lines trip off because of lightning, the remaining line is overloaded at 0.4% which can be considered negligible. The PSCM 2018 is nearly immune to the SEWE 1. The additional line located in Area A also diminishes the vulnerability of Area B by rerouting power flows. For the SEWE 2, the vulnerability is lowered by almost two orders of magnitude. The vulnerability of the MZV 1 is zero whereas the one of the zone 2 is only lowered. The inter and extra zone vulnerability is negligible. For both of the SEWE, the vulnerability of the areas A and B diminishes because of the additional line.

The rerouting of approximately 550 MW by the SVALLO1A-FCORNI1A line drains power flows out of the vulnerable areas. Around 100 MW do not flow from the Areas A to B which diminishes its vulnerability. Approximately 200 MW is withdrawn from the 220 kV network in Area A leading to more resilience. The additional line free margins in many other lines of the region. It is possible that congestion could appear in the French network. But network changes of 2018 outside Switzerland have not been taken into account.

For both of the thunderstorm scenarios, the vulnerability decreased by the addition of the SVALLO1A-FCORNI1A line. Obviously, its effect on the Area B is lower than the Area A in which the countermeasure is located. However, this unique additional line is able to make the network more resilient in the two distant areas. It is worth mentioning that this countermeasure proposal is an illustrative case of a limited number of plausible scenarios. This alternative scenario for 2018 aims primarily to illustrate the methodology by showing its



---

capacity to discover vulnerable areas, and searching for a way of alleviating them.

## 6.3 Conclusions

The analysis of the CMCs suggests that Areas A is a bigger threat to the security of supply than Area B. Indeed, transmission line overloads of A could potentially lead to line and power plant disconnections. This is also compatible with the zonal vulnerability ratio which indicates the most of the vulnerability is located within Area A. The vulnerability seems to be the consequence of the relative inadequacy between high local productions and transmission capacity. Both relate to the topography fostering dams and hydro power plants while hampering the construction of power lines. Although the PS 2018 is not completely immune to plausible CMCs, its level of vulnerability could be deemed acceptable. Indeed, complete immunity is not an achievable objective by reason of its inordinate cost. But if the vulnerability is deemed excessive, countermeasures can be proposed to reduce it. Because of the complex nature of the problem, the proposed alternatives of development should be considered as an illustration of the methodology and not as official recommendations.

In the particular case of the PS 2018 subject to the SEWE 1 and 2, the construction of an overhead transmission line lowers the level of vulnerability of several orders of magnitude. The addition of the SVALLO1A-FCORNI1A line to the network vanishes the vulnerability in Area A and reduces greatly the one in Area B. Minor changes regarding the whole network can improve considerably resilience leading to better security of supply. The augmented network resilience could also benefit other scenarios not simulated here. For example, normal weather conditions coupled with transmission lines maintenances, as well as other extreme weather conditions such as winter storms.

Even though the PSCM 2018 is a less vulnerable alternative than the PS 2018, the SVALLO1A-FCORNI1A line has in all cases a lower priority compared to strategic network modifications included in the PS 2018. These changes are necessary to connect the coming pumped-storage power plants. Besides, these transformations assure a good level of security of supply during normal weather conditions. Nevertheless, the proposed alternative is a possible way of developing a more resilient transmission network.



---

## 7 Conclusions

*This chapter presents the conclusions of the research. It starts with an overview and then the main findings are highlighted. After that, the main contributions and limitations are summarized. Finally, possible future works are outlined.*

### 7.1 Overview of the research

The objective of this research is the assessment of the vulnerability of transmission networks subject to extreme weather conditions. They provoke common mode contingencies of overhead transmission lines impeding the transfer of electricity from the production sites to distribution networks. These simultaneous failures endanger the security of supply because transmission networks are usually devised and operated according to the N-1 criterion, that is to say, to only withstand single outages. Therefore, common mode contingencies can cause exceeding security limits possibly leading to further disconnections of transmission infrastructures and large disturbances. The planning of network structure taking into account plausible and severe coincident outages assists in the reduction of vulnerability.

In this research, the vulnerability is measured in terms of probability and severity of common mode contingencies aggregated into an index quantifying the overall level of vulnerability. The probability is a complex function of the space-time evolution of extreme weather events, the geographic distribution of transmission lines and the physical resistance the sometimes raging natural environment. Since the number of possible common mode contingencies is tremendous for real network, only the most probable are taking into account in the vulnerability assessment. The severity is evaluated by a contingency analysis based on an AC power flow model of the electric power system. This model calculates branch current through transmission lines and voltage at buses. It gives a static image of the network state since it assumes that all transients have vanished. The severity is an aggregated index composed by the combination of current overloads and unsafe voltage deviations.

The vulnerability index is projected into two dimensions in order to identify weak zones of the network. This projection ends in the matrix of vulnerability. The first dimension consists of the transmission lines included in the most probable and severe common mode contingencies. The second contains the transmission lines and buses undergoing violation of security limits. The matrix of vulnerability allows simple linking of the infrastructures suffering from weather related outages to those which exhibit overcharges. Then, the transmission infrastructures of both dimensions are aggregated in major zones of vulnerability. They are independent regions of the network responsible of most of the vulnerability.

Consequently, the causes of vulnerability of these zones are inferred to identify appropriate countermeasures for reducing vulnerability. They are possible actions to be taken if the

---

overall vulnerability is deemed excessive. For mature electric power systems, the risk of major disturbances is low because of past adverse experiences leading to reinforcement measures. In this case, countermeasures are likely to not be justified if they only are useful during rare extreme weather events. Therefore, countermeasures should be considered as alternatives to development plans of the system, and thus, also profitable during normal weather conditions.

The approach used to model electric power systems and extreme weather events is based on scenarios. They allow the construction of a simplified but truthful replica of complex systems under uncertainty. Two types of scenarios are required to assess vulnerability. First, scenarios of extreme weather event store the space-time evolution of particular past or simulated weather events. The primary hazardous features threatening the physical integrity of transmission lines such as wind speed or lightning impacts compose these scenarios. They can be seen as a movie of the extreme weather event sweeping across the transmission network. The second type of scenario represents specific states of the electric power system under investigation. These scenarios are subdivided into three models. The electric model stores all the relevant electric characteristics of the power systems. It is based on an AC power flow model used in contingency analysis to obtain an evaluation of the severity of common mode contingencies. The geographic model locates each of the transmission line of the electric model over the territory. This model and the scenarios of extreme weather event are superimposed to estimate the transmission line exposure. Finally, the reliability model links the scenarios of extreme weather event with those of electric power system to estimate the probability of common mode contingencies. This model is composed by two opposed processes. First, the disconnection process mimics the behavior of transmission lines subject to weather in terms of rate of failure. On the other hand, the reconnection process simulates, in terms of reconnection rate, the automatic security systems or operators turning back on failed lines. The two rates are used to evaluate the temporal probability of each transmission line or any combinations of them of being unavailable.

The methodology is applied to the Swiss transmission network in 2006 and 2018 impacted by two extreme thunderstorm events. Thunderstorms have been chosen because of their relative high frequency of occurrence and their complex space-time correlations. The Swiss electric power system will undergo major modifications within the next years and its transmission network will adapt to the rise in consumption, increasing transit power flows and new pumped-storage hydro power plants. These adjustments are an opportunity to assess the change in vulnerability between 2006 and 2018 to possibly propose alternatives to the current development plans. One has to insist that the objective of this application is not to draw final conclusions about the vulnerability of the Swiss transmission network. Rather, this application should be considered as an illustration of the methodology taking into account the most relevant characteristics of the Swiss network.

Two major zones of vulnerability are found in the scenarios under investigation at peak demand. The existence of these zones in 2006 and 2018 suggests the main cause of vulnerability is not tackled by the modifications proposed by the scenario of 2018. It seems that the topography plays a key role in the vulnerability of these zones. Indeed, these two mountain areas are prone to the establishment of large hydro power plants and a low consumption whereas transmission lines are difficult to build a variety of reasons. It is worth

---

mentioning that the vulnerability of these regions is not so severe that they would require radical transformations. As a result, only one countermeasure has been proposed consisting of the addition of a 380 kV line mounted in parallel to an existent one. In this case, the vulnerability of both regions decreases by several orders of magnitude even in the remote one. This demonstrates that vulnerability can be reduced by minimal changes in the network structure.

## 7.2 Main findings of the research

The main findings of this research are summarized as follow:

1) Most of the probable and severe common mode contingencies are composed by line close to each other. The limited range in the space-time correlations of weather events favors proximate lines failing simultaneously. Moreover, these lines are more likely to induce overloads when tripping off because of the electric proximity. These observations are valid to a certain extent for all type of extreme weather conditions and transmission networks. Therefore, the N-1 criterion could be broadened to an N-2 criterion for overhead transmission lines ending at the same substation, mounted on the same pylons or whose paths are closely parallel.

2) Some areas regroup the majority of the probable and severe common mode contingencies and their hazardous consequences. These major zones of vulnerability are vulnerable areas in the electric power systems that have priority at the time of vulnerability diminution. A reduce number of network modifications are able to augment the resilience of several vulnerable areas. This is the case of the SVALLO1A-FCORNI1A line of the case study. This line alleviates the main cause of vulnerability by draining an important amount of power from loaded lines from two major zones of vulnerability. It is not guaranteed that such a relieving procedure can always be found in general, but it will likely be more beneficial on the long run than small local actions.

3) A methodology based on scenarios is able to cope with the inherent complexity and uncertainty of interacting systems similar to those under examination. One of the key advantages of the scenario-based approach is that the modeler learns how the systems work at the time of building the cases. Scenarios are easily updated when new pieces of information are available, which is important the full range of information is rarely accessible from the initiation of research. Finally, all imaginable scenarios can be created. This property allows prospective vulnerability assessments of electric power systems, even for extreme weather events which have not actually occurred in the past.

4) GIS is of great help when building geographic models and calculating the exposure of segments. Without the use of the current GIS software, these tasks would have been extremely burdensome or even impossible. More generally, GIS could improve and facilitate the planning and operation of transmission networks. Although it is currently employed in electric utilities, its capabilities have certainly not been fully used. Bridges between geographical sciences and electrical engineering could foster innovative solutions tackling

---

future needs of the industry.

5) The methodology is implemented with standard GIS and power flow analysis software which are widely used in the industry and academics. Unfortunately, these two programs are not made to work together and problems of data integrity and coherence among models arose during the creation of scenarios and simulations. These problems were solved by investing in a remarkable programming and debugging effort. However, most of the resources should be invested in the development of representative and plausible scenarios as well as interpretation of results. As the application has shown, integrated and reliable software of vulnerability analysis could be readily developed to facilitate vulnerability assessments during extreme weather conditions.

### **7.3 Main contributions and limitations**

The first main contribution consists of the evaluation of the subjective probability of common mode contingencies taking into account to the following characteristics:

- Space-time correlations of extreme weather events
- Geographic distribution of transmission lines
- Time-dependent disconnection and reconnection processes of transmission lines

These characteristics have never previously been associated in vulnerability assessments of large transmission network impacted by extreme weather events. The recourse to GIS as a basis for dynamic simulations is also quite a novel approach since it was mainly developed for static analyses such as cartography. The mixing of these three points allows a spatiotemporal evaluation of the unavailability of any transmission lines or any combinations of them. This is very important in case of extreme weather conditions since failures in common modes are likely and represents threats to the security of supply. Vulnerability assessments are enhanced by taking space-time dimensions into consideration.

This leads to the second main contribution regarding the concept of major zone of vulnerability. First, the overall vulnerability is defined by the sum of partial vulnerability induced by common mode contingencies. Therefore, vulnerability is considered as an extensive property of transmission networks. It is defined as the product of the probability by the severity of a given power line contingency. Both of these vulnerability components are strongly related to space and time as shown above for the probability. In the case of severity, the space-time dimensions pertain to the location of production and consumption centers combined with the topology and capacity of the network. The association of the space-time dimensions of probability and severity leads to major zones of vulnerability. In this research, this intuitive concept has been openly defined in the methodological part and validated in the application. Major zones of vulnerability aggregate numerous outcomes of simulation in a unique fashion that facilitates the understanding of the causes of vulnerability and the search for countermeasures.

One limitation pertains to the plausibility and relevance of the scenarios, exact states of the

---

Swiss and European electric power systems are not known exactly since they are dependent on multiple decisions made by numerous actors during the coming years. Equally important, extreme weather events are not predictable regarding the details required by the scenarios. The inherent uncertainty about complex systems and the difficulty to model them deter any predictions of vulnerability. However, the objective is much more reasonable since aims at assessing the vulnerability of plausible scenarios. This approach enhances the comprehension of the underlying mechanisms of the vulnerability and this knowledge is valuable at the time of devising strategic electricity infrastructures.

Another limitation is the measure of vulnerability derived only on violation of security limits. The contingency analysis based on an AC power flow model gives a static picture of the state just after simultaneous contingencies. The vulnerability analysis is limited at the transmission network level. On the other hand, a thorough analysis should take into account the negative externalities for the society. It would require an evaluation of the consequences of contingencies which entails dynamic simulations.

In contrast to some risk analyses, this vulnerability analysis is not able to evaluate the balance between costs of countermeasure and reduction of cost due to more resilient networks. Justification of countermeasures has to take place in a supplementary analysis considering the inherent uncertainties of the problem. However, the methodology provides guidelines fostering reasonable countermeasures.

## 7.4 Future works

The methodology presented in this thesis can be further improved in a number of ways. First, the disconnection process could take into account several mechanisms of failure acting at the same time, such as fugitive failures from short circuits or permanent failures due to mechanical damages. The reconnection process could also consider different mechanisms for fixing such automatic circuit recloser or actions of repair teams. The former is important when mechanical damages are likely as in during a hurricane. The second possible improvement concerns the subjective probability. Another possible candidate could be the fuzzy set theory, which properly deals with incomplete or imprecise information. Finally, the severity could be expressed in term of energy not served by evaluating the consequences of contingencies at the consumer level.

Winter storms are possible threats to the Swiss transmission network. New major zones of vulnerability are likely to be discovered with this new extreme weather condition. Indeed, their space-time correlations and the winter power flows are markedly different than those studied in this research. It is also worth mentioning that global warming could radically change the climate for which the electric power system has been designed. Distribution networks should not be neglected since they are especially sensitive to environmental dangers.

The methodology proposes a vulnerability assessment for planning purposes. It could be adapted to real-time or day ahead assessments. In these cases, the uncertainty about network

---

states and weather conditions would be reduced, and plausible contingencies could be taken into account to prepare and implement short term countermeasures.

In the long run, electric power systems will change due to environmental constraints and new technologies. In a few decades, greener and smarter will describe the best of these systems. It is imaginable that intermittent and local sources of energy could partially supply consumers while the rest would be remotely provided via large center of production such as wind or solar farms. Information technology would connect and coordinate the different parts of the system to assure its safety and efficiency. This futuristic system would also be subject to new forms of vulnerability not yet known, and new tools will be required to design resilient hybrid systems combining information and energy. In these conditions, the use of dynamic simulations combining geographic and electric models would be appropriate to challenge the complexity of future vulnerability issues.



---

## 8 Bibliography

- AES-VSE (2005) Statistique 2005 sur la disponibilité de la fourniture en électricité en Suisse. Lausanne, AES-VSE.
- AES-VSE (2006) Prévision 2006 sur l'Approvisionnement de la Suisse en Electricité jusqu'en 2035/2050. Lausanne, AES-VSE.
- AGUET, M. & IANOZ, M. (2004) *Haute tension*, Lausanne, Presse polytechnique universitaire romande.
- AGUET, M. & MORF, J. J. (1990) *Energie électrique*, Lausanne, Presses polytechniques et universitaires romandes.
- ALBERTO NUCCI, C. (2010) A survey on Cigre and IEEE procedures for the estimation of the lightning performance of overhead transmission and distribution lines. *Electromagnetic Compatibility (APEMC), 2010 Asia-Pacific Symposium on*.
- ALGUACIL, N., CARRIÓN, M. & ARROYO, J. M. (2009) Transmission network expansion planning under deliberate outages. *International Journal of Electrical Power & Energy Systems*, 31, 553-561.
- ALPIQ (2009) Pumped storage power station capacity increase investigated. Lausanne, [http://www.alpiq.com/news-stories/press-releases/press\\_releases.jsp?news=tcm:95-64834](http://www.alpiq.com/news-stories/press-releases/press_releases.jsp?news=tcm:95-64834).
- ALVEHAG, K., SODER, L. & IEEE (2008) *A Stochastic Weather Dependent Reliability Model for Distribution Systems*, New York, Ieee.
- ASCHER, H. & FEINGOLD, H. (1984) *Repairable systems reliability: Modeling, inference, misconceptions and their causes.*, New-York, Marcel Dekker.
- BALDICK, R., CHOWDHURY, B., DOBSON, I., DONG, Z. Y., GOU, B., HAWKINS, D., HUANG, H., JOUNG, M., KIRSCHEN, D., LI, F. X., LI, J., LI, Z. Y., LIU, C. C., MILI, L., MILLER, S., PODMORE, R., SCHNEIDER, K., SUN, K., WANG, D., WU, Z. G., ZHANG, P., ZHANG, W. J., ZHANG, X. P. & FORCE, E. P. C. T. (2008) Initial review of methods for cascading failure analysis in electric power transmission systems. *Ieee Power & Energy Society General Meeting, Vols 1-11*, 52-59-5633.
- BALDICK, R., CHOWDHURY, B., DOBSON, I., DONG, Z. Y., GOU, B., HAWKINS, D., HUANG, Z. Y., JOUNG, M., KIM, J., KIRSCHEN, D., LEE, S., LI, F. X., LI, J., LI, Z. Y., LIU, C. C., LUO, X. C., MILI, L., MILLER, S., NAKAYAMA, M., PAPIĆ, M., PODMORE, R., ROSSMAIER, J., SCHNEIDER, K., SUN, H. B., SUN, K., WANG, D., WU, Z. G., YAO, L. Z., HANG, P., ZHANG, W. J., ZHANG, X. P. & PREDICTIO, T. F. U. (2009) Vulnerability Assessment for Cascading Failures in Electric Power Systems. *2009 Ieee/Pes Power Systems Conference and Exposition, Vols 1-3*, 83-91-2078.
- BENISTON, M. (2004) Extreme climatic events: Examples from the alpine region. *Journal De Physique Iv*, 121, 139-149.
- BESSIS, J. (2007) *La probabilité et l'évaluation des risques*, Paris, Masson.
- BILLINGTON, R. & WENYUAN, L. (1994) *Reliability assessment of electric power systems using monte carlo methods*, New York, Plenum Press.
- BILLINGTON, R., WU, C. & SINGH, G. (2002) Extreme adverse weather modeling in transmission and distribution system reliability evaluation. *14th PSCC*. Sevilla.
- BILLINTON, R. & SINGH, G. (2006) Application of adverse and extreme adverse weather: modelling in transmission and distribution system reliability evaluation. *Generation, Transmission and Distribution, IEE Proceedings-*, 153, 115-120.
- BIROLINI, A. (2007) *Reliability engineering: theory and practice*, Berlin, Springer.

- 
- BLACHE, K. M. & SHRIVASTAVA, A. B. (1994) Defining failure of manufacturing machinery and equipment. *Reliability and Maintainability Symposium, 1994. Proceedings., Annual*.
- BOSSEL, H. (1994) *System simulation and modelling*, Wiesbaden, Verlag Vieweg.
- BOX, G. E. P., JENKINS, G. M. & REINSEL, G. C. (2008) *Time series analysis: Forecasting and control*, Hoboken, John Wiley and Sons.
- BRÉMAUD, P. (2001a) *Markov chains: Gibbs fields, monte carlo simulation, and queues*, New-York, Springer.
- BRÉMAUD, P. (2001b) *Markov chains: Gibbs fields, monte carlo simulation, and queues*. New-York, Springer.
- BRESLIN, P., FRUNZI, N., NAPOLEON, E. & ORMSBY, T. (1999) *Getting to know ArcView GIS: the geographic information system (GIS) for everyone*, Redlands, ESRI.
- BROSTROM, E., AHLBERG, J. & SODER, L. (2007) Modelling of Ice Storms and their Impact Applied to a Part of the Swedish Transmission Network. *Power Tech, 2007 IEEE Lausanne*.
- BUSARELLO & COTT (2010) The high-end power system analysis tool. Erlendbach.
- CARRERAS, B. A., NEWMAN, D. E., DOBSON, I. & POOLE, A. B. (2004) Evidence for self-organized criticality in a time series of electric power system blackouts. *Circuits and Systems I: Regular Papers, IEEE Transactions on*, 51, 1733-1740.
- CEC (2006) Green Paper on a European Strategy for Sustainable, Competitive and Secure Energy. Brussel, Commission of the European Communities.
- CEC (2007) Priority Interconnection Plan. Brussel, Commission of the European Communities.
- CHRISMAN, N. R. (1999) What Does 'GIS' Mean? *Transactions in GIS*, 3, 175-186.
- COM (2003) Undergrounding of Electricity Lines in Europe. Brussels, Commission of the European Communities.
- CORWIN, J. & MILES, W. (1979) Impact Assessment of the New York City Blackout. Palo Alto CA, SCI inc.
- COX, A. B. & GIFFORD, F. (1997) An overview to geographic information systems. *The Journal of Academic Librarianship*, 23, 449-461.
- CRESSIE, N. A. C. (1993) *Statistics for Spatial Data*, Wiley-Interscience.
- DE CONTI, A., PEREZ, E., SOTO, E., SILVEIRA, F. H., VISACRO, S. & TORRES, H. (2006) Calculation of Lightning-Induced Voltages on Overhead Distribution Lines Including Insulation Breakdown. *Power Delivery, IEEE Transactions on*, PP, 1-1.
- DEO, P. P. (2007) *Power system analysis*, Pune, Technical Publication Pune.
- DOBESCH, H., DUMOLARD, P. & DYRAS, I. (2007) *Spatial interpolation for climate data: The use of GIS in climatology and meteorology*, London, Wiley-ISTE.
- DOBSON, I. (2002) Examining Criticality of Blackouts in Power System Models with Cascading Events. *Hawaii International Conference on System Sciences*. Hawaii
- DOORMAN, G., KJOLLE, G., UHLEN, K., HUSE, E. S. & FLATABO, N. (2004) Vulnerability of the nordic power system. Trondheim, SINTEF.
- DORMAND, J. R. & PRINCE, P. J. (1980) A family of embedded Runge-Kutta formulae. *Journal of Computational and Applied Mathematics*, 6, 19-26.
- DUENAS-OSORIO, L. & VEMURU, S. M. (2009) Cascading failures in complex infrastructure systems. *Structural Safety*, 31, 157-167.
- ENTSO-E (2008) Statistical Year Book. Brussels, European Network of Transmission System Operators for Electricity.
- ENTSO-E (2009a) P3 – Policy 3: Operational Security. ENTSO-E.
- ENTSO-E (2009b) System Adequacy Forecast for 2010-2025. Brussels, European Network of Transmission System Operators for Electricity.
- ENTSO-E (2010) Statistical Year Book. Brussels, ENTSO-E.
- ESRI (2010a) ArcInfo: the complete desktop GIS. ESRI.
-

- 
- ESRI (2010b) Map and aps for everyone.
- EURELECTRIC (2004) Security of Supply. Brussels, Eurelectric.
- EWIS (2007) European Wind Integration Study (EWIS) Towards a Successful Integration of Wind Power into European Electricity Grids.
- FERSON, S. & GINZBURG, L. R. (1996) Different methods are needed to propagate ignorance and variability. *Reliability Engineering & System Safety*, 54, 133-144.
- FINK, L. H. & CARLSEN, K. (1978) Operating under stress and strain. *IEEE Spectrum*. IEEE.
- FINKE, U. & KREYER, O. (2002) Review of existing lightning location systems. Hannover, Institute für Meteorologie und Klimatologie.
- FUCHS, E. F. & MASOUM, M. A. S. (2008) *Power Quality in power systems and electrical machines*, Burlington, Elsevier Academic Press.
- GILGEN, H. (2006) *Univariate time series in geosciences: Theory and examples*, Berlin, Springer-Verlag.
- GOMES, P. (2004) New strategies to improve bulk power system security: lessons learned from large blackouts. *Power Engineering Society General Meeting, 2004. IEEE*.
- GOMES, P., DE LIMA, A. C. S. & DE PADUA GUARINI, A. (2004) Guidelines for power system restoration in the Brazilian system. *Power Systems, IEEE Transactions on*, 19, 1159-1164.
- GRAINGER, J. J. & STEVENSON, W. D. (1994) *Power system analysis*, Hightstown, McGraw-Hill.
- GROSS, J. (2003) *Linear regression*, Heidelberg, Springer-Verlag, chapter 3.
- GUIKEMA, S. D. (2009) Natural disaster risk analysis for critical infrastructure systems: An approach based on statistical learning theory. *Reliability Engineering & System Safety*, 94, 855-860.
- HAN, S.-R., GUIKEMA, S. D., QUIRING, S. M., LEE, K.-H., ROSOWSKY, D. & DAVIDSON, R. A. (2009) Estimating the spatial distribution of power outages during hurricanes in the Gulf coast region. *Reliability Engineering & System Safety*, 94, 199-210.
- HARDIMAN, R. C., KUMBALE, M. & MAKAROV, Y. V. (2004) An advanced tool for analyzing multiple cascading failures. *Probabilistic Methods Applied to Power Systems, 2004 International Conference on*.
- HARVEY, F. (2008) *A primer of GIS: fundamental geographic and cartographic concepts*, New York, Guilford Press.
- HONGBIAO, S. & KEZUNOVIC, M. (2005) Static Security Analysis based on Vulnerability Index (VI) and Network Contribution Factor (NCF) Method. *Transmission and Distribution Conference and Exhibition: Asia and Pacific, 2005 IEEE/PES*.
- HUANG, Z., ROSOWSKY, D. V. & SPARKS, P. R. (2001) Hurricane simulation techniques for the evaluation of wind-speeds and expected insurance losses. *Journal of Wind Engineering and Industrial Aerodynamics*, 89, 605-617.
- IPCC (2001) Climate Change. The IPCC Third Assessment Report. Volumes I (Science), II (Impacts and Adaptation) and III (Mitigation Strategies). Cambridge, Cambridge University Press.
- IPCC, W. G. I. (2007) IPCC Fourth Assessment Report: Climate Change 2007: Impacts, Adaptation and Vulnerability Geneva, IPCC.
- ISERLES, A. (1996) *Numerical analysis of differential equations*, Cambridge, Cambridge University Press.
- JAYNES, E. T. (2003) *Probability theory: the logic of science*, Cambridge University Press.
- KELLEY, C. T. (2003) *Solving nonlinear equations with Newton's method*, Philadelphia, SIAM.
- KIESSLING, F., NEFZGER, P., NOLASCO, J. F. & KAJINTZYK, U. (2003) *Overhead power lines: planning, design, construction*, New-York, Springer Verlag.
-

- 
- KLIR, G. J. & SMITH, M. (2001) On measuring uncertainty and uncertainty-based information: Recent development. *annals of mathematics and artificial intelligence*, 32, 5-33.
- KNIGHT, U. G. (2001) *Power systems in emergencies*, Chichester, John Wiley & Sons LTD.
- KUMBALE, M., HARDIMAN, R. & MAKAROV, Y. (2008) A methodology for simulating power system vulnerability to cascading failures in the steady state. *European Transactions on Electrical Power*, 18, 802-808.
- LI, L. & REVESZ, P. (2004) Interpolation methods for spatio-temporal geographic data. *Computers, Environment and Urban Systems*, 28, 201-227.
- LI, W. (2005) *Risk assessment of power systems*, Piscataway, IEEE Press.
- LI, W., XIONG, X. & ZHOU, J. (2009) Incorporating fuzzy weather-related outages in transmission system reliability assessment. *Generation, Transmission & Distribution, IET*, 3, 26-37.
- LIU, H., DAVIDSON, R. A. & APANASOVICH, T. V. (2008) Spatial generalized linear mixed models of electric power outages due to hurricanes and ice storms. *Reliability Engineering & System Safety*, 93, 897-912.
- LUEMONGKOL, T., WANNAKOMOL, A. & KULWORAWANICHPONG, T. (2009) Application of Satellite Imagery for Rerouting Electric Power Transmission Lines. IN TRILLING, L., PERKINS, S., DIONYSIOU, D., PERLOVSKY, L., DAVEY, K., LANDGREBE, D., MARINO, M. A., RUSSELL, D. L., COLLICOTT, S. H., CECCARELLI, M. & LUND, J. W. (Eds.) *Recent Advances in Energy and Environment - Proceedings of the 4th Iasme/Wseas International Conference on Energy and Environment*. Athens, World Scientific and Engineering Acad and Soc.
- MAKAROV, Y. V., RESHETOV, V. I., STROEV, V. A. & VOROPAI, N. I. (2005) Blackout prevention in the United States, Europe, and Russia. *Proceedings of the Ieee*, 93, 1942-1955.
- MAO, A., YU, J. & GUO, Z. (2006) Electric power grid structural vulnerability assessment. *Power Engineering Society General Meeting, 2006. IEEE*.
- METEORAGE (2010) Meteorage: Making the most of lightning. Available at: <http://www.meteorage.com/#>.
- MILLS, S. J., GERARDO CASTRO, M. P., LI, Z., CAI, J., HAYWARD, R., MEJIAS, L. & WALKER, R. A. (2004) Evaluation of Aerial Remote Sensing Techniques for Vegetation Management in Power-Line Corridors. *Geoscience and Remote Sensing, IEEE Transactions on*, PP, 1-12.
- MODARRES, M., KAMINSKIY, M. & KRISVTSOV, V. (1999) *Reliability engineering and risk analysis: A practical guide*, New York, Marcel Dekker.
- MONTEIRO, C., RAMIREZ-ROSADO, I. J., MIRANDA, V., ZORZANO-SANTAMARIA, P. J., GARCIA-GARRIDO, E. & FERNANDEZ-JIMENEZ, L. A. (2005) GIS spatial analysis applied to electric line routing optimization. *Ieee Transactions on Power Delivery*, 20, 934-942.
- NAG, O. & SENGUPTA, S. (2008) Appendix. IN COMPANY, C. P. (Ed.) *Introduction to geographical information systems*. New Dehli, Ashol Kummer Mittal.
- NERC (2008) Long-term reliability assessment for 2008-2017. Princeton, Nerc.
- NERC (2010) Reliability standards complete set. NERC.
- NOVOSEL, D., BEGOVIC, M. M. & MADANI, V. (2004) Shedding Light on Blackouts. *IEEE power and energy magazine*.
- OFEN (2009a) Rapport sur les résultats de la procédure d'audition sur le système d'examen et d'évaluation «Câblage - ligne aérienne» pour les lignes à haute tension Bern, OFEN.
- OFEN (2009b) Rapport sur les résultats de la procédure d'audition sur le système d'examen et d'évaluation «Câblage - ligne aérienne» pour les lignes à haute tension 220/380 kV (sans attribution de points en fonction des coûts) Bern, OFEN.
- OFEN (2009c) Statistique Suisse de l'Electricité en 2008. Bern, Office fédéral de l'énergie
-

- 
- OFEN (2010) Projet ligne 380 kV Chatelard-Rosel: Rapport explicatif. Bern, OFEN.
- OFEN & ARE (2001) Transmission Lines Sectoral Plan. Bern, Office fédéral de l'énergie Office fédéral du développement territorial.
- PATECORNELL, M. E. (1996) Uncertainties in risk analysis: Six levels of treatment. *Reliability Engineering & System Safety*, 54, 95-111.
- PHILLIPS, A. (2004) Handbook for Improving Overhead Transmission Line Lightning Performance. Palo Alto, EPRI, 28-29.
- PIKETTY, G., TRINK, C. & ABORD DE CHATILLON, R. (2000) La Sécurisation du Système Electrique Français. Paris, Secrétariat d'état à l'industrie.
- POLYANIN, A. D. & ZAITSEV, V. F. (2003) *Handbook of Exact Solutions for Ordinary Differential Equations*, Boca Raton, CRC Press.
- POURBEIK, P., KUNDUR, P. S. & TAYLOR, C. W. (2006) The anatomy of a power grid blackout - Root causes and dynamics of recent major blackouts. *Power and Energy Magazine, IEEE*, 4, 22-29.
- RAPPAZ, J. & PICASSO, M. (2000) *Introduction à l'analyse numérique*, Lausanne, Presses polytechniques et universitaires romandes.
- RAUSAND, M. & HOYLAND, A. (2004) *System Reliability Theory*, Hoboken, Wiley-Interscience.
- RINGLAND, G. (2006) *Scenario planning: Managing the future*, Chichester, John Wiley and Sons Ltd.
- SAKIS MELIOPOULOS, A. P. (1988) *Power system grounding and transients: An introduction*, New York, Marcel Dekker.
- SCHÄTTLER, U., DOMS, G. & SCHRAFF, C. (2009) A description of the nonhydrostatic regional COSMO-model: Part VII. Offenbach, Consurtium for small-scale modelling.
- SCHIESSER, H. H., HOUZE, R. A. & HUNTRIESER, H. (1995) The Mesoscale Structure of Severe Precipitation Systems in Switzerland. *Monthly Weather Review*, 123, 2070-2097.
- SCHIESSER, H. H., SCHMID, W., HOUZE, R. A., BAUER, B. & AMER METEOROL, S. O. C. (1996) *A tornado-producing mesoscale convective system in northern Switzerland*, Boston, Amer Meteorological Soc.
- SCHMID, W., SCHIESSER, H. H. & BAUER-MESSMER, B. (1997) Supercell storms in Switzerland: case studies and implications for nowcasting severe winds with Doppler radar. John Wiley & Sons, Ltd.
- SCHWIERZ, C., KÖLLNER-HECK, P., ZENKLUSEN MUTTER, E., BRESCH, D., VIDALE, P.-L., WILD, M. & SCHÄR, C. (2010) Modelling European winter wind storm losses in current and future climate. *Climatic Change*, 101, 485-514.
- SHAFER, G. (2009) A betting interpretation for probabilities and Dempster-Shafer degrees of belief. *International Journal of Approximate Reasoning*, In Press, Corrected Proof.
- SILVAST, A. & KAPLINSKY, J. (2007) Project UNDERSTAND: White Paper on Security of European Electricity Distribution. Eskilstuna, Swedish energy agency.
- SNAIDER, R. J. (2005) Operational uses of weather information in GIS based decision support systems. Burnsville, Meteorlogix.
- STANTON, K. N. (1969) Reliability Analysis for Power System Applications. *Power Apparatus and Systems, IEEE Transactions on*, PAS-88, 431-437.
- STOTT, B. (1974) Review of load-flow calculation methods. *Proceedings of the Ieee*, 62, 916-929.
- STOTT, B., ALSAC, O. & MONTICELLI, A. J. (1987) Security analysis and optimization. *Proceedings of the Ieee*, 75, 1623-1644.
- SUNDELL, J., BECK, D., HARRIS, J. L. & PIERRE, I. (2006) Impacts of Severe Storms on Electric Grids. 2006, Eurelectric.
- SUTER, S., KONZERLMANN, T., MÜHLHÄUSER, C., BERGERT, M. & HEIMO, A. (2006) SwissMetNet- The New Automatic Meteorological Network of Switzerland:
-

- 
- Transition From Old to New Network, Data Management and First Results. Zürich, Meteosuisse.
- SWISSTOPO (2010) Vector 25. Available at:  
<http://www.swisstopo.admin.ch/internet/swisstopo/en/home/products/landscape/vector25.html>.
- TLEIS, N. (2008) *Power systems modelling and fault analysis: Theory and practice*, Oxford, Elsevier.
- TLSSW (2007) Rapport Final du Groupe de Travail : Lignes de Transport d'Electricité et Sécurité de l'Approvisionnement. Bern, OFEN.
- UCTE (2008) Memo. Brussels, Union for the coordination of transmission electricity.
- VAN DER HELM, R. (2006) Towards a clarification of probability, possibility and plausibility: How semantics could help futures practice to improve. *Foresight*, 8, 17-7.
- VAN HULLE, F. (2009) Developing Europe's power market for the large-scale integration of wind power. European Wind Energy Association.
- VARADAN, S. & VAN CASTEREN, J. (2009) Transmission planning risk indices - what now? *Power Systems Conference and Exposition, 2009. PSCE '09. IEEE/PES*.
- VARUM, C. A. & MELO, C. (2010) Directions in scenario planning literature - A review of the past decades. *Futures*, 42, 355-369.
- WENYUAN, L. (2005) *Risk assessment of power systems*, Piscataway, IEEE Press.
- WILLIS, H. L. (2004) *Power Distribution Planning Reference Book*, New York, Marcel Dekker.
- WINKLER, J., DUEÑAS-OSORIO, L., STEIN, R. & SUBRAMANIAN, D. (2010) Performance assessment of topologically diverse power systems subjected to hurricane events. 95, 323-336.
- WINKLER, R. L. (1996) Uncertainty in probabilistic risk assessment. *Reliability Engineering & System Safety*, 54, 127-132.
- ZHANG, P. (2003) TRELSS Application Manual. Palo Alto, EPRI.
- ZHANG, T. & HORIGOME, M. (2001) Availability and reliability of system with dependent components and time-varying failure and repair rates. *Reliability, IEEE Transactions on*, 50, 151-158.

---

## 9 Appendix

### 9.1 Power system analysis

#### 9.1.1 AC power flow model

The derivation of the power flow equations starts with the bus admittance matrix of the network  $Y_{bus}$ . It is an  $n \times n$  symmetric matrix describing a power system with  $n$  buses. It represents the nodal admittance of the buses in a power system. In a real network, it is quite sparse. The admittance  $Y^{i,j}$  between the bus  $i$  and  $j$  is derived from the single-line diagram of the network represented by their nominal  $\pi$  equivalent circuit in the per-unit system. Fuchs presents a method to build this equivalent circuit and the admittance matrix from the parameters of Table 3, see Chapter 7 of (Fuchs and Masoum, 2008). Since transmission networks are normally operated with balanced three-phase circuits, the calculation of only one phase is necessary. Indeed, the other phases just lag or lead with a phase of  $\pm 120^\circ$ .

In order to derive the power flow equations, the admittance is defined as:

$$Y^{i,j} = G^{i,j} + jB^{i,j} \quad (9.1)$$

Where  $G^{i,j}$ ,  $B^{i,j}$  are respectively the conductance and susceptance between bus  $i$  and  $j$ . The voltage  $V^i$  at bus  $i$  is typically in polar coordinates.

$$V^i = |V^i| \cdot (\cos(\theta^i) + j \sin(\theta^i)) \quad (9.2)$$

Where  $\theta^i$  is the angle of voltage at bus  $i$ . According to the Kirchhoff's current-node law, At any bus  $i$  of an electrical network, the sum of currents flowing into that bus is equal to the sum of currents flowing out of that node.

$$I^i = Y^{i,1} \cdot V^1 + Y^{i,2} \cdot V^2 + \dots + Y^{i,N} \cdot V^N = \sum_{n=1}^N Y^{i,n} \cdot V^n \quad (9.3)$$

The net real  $P^i$  and reactive  $Q^i$  power entering the network at the bus is found by multiplying (9.3) by the complex voltage  $V^{i*}$ , where  $*$  denotes the complex conjugate.

$$P^i - jQ^i = \sum_{j=1}^N V^{i*} Y^{i,j} V^j \quad (9.4)$$

Substituting (9.1) in (9.4) and equating the real and reactive parts gives the equation of the

AC power flow model. Steps of calculation can be found in the appendix C of (Wenyuan, 2005).

$$P_G^i - P_L^i = \sum_{j=1}^N |V^i| \cdot |V^j| \cdot (G^{i,j} \cos(\theta^{i,j}) + B^{i,j} \sin(\theta^{i,j})) = f^i \quad (9.5)$$

$$Q_G^i - Q_L^i = \sum_{j=1}^N |V^i| \cdot |V^j| \cdot (G^{i,j} \sin(\theta^{i,j}) - B^{i,j} \cos(\theta^{i,j})) = g^i \quad (9.6)$$

$$\text{Where } \theta^{i,j} = \theta^i - \theta^j \quad (9.7)$$

Subscripts  $G$  and  $L$  denote respectively generator and load.

A system of nonlinear equations is built with these two equations for the  $n$  buses. The two equations of the slack bus SB ( $i = 1$ ) are omitted because its voltage and angle are known by definition. For PQ bus, the active and reactive powers are known contrary to the bus voltage and phase angle. For the  $m$  PV buses, the active power and voltage magnitude is known. In this case, the reactive power equation is omitted.

$$\begin{cases} P^2 = f^2(|V^2|, \dots, |V^n|, \theta^2, \dots, \theta^n) \\ \vdots \\ P^n = f^n(|V^2|, \dots, |V^n|, \theta^2, \dots, \theta^n) \\ Q^{m+2} = g^{m+2}(|V^{m+2}|, \dots, |V^n|, \theta^{m+2}, \dots, \theta^n) \\ \vdots \\ Q^n = g^n(|V^{m+2}|, \dots, |V^n|, \theta^{m+2}, \dots, \theta^n) \end{cases} \quad (9.8)$$

This system  $2n - m - 2$  equations for  $2n - m - 2$  unknown quantities can be solved with the Newton-Raphson methods which are fully described in Chapter 9 of (Grainger and Stevenson, 1994). Once the voltages and their angles are known, the transit from  $i$  to  $j$  of power in the transmission line is given by

$$P^{i,j} = -P^{j,i} = \frac{|V^i| \cdot |V^j|}{X^{i,j}} \cdot \sin(\theta^{i,j}) \quad (9.9)$$

$$Q^{i,j} = C^i \cdot |V^i|^2 - \frac{|V^i|^2}{X^{i,j}} + \frac{|V^i|^2 \cdot |V^j|^2}{X^{i,j}} \cdot \cos(\theta^{i,j}) \quad (9.10)$$

Where  $C^i$  is the shunt capacitance and  $X^{i,j}$  the branch reactance

The derivation of these two equations are made in the Chapter 6.11 of (Sakis Meliopoulos, 1988). They are valid for short and medium length transmission lines where the branch resistance is neglected. In the same reference, the generalized equations for (9.9) and (9.10) are also provided. The current flow from  $i$  to  $j$  is simply derived from the bus voltages and the



---

line admittance by

$$I^i = Y^{i,j} \cdot (V^i - V^j) \quad (9.11)$$

### 9.1.2 DC power flow model

A simplified linear model, the DC power flow model, allows faster calculations at the price of imprecision. This model can be used for fast screening of severe CMCs prior to a more time consumer AC power flow model. The DC power-flow is based on the following assumptions

- 1) The voltage difference between two buses is small

$$\sin(\theta^{i,j}) = \theta^i - \theta^j \quad (9.12)$$

$$\cos(\theta^{i,j}) = 0$$

- 2) All voltages are assumed to be 1.0 p.u.

Under these assumptions, (9.9) can be further simplified

$$P^{i,j} = -P^{j,i} = \frac{\theta^i - \theta^j}{X^{i,j}} \quad (9.13)$$

$$Q^{i,j} = 0 \quad (9.14)$$

Since the power injected at a bus is equal to the power leaving the bus

$$P^i = \sum_j P^{i,j} = \sum_j \frac{\theta^{i,j}}{X^{i,j}} \quad (9.15)$$

Knowing the real power injection  $P^i$  and the branch inductance  $X^{i,j}$ , the angles difference  $\theta^{i,j}$  are found by solving the linear system. The power transit from  $i$  to  $j$  in the transmission line is easily carried out by injecting the  $\theta^{i,j}$  in (9.13).

### 9.1.3 Contingency analysis

Contingency analysis aims at assessing the static security of electric power systems when one or several of their elements trip off such as three-phase circuits, transformers, generators, loads or busbars. Thereafter, it is assumed that only power lines (three-phase circuit) can be disconnected due to extreme weather events. Several different methods of contingency

analysis have been reported in the literature. Many of them implement the network contribution factor method (Hongbiao and Kezunovic, 2005), which is fast but not accurate for high-order contingencies. Since this type of contingency is prevalent in this research, a contingency analysis based on an AC power flow analysis is retained. No approximation is made since a full power flow analysis is performed for each CMC. The method consists of the following steps:

- Determine the parameters of the electric model (Chapter 3.3.1)
- Identify the set  $\Gamma^m$  of plausible CMCs (Chapter 3.5)
- Perform a power flow analysis for each plausible CMC by disconnecting the correspondent power lines (Chapter 9.1.1)
- Identify the resultant violation of security limits

Two types of static security limits are considered for each CMC. First, the branch current must be below the maximum current  $I_{rating}^l$  transiting in line  $l$ . Secondly, the bus voltage  $V^i$  must not deviate more than the admissible voltage deviation  $V_{adm}^i$  around the nominal bus voltage  $V_{nom}^i$ . The following figure shows the process of the contingency analysis used for the CMC severity assessment of Chapter 3.6.

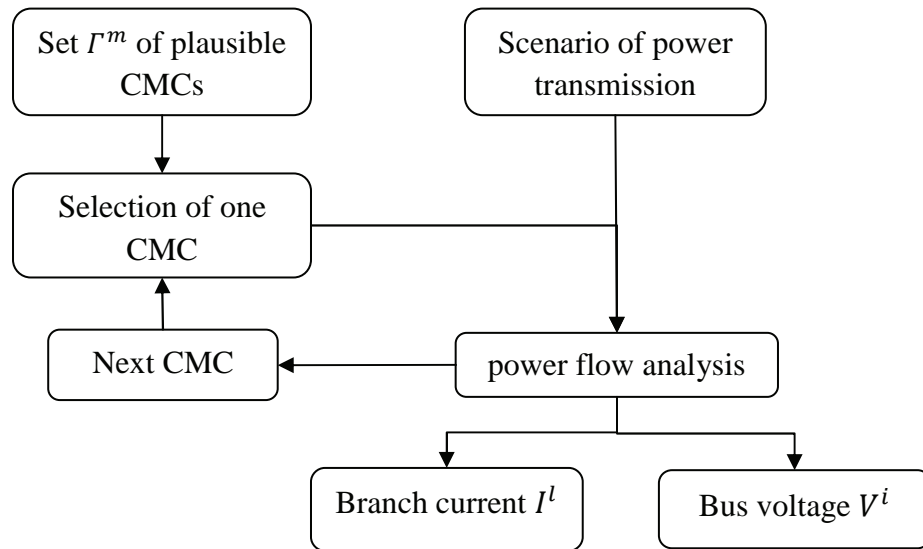


Figure 26: Process of the contingency analysis

---

## 9.2 Concepts from reliability theory

### *Definitions*

Here is a description of the most important definitions of concept of reliability theory. Birolini gives an introduction of reliability theory which inspired this chapter (Birolini, 2007)

The reliability or survival function is the probability that an item will perform its required function later than the specified time  $T$ .

$$R(t) = \Pr(T > t) \quad (9.16)$$

Where  $T$  is a continuous random variable denoting the time to failure. The complement of  $R(t)$  noted  $F(t)$  is the probability that an item will not perform its function later than  $T$ . The reliability function and its complement are cumulative distribution functions. The probability density function  $f(t)$  is the derivative of  $F(t)$ .

$$f(t) = \frac{dF(t)}{dt} = \frac{d}{dt}(1 - R(t)) = -\frac{dR(t)}{dt} \quad (9.17)$$

The hazard function  $h(t)$  is the probability that an item fails during  $dt$  at time  $t$  knowing it was functioning until  $t$ . The hazard function is denoted by  $\lambda(t)$  in the Chapter 3.3.3, also mentioned as the rate of failure.

$$h(t) = \frac{\Pr(t \leq T < t + dt \mid T \geq t)}{dt} = \frac{f(t)}{R(t)} \quad (9.18)$$

The relation between the hazard function and the reliability function is given by

$$R(t) = e^{-\int_0^t h(u)du} \quad (9.19)$$

### *Exponential model*

The exponential model is used in reliability engineering to model the process of failure or reconnection with a constant failure rate. This process is memoryless, namely items do not wear out with time. The probability of failure has the following formulation.

---

Probability density function:

$$f(t, \lambda) = Pr (t = T) = \begin{cases} \lambda \cdot e^{-\lambda t} & t \geq 0 \\ 0 & t < 0 \end{cases} \quad (9.20)$$

Cumulative distribution function:

$$R(t, \lambda) = Pr (T > t) = \begin{cases} e^{-\lambda \cdot t} & t \geq 0 \\ 0 & t < 0 \end{cases} \quad (9.21)$$

Where  $T$  is a continuous random variable denoting the time to failure of an item.

Hazard rate function:

$$h(t, \lambda) = \frac{f(t, \lambda)}{R(t, \lambda)} = \lambda \quad (9.22)$$

An interesting property of the exponential model arises for a series of  $n$  items with constant failure rate. The resultant reliability function is the product of the item's reliability. Interdependency among items is assumed.

$$R^S(t) = \prod_{i=1}^n R^i(t) = \prod_{i=1}^n \exp(-\lambda^i \cdot t) = \exp\left(t \cdot \sum_{i=1}^n \lambda^i\right) \quad (9.23)$$

Combining (9.18) with (9.23) yields to

$$h^S(t, \lambda) = \frac{dR^S(t)}{R^S(t)} = \sum_{i=1}^n \lambda^i \quad (9.24)$$

The rate of failure of a system composed by items in a series with constant failure rates equals the sum of those constant failure rates. This property is very important when modeling systems of subsystems in series like in Chapter 3.3.3 when developing the reliability model. A similar approach can be used in the general case of a non constant hazard function or rate of failure. In this case, the reliability function is given by (9.19):

$$R^S(t) = \prod_{i=1}^n R^i(t) = \prod_{i=1}^n \exp\left(-\int_0^t h^i(u) du\right) = \exp\left(-\int_0^t \sum_{i=1}^n h^i(u) du\right) \quad (9.25)$$

By identification to (9.19), the hazard function of a system is

$$h^S(t, \lambda) = \sum_{i=0}^n h^i(u) \quad (9.26)$$

Therefore, hazard function of a system composed by  $n$  independent components in series is the sum of the component's hazard functions.

### 9.3 Equivalence between the index and the matrix of vulnerability

The aim of this chapter is to demonstrate the equality between the sum of the element of the matrix of vulnerability and the aggregated index of vulnerability:

$$\sum_{k=1}^{N^\ell} \sum_{l=1}^{N^\ell} \sum_{i=1}^{N^\ell} v^{k,l,i} = V$$

First, the element of the matrix are expressed as the sum of probability and severity for all CMCs of the set  $\Gamma^m$ .

$$\sum_{k=1}^{N^\ell} \sum_{l=1}^{N^\ell} \sum_{i=1}^{N^\ell} v^{k,l,i} = \sum_{k=1}^{N^\ell} \sum_{l=1}^{N^\ell} \sum_{i=1}^{N^\ell} \sum_{m=1}^{N^m} \sum_{c=1}^{N_{cm}^m} \hat{U}_m^c \cdot \tilde{S}_m^c \cdot \gamma(k, m, c) \quad (9.27)$$

The permutation of the sums yields to:

$$= \sum_{m=1}^{N^m} \sum_{c=1}^{N_{cm}^m} \hat{U}_m^c \cdot \sum_{l=1}^{N^\ell} \sum_{i=1}^{N^\ell} \tilde{S}_m^c \cdot \sum_{k=1}^{N^\ell} \gamma(k, m, c) \quad (9.28)$$

According to (3.44)

$$\sum_{l=1}^{N^\ell} \sum_{i=1}^{N^\ell} \tilde{S}_m^c = S_m^c \quad (9.29)$$

Therefore (9.28) can be further simplified:

$$= \sum_{m=1}^{N^m} \sum_{c=1}^{N_{cm}^m} \hat{U}_m^c \cdot S_m^c \cdot \sum_{k=1}^{N^\ell} \gamma(k, m, c) \quad (9.30)$$

By definition of  $\gamma$ , for any couple  $(m, c)$ :

$$\sum_{k=1}^{N^\ell} \gamma(k, m, c) = 1 \quad (9.31)$$

Thanks to (9.31), equation (9.30) can be further simplified:

$$= \sum_{m=1}^{N^m} \sum_{c=1}^{N_{cmc}^m} \hat{U}_m^c \cdot S_m^c = V \quad (9.32)$$

The equality between the sum of the element of the matrix of vulnerability and the aggregated index of vulnerability is demonstrated.

## 9.4 Scenarios of extreme thunderstorm event

The following map shows the lightning impact of SEWE 1 (blue) and 2 (green) at less than 2.5 kilometers from the transmission network of the PS 2018.

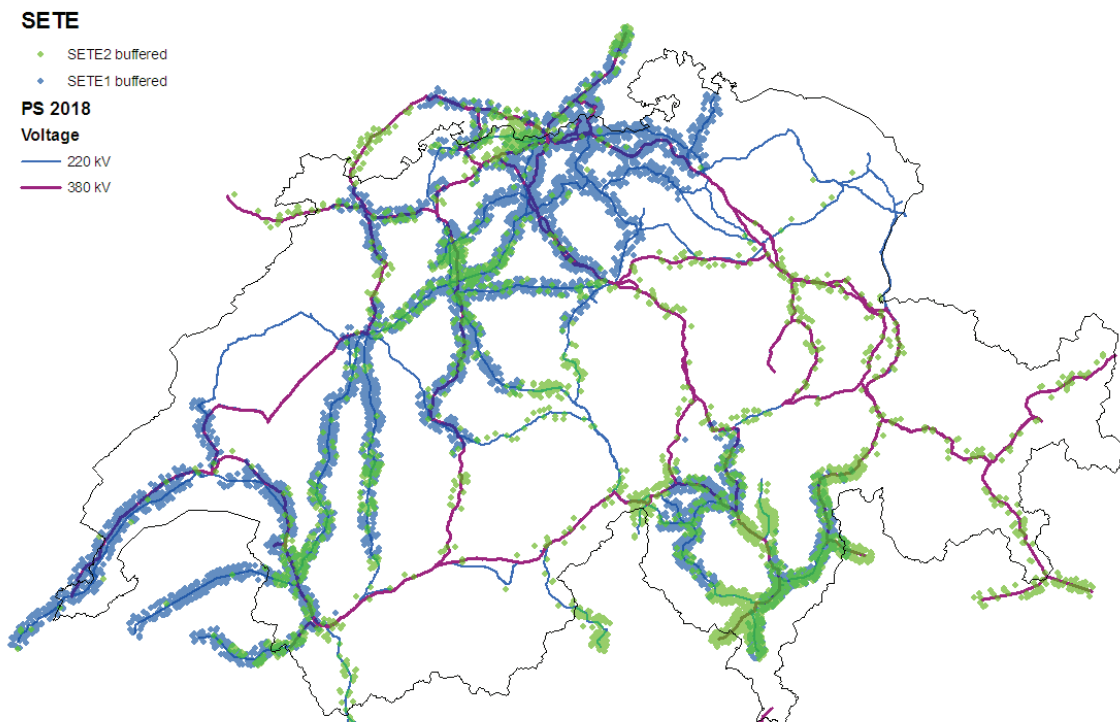


Figure 27: Map of lightning strikes close to transmission lines for SEWE 1 and 2

The two following graphs describe the evolution of the number of lightning impacts every 20 minutes at less than 2.5 kilometers from the transmission network of the PS 2018.

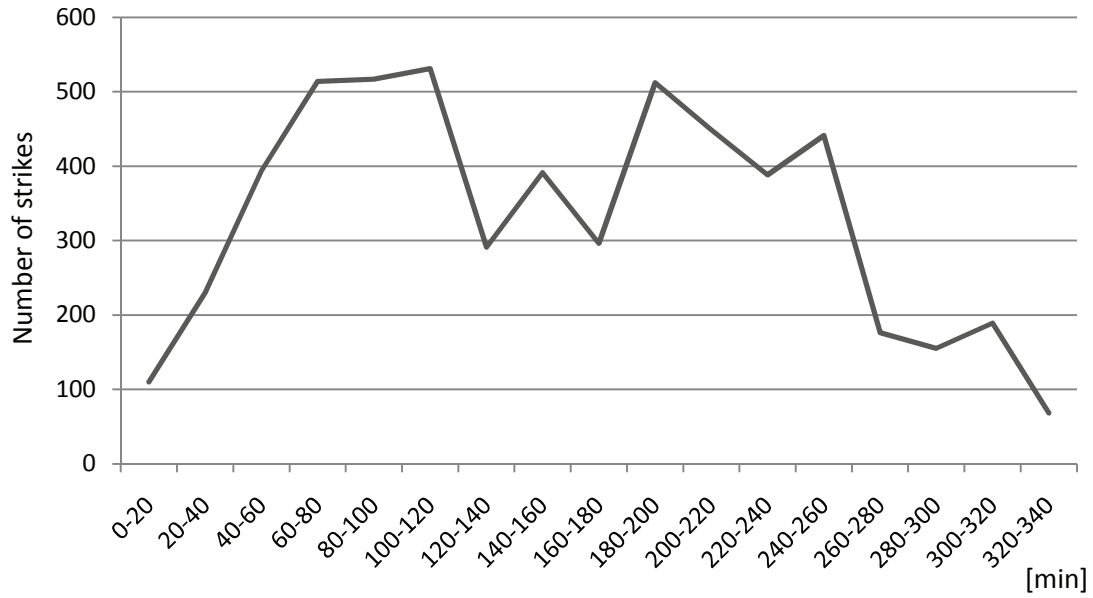


Figure 28: Lightning impacts at 2.5 km from transmission lines for SEWE 1

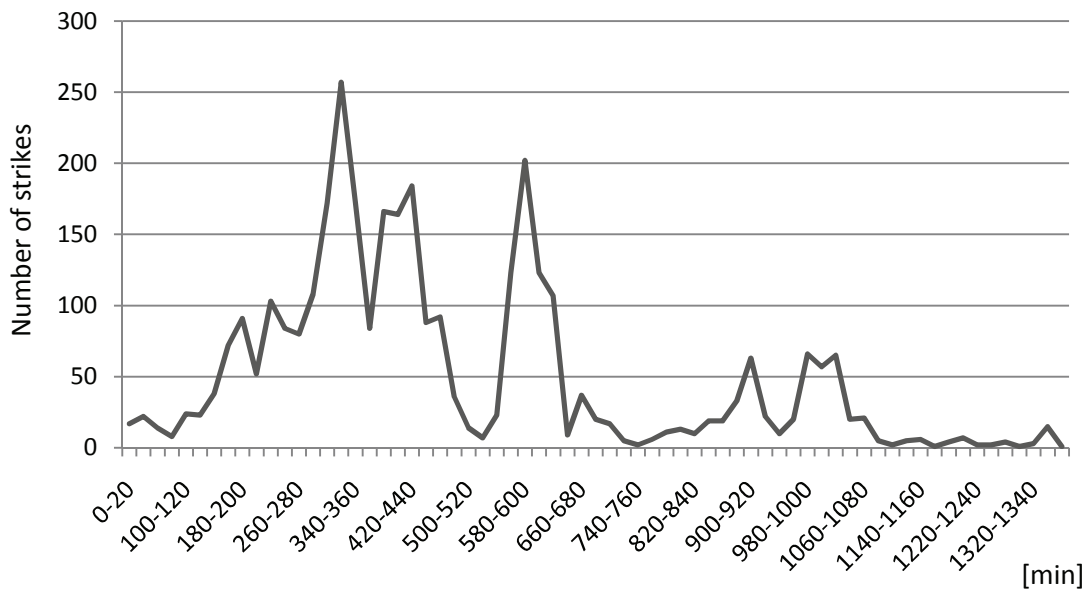


Figure 29: Lightning impacts at 2.5 km from transmission lines for SEWE 2

## 9.5 Scenarios of power transmission system

### 9.5.1 Characteristics of the electric models

Here are some relevant characteristics of the RS 2006 and PS 2018. Table 22 shows the number of different components of the AC power flow model of the European transmission network of the RS 2006 and PS 2018. Table 23 presents the generator of the Swiss transmission system for the RS 2006 and PS 2018 according to their type and installed capacity. The generator name referred to the name of the bus where they are connected, see electric schema of Chapter 9.5.2. Highlighted generators are located in Areas A (light grey) or B (darker grey) of the schema.

Table 22: Number of elements of the AC flow model

	European network	RS 2006	PS 2018
Coupler	611	19	19
Line	7753	211	248
Load	3426	61	75
Generators	946	39	52
Transformer	1368	16	25
Bus	6591	176	183

Table 23: Installed capacity in Switzerland (> 100 MW)

Location	Type	RS 2006	PS 2018	Installed gen. capacity [MW]	Installed pump capacity [MW]
Avegno	Hydro	X	X	120	0
Bâtiaz	Hydro	X	X	180	0
Bavona	Hydro	X	X	172	0
Beznau 1	Nuclear	X	X	391	0
Beznau 2	Nuclear	X	X	391	0
Biasca	Hydro	X	X	424	0
Bitsch	Hydro	X	X	330	0
Caveragno	Hydro	X	X	108	0
Chamoson	Hydro		X	1200	0
Fionnay GD	Hydro	X	X	312	0
Nendaz	Hydro	X	X	384	0
Chandoline	Pumped-storage		X	140	-70
Gösgen	Nuclear	X	X	1000	0



Grimsel	Pumped-storage		X	800	-780
Handeck	Pumped-storage	X	X	340	-50
Innertkirchen	Pumped-storage	X	X	350	-10
Leibstadt	Nuclear	X	X	1171	0
Limmern	Pumped-storage		X	1000	-1000
Mapragg	Pumped-storage	X	X	300	-162
Mühleberg	Nuclear	X	X	368	0
Pradella	Pumped-storage	X	X	360	-360
Riddes	Hydro	X	X	285	0
Fionnay FMM	Hydro	X	X	150	0
Robiei	Pumped-storage	X	X	160	-150
Stalden	Pumped-storage	X	X	300	-165
Tierfehd	Pumped-storage	X	X	400	-140
Vallorcine	Hydro	X	X	186	0
Vallorcine	Pumped-storage		X	600	-600
Veytaux	Pumped-storage	X	X	240	-240

### 9.5.2 *Electric schemas*

The three following pages are dedicated to the electric schema divided in the west, central and east parts. The schema is presented as a geographic map to help the localization of the infrastructures. The 220 kV and 380 kV overhead power lines and buses are respectively green and red. Solid lines and buses of a single color are infrastructures directly captured from the RS 2006. Dotted lines and bicolor buses are new infrastructures of the PS 2018. Yellow generators symbol are new or upgraded hydro power plants. Table 24 gives an indication about the nature of the modifications between the RS 2006 and the PS 2018.

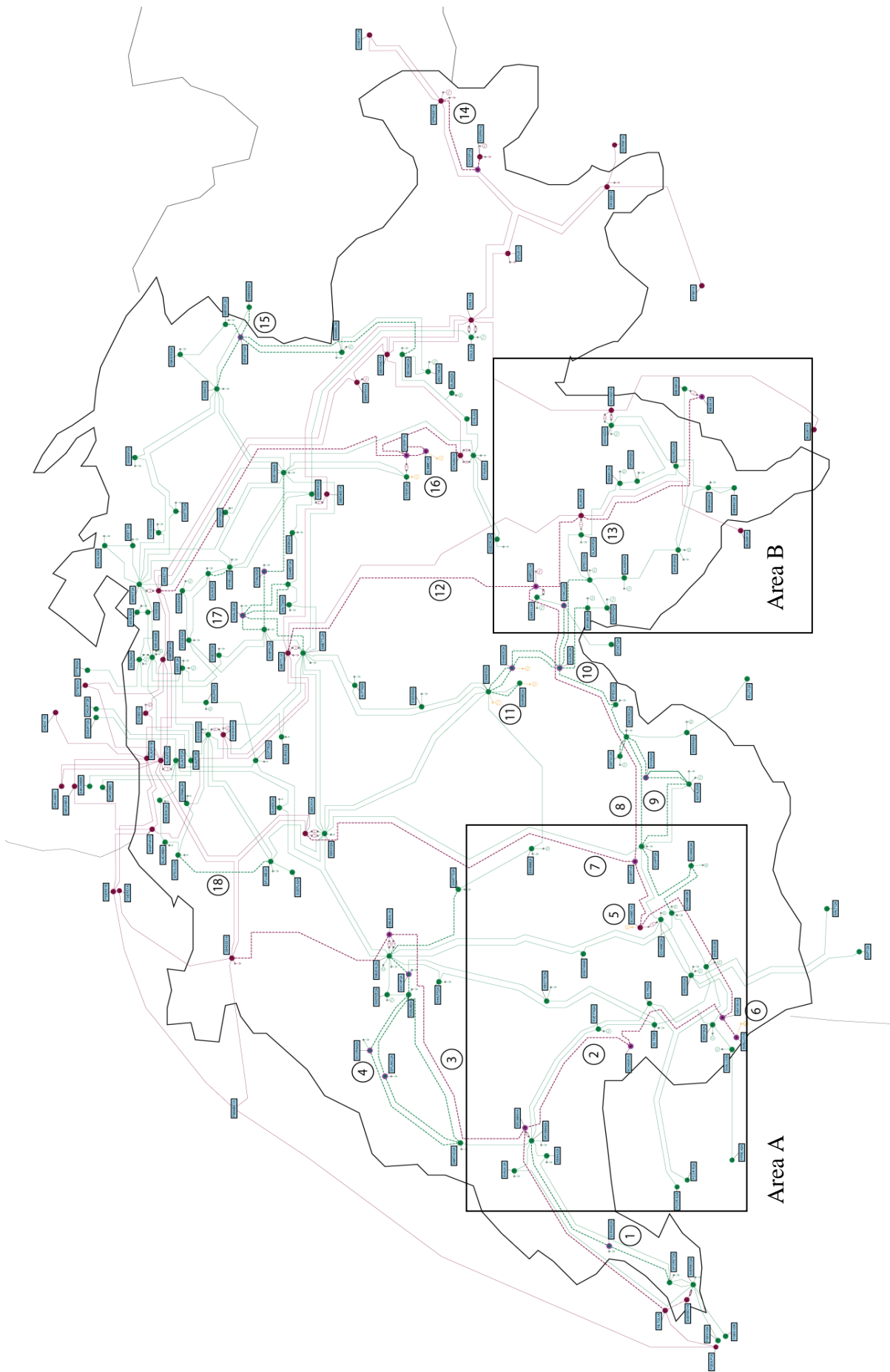


Figure 30: Electric schema of the PS 2018

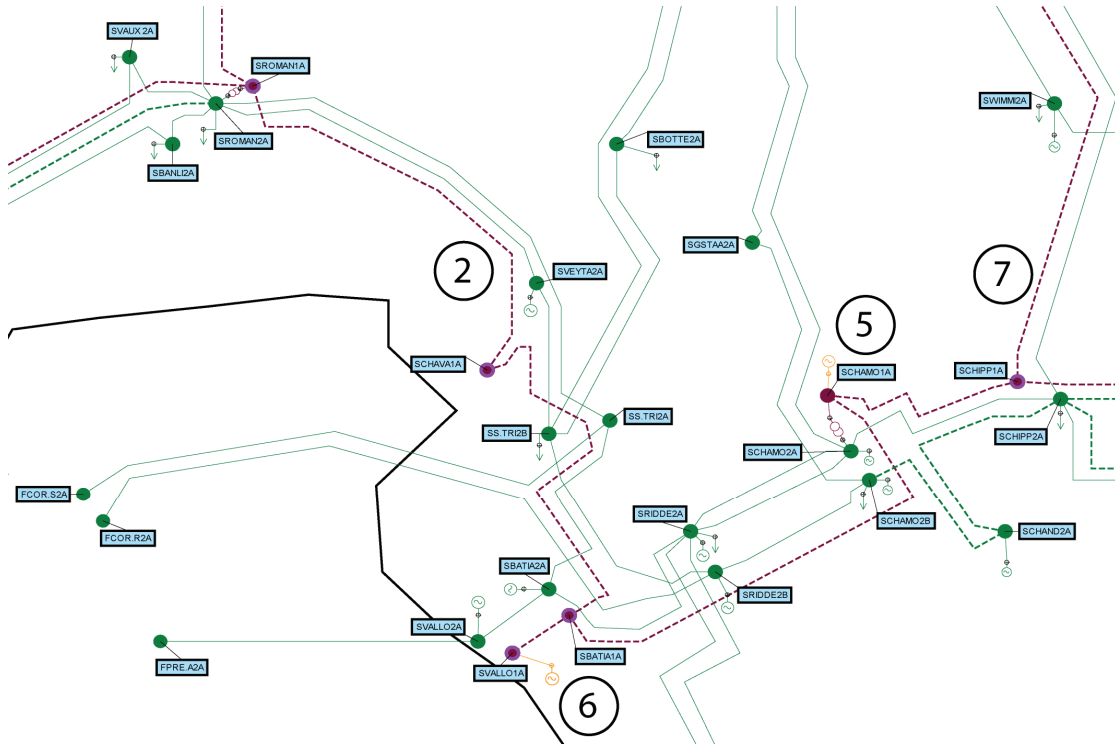


Figure 31: Zoom in area A

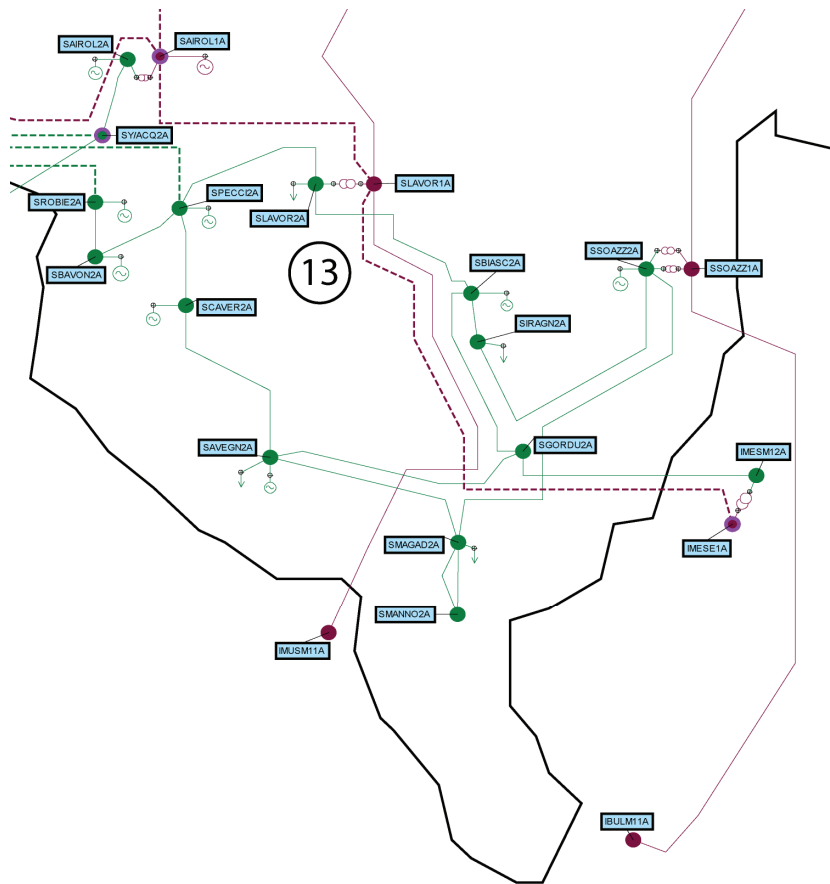


Figure 32: Zoom in area B

Table 24: Comments on the electric schemas of the PS 2018

**Label Description of the main modifications**

Label	Description of the main modifications
1	New substation at Crans. The 220 kV line Foretaille - Romanel is divided in two segments.
2	The 380 kV line Bois-Tollot - Chamoson is divided in four segments connecting three new buses at Chavalon, Bâtiaz and Romanel.
3	Construction of the 380 kV line from Romanel to Bassecourt via Mühleberg. New 220 kV line from Method to Mühleberg via Galmiz and and a new substation at Schiffenen.
4	New 220 kV substation at Cornaux and Planchamps connected to Method and Galmiz.
5	New 380 kV line Chamoson - Chippis. Connection of the Bieudron hydro power plant of 1200 MW at Chamoson.
6	New 380 kV line connecting a 600 MW hydro power plant of Nant de Drance to Bâtiaz.
7	Operation of one of the line Bickigen - Chippis at 380 kV.
8	New 380 kV line from Chippis to Airolo.
9	Multiple modifications of the 220 kV lines between Chippis to Ulrichen.
10	Construction of a substation at Ulrichen inducing topology changes.
11	Extension of three hydro power plant in Innertkirchen, Grimsel and Handeck for a total of 800 MW inducing topology modifications.
12	Operation of one of the line Mettlen - Airolo at 380 kV.
13	New 380 kV interconnection line between Airolo and Mese.
14	New 380 kV line between Ova Spin and Pradella.
15	Construction of a substation at Rütli inducing topology changes.
16	Construction of the Limmern hydro power plant of 1 GW inducing modification of the 380 kV line between Breit and Tavanasa.
17	New substations at Waldegg and Thalwil entailing the construction of six 220 kV power lines.
18	New 220 kV power line between Flumenthal and Froloo.

---

### 9.5.3 Geographical models

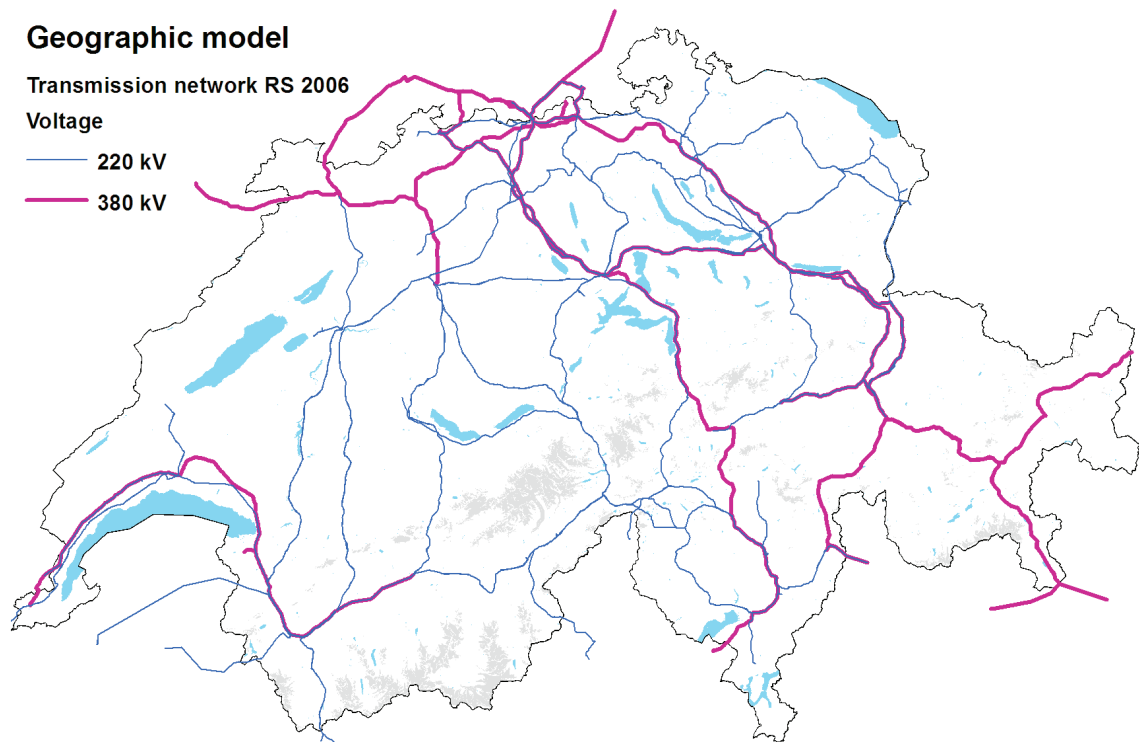


Figure 33: Map of the geographic model of the RS 2006

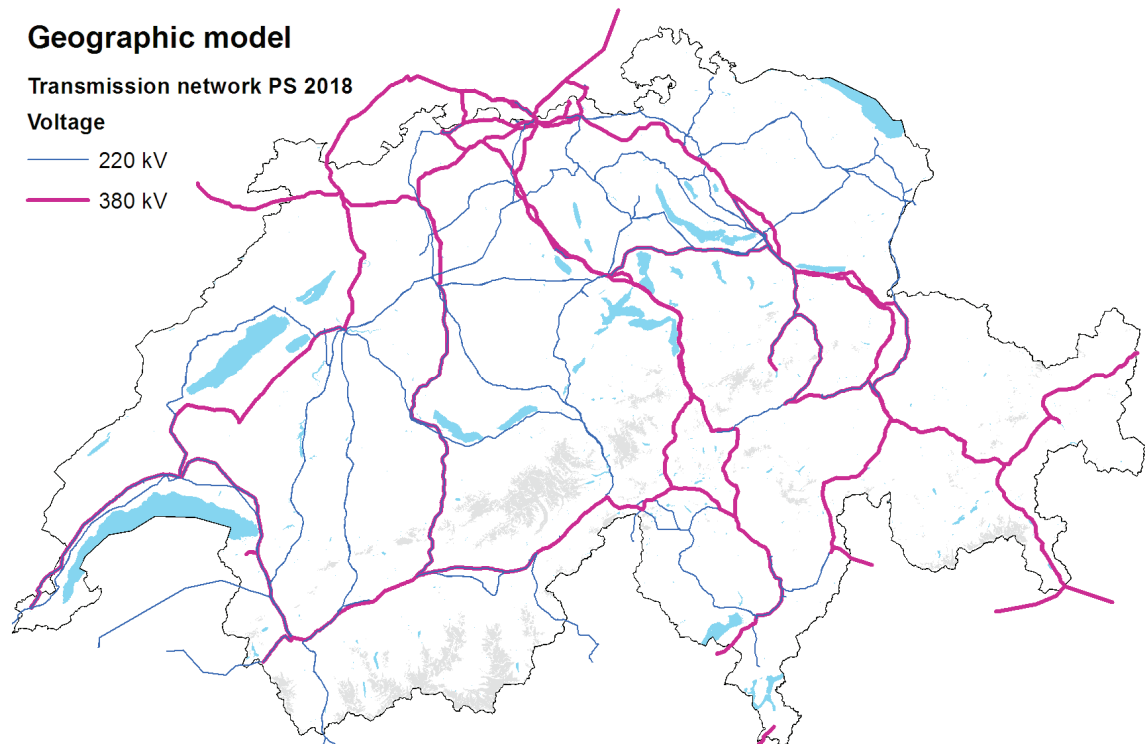


Figure 34: Map of the geographic model of the PS 2018

Table 25: Statistics of the geographic models

	2006	2018	Increase	Total increase
# of 220 kV lines	157	185	28	
# of 380 kV lines	54	63	9	37
Length of 220 kV lines [km]	4406	4889	483	
Length of 380 kV lines [km]	2246	2620	374	857
# of exposure points 220 kV	1919	2141	222	
# of exposure points 380 kV	953	1111	158	380

Table 26: Attributes of fifth first lines of the geographic model 2006

ID	Voltage	Length	Summer peak name	Summer off-peak name	# Segments
1	220	8897	SFROLO2A-SLACHM2A-1	SFROLO2A-SLACHM2A-1	4
2	380	33795	SASPHA1B-FSIERE1C-1	SASPHA1A-FSIERE1C-1	15
3	220	26713	SFROLO2A-SORMAL2A-1	SFROLO2A-SORMAL2A-1	12
4	220	7553	SBIRR 2A-SNIEDE2B-1	SBIRR 2A-SNIEDE2B-1	4
5	220	12732	SBIRR 2A-SRUPPE2A-1	SBIRR 2A-SRUPPE2A-1	6

Table 27: Attributes of six first segments in the geographic model 2006

ID segment	ID Line	Coordinate X	Coordinate Y	$R^1$ or $R^2$	Length [m]
1	1	610417	261515	2.4E-02	2500
2	1	612266	262852	2.4E-02	2500
3	1	615272	262066	2.4E-02	2500
4	1	617538	263246	2.4E-02	2500
5	2	623920	266043	7.0E-03	2500
6	2	624353	267847	7.0E-03	2500

## 9.6 Data of the reference scenario

Table 28: Estimation of the average unavailability

	2001	2003	2004	Sources
<b>A</b> Unavailability [h]	221	685	407	AES-VSE statistics
<b>B</b> Number of line	211	211	211	AES-VSE statistics
<b>C</b> Unavailability per line [h]	1.0	3.2	1.9	A/B
<b>D</b> Hours per year	8760	8760	8760	-
<b>E</b> Unavailability	1.2E-04	3.7E-04	2.2E-04	$U^l = C/D$
<b>F</b> Average unavailability		2.4E-04		$\bar{U}^l = \text{Mean}(E)$

Table 29: Normalized vulnerability of the reference scenario

	$m = 2$	$m = 3$	Sources
<b>G</b> Sum severity	0.06	0.16	Contingency analysis
<b>H</b> Unavailability	5.6E-08	1.3E-11	$F^m$
<b>I</b> Vulnerability	3.2E-09	2.2E-12	G*H
<b>J</b> Number CMC	20000	40000	Choice
<b>K</b> Vulnerability		1.6E-13	$V^{ref} = I1/J1 + I2/J2$

---

# 10 Curriculum vitae

**RAPHAEL BARBEN**, Electrical Engineer EPF

## Basic information

E-mail: raphael.barben@a3.epfl.ch

Citizenship: Swiss

Date of birth: September 29, 1979

## Education

2006-2010 **Ecole Polytechnique Fédérale de Lausanne**

Doctoral candidate and research assistant

Thesis: *Vulnerability assessment of the electric power supply under extreme weather conditions*

1999-2005 **Ecole Polytechnique Fédérale de Lausanne**

Master of Science in Electrical Engineering

Master project: *Application of neural networks to maximize the profit of hydro power plants*

Semester project: *Search of equilibriums with game theory in liberalized electricity markets*

1996-1999 **High School Auguste Piccard, Lausanne**

Secondary School Diploma

## Languages and technical skills

French: Native \ English: Advanced \ German: Beginner

Software: Microsoft office, Matlab-Simulink, Neplan, ArcInfo

Programming languages: C++, Pascal, SQL

## Publications and presentations

- Barben R, Gnansounou E., 2010, *Identification of plausible common mode contingencies in transmission networks triggered by extreme weather events*, paper submitted to International Journal of Electrical Power & Energy Systems.
- Barben R, Gnansounou E., 2010, *Identification of zones of vulnerability in transmission networks due to extreme weather conditions*, paper submitted to International Journal of Electrical Power & Energy Systems.
- Project report: *Assessment of the vulnerability of supply under extreme weather conditions*, funded by SwissElectric Research (started in 2006 and ended in 2009).
- Moser C., Burri P., Gnansounou E., Barben B., *Climate change and its influence on the planning and operation of electric power systems*, conference paper C3-102 for Cigré session 42, Paris (August 2008).
- Presentation: *Vulnerability of Electric Supply under Extreme Weather Conditions*, Cigre/Cired Conference ETH Zurich (March 1, 2007).
- Gnansounou E., Barben R., *La vulnérabilité de l’approvisionnement en électricité lors d’événements météorologiques extrêmes*, Bulletin AES-VSE (September 2007).